UNIVERSITAT DE BARCELONA

Solubility and Dissolution Rate of Active Pharmaceutical Ingredients: Dissolution Media and Effect of Enhancers

Diego Sebastián Lucero Borja

2021 DOCTORAL THESIS DIEGO SEBASTIÁN LUCERO BORJA

SOLUBILITY AND DISSOLUTION RATE OF ACTIVE PHARMACEUTICAL INGREDIENTS:

Dissolution Media and Effect of Enhancers

DIEGO SEBASTIÁN
LUCERO BORJA

UNIVERSITAT DE BARCELONA

UNIVERSITY of BARCELONA

ANALYTICAL CHEMISTRY AND THE ENVIRONMENT

DOCTORATE PROGRAMME

Solubility and Dissolution Rate of Active Pharmaceutical Ingredients:

Dissolution Media and Effect of Enhancers

Doctoral thesis presented by

DIEGO SEBASTIÁN LUCERO BORJA

DIRECTED BY:

- CLARA RÀFOLS LLACH
- XAVIER SUBIRATS VILA

University Of Barcelona – Department of Chemical Engineering and Analytical Chemistry

La Dra. Clara Ràfols Llach, catedrática del Departamento de Ingeniería Química y Química Analítica de la Universidad de Barcelona, y el Dr. Xavier Subirats Vila, profesor agregado del mismo Departamento,

HACEN CONSTAR,

Que la presente memoria titulada: “Solubility and Dissolution Rate of Active Pharmaceutical Ingredients: Dissolution Media and Effect of Enhancers”, ha sido realizada bajo su dirección por el Sr. Diego Sebastián Lucero Borja y que todos los resultados presentados son fruto de las experiencias realizadas por el citado doctorando.

Y para que así conste, expiden el presente certificado.

Barcelona, mayo 2021

Clara Ràfols Llach Xavier Subirats Vila

Dedicated to:

Jorge, Isabel, Jorge, Hipatia, Tatty

Happiness is a comfortable consequence of things well done.

Acknowledgements:

To all the people that made of my stay at Barcelona an incredible experience.

I am very thankful with the people in Laboratory 362 and the entire group of undergraduate, masters and doctorates that have crossed around during these 4 years. Very grateful with all of you.

Especial acknowledgement to Clara, Xavi, Elisabeth, Eli, Susana and Martí, for their advising and strong and nice conversations.

A strong recognition to the – in its time – Ecuadorian progressive government for the scholarship provided to develop this work.

INDEX

ACRONYMS

ABL	Aqueous Boundary Layer
Ac/P	Acetate/Phosphate buffer solution
API	Active Pharmaceutical Ingredient
ADME	Absortion, Distribution, Metabolization and Elimination
BCS	Biopharmaceutics Clasification System
BDM	Biorelevant Dissolution Media
BPP	Buffer Potasium Phosphate
Bzt	Benzthiazide
CAP	Captisol
CAV	Cavasol
CE	Capillary Electrophoresis
$[C]_f$	Final Concentration in DR assays
CheqSol	Chasing Equilibrium Solubility
DCS	Developavility Classification System
DR	Dissolution Rate
DSC	Differential Scanning Calorimetry
FaSSIF	Fasted State Simulation Intestinal Fluid
FeSSIF	Fed State Simulation Intestinal Fluid
GIT	Gastrointestinal tract
Glm	Glimepiride
HB	Hydrogen Bond
HH	Henderson – Hasselbalch
HPLC	High Performance Liquid Chromatography
I	Ionic strength
Iso	Isoxicam
K_a	Thermodynamic dissociation constant
K_a^C	Dissociation constant in concentration scale
K_{a-app}	Apparent dissociation constant
K_a^{Gibbs}	Gibbs acidity constant

ACRONYMS

KLU	Klucel
KOL	Kollidon
MM	Maleic/Maleate Buffer solution
Pio	Pioglitazone
Pir	Piroxicam
PVP	Polyvinylpyrrolidone
PXRD	Powder X-Ray Diffraction/Diffractometry
S	Thermodynamic Solubility
S_0	Intrinsic Solubility
$S_{0\text{-app}}$	Apparent intrinsic solubility
S630	Type of polyvinylpyrrolidone
SF	Shake Flask
Sib	Sibutramine
S_K	Kinetic Solubility
TGA	Thermogravimetric Analysis

ABSTRACT

The present doctoral thesis is focused on the effect of pH, enhancers and biorelevant media in the Solubility and the Dissolution Rates of some selected acidic active pharmaceutical ingredients (API). Because of the effect of these physicochemical parameters in the bioavailability of drugs and their pharmacological action, deepen the knowledge on the factors affecting the dissolution properties is of paramount importance in the drug development process.

Solubility and dissolution rates are examined in different aqueous solutions and buffering systems, accounting for the pH values of main interest in the gastrointestinal tract (2.0, 5.8 and 6.5), together with dissolution media that simulate intestinal fluids in fasted (FaSSIF) and fed states (FeSSIF). It is also determined in these media and discussed the effect of some excipients intended as dissolution enhancers, such as cyclodextrins, polyvinylpyrrolidones and hydroxypropylcellulose. Finally, differential scanning calorimetry was used to identify solid-solid interactions between excipients and APIs. As a complementary investigation, this thesis also presents a comparative study of the reference shake-flask and potentiometric CheqSol methods for the determination of solubility, including APIs with different acid/base properties (acidic, amphoteric and basic).

The study confirms that solubility is pH dependent, and an accurate pK_a determination of the drugs is needed to detect the presence of concurrent aggregation or complexation reactions affecting the amount of compound dissolved. As expected, the addition of excipients increases the solubility of APIs, but in different degrees depending on the drug, excipient, and pH

conditions. Solubility in simulated intestinal fluids is generally improved, and the addition of excipients might increase, diminish or even cancel the enhancement, depending on the matrix formed. Interestingly, the factors improving the solubility of an API do not necessarily enhance its dissolution rate. The release of the drug from its compressed solid form (tablet) is a complex process, involving an aqueous boundary layer between the solid and the bulk solution.

The results of this thesis point out the need of systematic and detailed dissolution studies in the step of pharmaceutical formulation, as long as the enhancement produced by a particular excipient in a singular dissolution medium can be characteristic of an individual API, and these results cannot be uncritically extended to other drugs.

1 INTRODUCTION

1.1 General Considerations for Pharmaceutical Formulation

In the pharmaceutical industry, the development of a drug until it is accessible to the people involves many stages. Everything starts in the discovery of a new active pharmaceutical ingredient, either by natural origin, organic synthesis or from chemical modification of anyone already in existence. Next step is to define the action mechanism of the molecule that can be used to cure any illness, ensuring that it works in the way that it was thought to work, also, their possible toxicity, side effects, etc.

This is followed by clinical studies and finally, if this stage is passed, the drug is now ready to commercialization. A brief summary of all these steps can be seen at Figure 1[1].

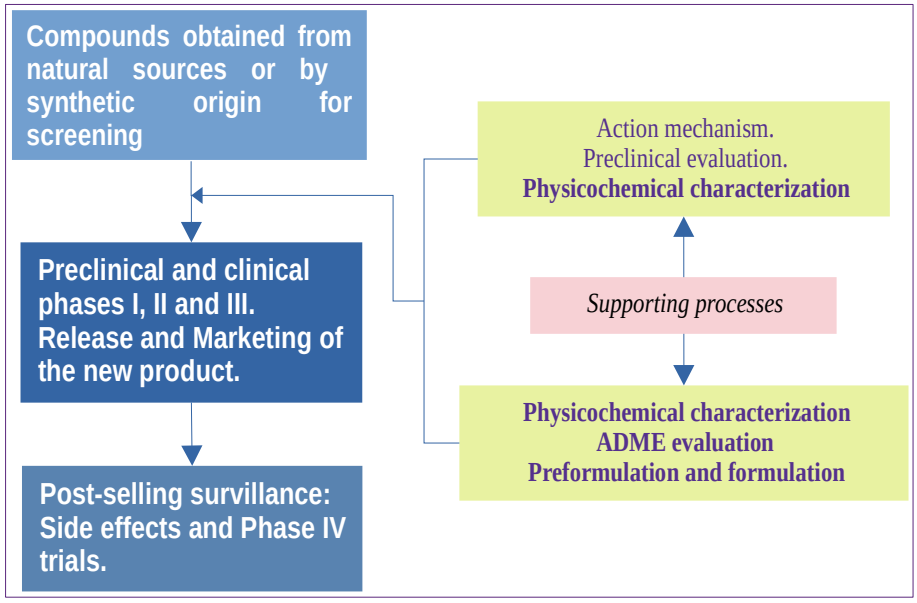

Fig 1: Development stages and cycle of life of a pharmaceutical product.

An intermediate stages of all this process is the pre-formulation and

formulation[2, 3], this is, to give to the active pharmaceutical ingredient enough stability during its administration in the preclinical evaluation, and the longest possible half-life time until it cannot be used or expires when it is commercialized. The preformulation and formulation are determined by the possible administration way of the drug (parenteral or enteral) and will set the best pharmaceutical form that fits better with that administration way. Then the medicine is completely developed according to the physicochemical and pharmaceutical properties of the API.

At this moment, two big research points have been called. The first one is in which the active pharmaceutical ingredient is fully characterised by the determination of its relevant physicochemical properties, and the second one is the preformulation and formulation of the pharmaceutical form.

The most important physicochemical parameters that are useful in drug development are: Acidity Constant, Solubility, Partition Ratio and Dissolution Rate, because these will affect directly over the entire pharmacokinetic processes involved under ***ADME studies***, this is: ***A***bsorption, ***D***istribution, ***M***etabolism and ***E***limination[4].

For an oral administered drug, the **Absorption** is the process where the drug pass from the intestinal fluids to the blood through the epithelial cells of the jejunum-ileum. Once the drug is in the blood, it is **Distributed** to all the body via circulatory system. In this case, the blood makes that the drug goes first to the liver, undergoing a First Step **Metabolization.** Then the metabolized compound goes out of the liver and it is distributed through the body, together with the drug portion that was not metabolized.

In many cases the part that was not altered by the liver, exerts the therapeutic

effect, but sometimes it is the metabolite which has a therapeutic effect. After these steps, the drug suffers a second metabolization step inside the cell (in cytoplasm or by any cellular organelle), and it is afterwards excreted to the blood. Finally, the blood will be filtered by the kidneys and the drug and its metabolites are **Eliminated or cleared** from the body[5].

The **Pharmacokinetic Process** of the drug is defined as the measurement of the concentration of the drug inside the body in function of time during each one of the **ADME steps**, allowing to study the onset, duration and intensity of this concentration in the different biological compartments**.** The pharmacokinetic of a drug will depend on the lipophilicity and solubility of the pharmaceutical ingredient, and both of them are dependent on the ionisation degree of the drug. These processes must be differentiated from the **Pharmacodynamics** of the drug, which is the study of how the active ingredient works or affects on the body, that is related to the pharmacological action, side effects and action mechanism[3].

1.2 Physicochemical parameters of interest in pharmaceutical formulation

1.2.1 Acidity constant (pK_a)

When the active ingredient is administered by oral dose, its absorption is related to the fraction solubilized in the gastrointestinal fluid, being the higher the solubility, the higher the absorption. The solubility of the compound is dependent on its ionisation degree. Although the ionised form is more soluble, usually it has very low absorption, and it is normally the neutral form the one that is absorbed. Then, a proper determination of the acidity constant is crucial because of the role of ionisation in the total concentration of the drug available

to pass by gastrointestinal membrane.

Once the absorbed drug is in the blood, its plasmatic proteins work as carriers of the API through the body to reach the specific action place or target organ. Usually it is the neutral form (poorly soluble) which is transported. The union to the proteins must be strong enough to allow the transport, but weaker than the union to receptors in the active site of the target organ. If the union to proteins is too strong, the compound cannot be released in the target organ and this could lead to saturation of the blood causing not only decrease of the pharmacological action but toxicity. In the other hand, if this union to proteins is not strong enough, the API could not be transported and could cause bioaccumulation in a specific place, because of its lipophilicity, leading also to toxicity. In these cases, the low ionisation degree can make difficult the elimination of the drug.

The metabolization in first step of APIs produces ionic metabolites that are easily eliminated by urine, being the more the ionisation degree, the easier the metabolization. Meanwhile, the free fraction of API that did not suffer a first step metabolization is going to produce the pharmacological effect, and after exerting its action the API could be eliminated unmetabolized. This fraction reaches the kidneys to be eliminated by urine (the most common elimination way), and again the more the ionisation degree in this medium, the easier the elimination[5–7].

Then, the pK_a determination of the API is essential to know its ionisation degree in the different biological fluids, this is, the amount of ionised or neutral species of the drug at different pH values and media.

The dissociation equilibrium for a monoprotic acid and base are given in the following Equations:

for a monoprotic acid (AH)

$$AH_{(aq)} \rightleftarrows [A^-] + [H^+] \quad (1)$$

$$K_a = \frac{[A^-] \cdot [H^+]}{[AH]} \quad (2)$$

for a base (B)

$$BH^+_{(aq)} \rightleftarrows [B] + [H^+] \quad (3)$$

$$K_a = \frac{[B] \cdot [H^+]}{[BH^+]} \quad (4)$$

$$pK_a = -logK_a \quad (5)$$

However, constants given in Equations (2) and (4) are considering only concentrations (an ideal solution) and are not taking into account the possible interactions of these species with others presents in the solution. These interactions could be affecting the effective concentration of the species involved in the constant. The use of activities instead of concentrations allow to determine the effective concentrations under non-ideal conditions. These activities are dependent on the ionic strength of the solution, and the higher the concentration of ions, the higher the ionic strength and the interactions.

Considering activities K_a is expressed as follows:

$$K_a = \frac{a_{A^-} \cdot a_{H^+}}{a_{AH}} \quad (6)$$

Where *a* is the activity of the corresponding ion or neutral species, and this activity is in turn the product of the concentration of the corresponding species and its *coefficient of activity* (γ), obtaining Equation (7):

$$a_X = \gamma_X \cdot [X] \quad (7)$$

where X can be any of the species involved in the dissociation process.

Equation 6 correspond to the thermodynamic dissociation constant K_a (expressed in terms of activities), which is independent of the media concentration. Nevertheless, the dissociation constants are often determined in a medium of constant ionic strength, and then, reported as a concentration scale (K_a^C) which varies with the media electrolyte concentration. Then, both the thermodynamic K_a and the concentration ionisation constant K_a^C are related through the activity coefficients, thus:

$$K_a = \frac{\gamma_{A^-}[A^-]\cdot\gamma_{H^+}[H^+]}{\gamma_{AH}[AH]} \quad (8)$$

$$-\log K_a = -\log\frac{[H^+][A^-]}{[AH]} - \log\frac{\gamma_{A^-}\gamma_{H^+}}{\gamma_{AH}} \quad (9)$$

$$\mathrm{p}K_a = \mathrm{p}K_a^C - \log\frac{\gamma_{A^-}\gamma_{H^+}}{\gamma_{AH}} \quad (10)$$

At infinite dilution K_a^C becomes numerically equal to the thermodynamic constant K_a, since activity coefficients are equal to unity. The activity coefficients can be estimated from the Ionic Strength (*I*) of the medium by means of the Debye-Hückel Equation (Equation 11)[8, 9].

$$\log\gamma_i = \frac{-A\cdot z_i^2\sqrt{I}}{1+B\mathring{a}\sqrt{I}} \quad (11)$$

where z_i is the charge of the ionic species presents, *I* is the ionic strength of the solution (dissolution media or buffer used). *A* and B are Debye-Hückel parameters that are solvent, temperature and pressure dependent, $\mathring{a}$ represents the hydrated radius of the ion. The values for A and B$\mathring{a}$ at 25°C in water are 0.509 and 1.5 respectively. Davies Equation[8, 10, 11] replaces A and B$\mathring{a}$ for terms involving *I*:

$$\log\gamma = 0.5\,z^2\left(\frac{\sqrt{I}}{1+\sqrt{I}} - 0.3\,I\right) \quad (12)$$

Equation 11 is commonly used at ionic strength up to 0.1M nevertheless, in a recent unpublished work in our research group it has been proved that it is applicable until 0.15M of ionic strength. The Equation 12 in turn is used for *I* up to 0.5M, for higher concentrations other approaches should be used.

1.2.2 Thermodynamic and Intrinsic Solubility (S and S_0)

The Thermodynamic Solubility (*S*) refers to the amount of solid sample that can be completely dissolved in a given amount of solvent at a particular pH and temperature, as long as a solid phase exists in equilibrium with the solution phase.

On the other hand, the Intrinsic Solubility (S_0) is the equilibrium solubility of the neutral acid or base form of any ionisable compound at a pH where it is fully unionised[4].

For ionisable molecules *S* is pH-dependent, because according to the pK_a of the compound, the solute will be more or less dissociated when the pH changes, hence more or less quantity of substance will be dissolved. Equations (13 – 15) show the solubility equilibria for monoprotic acids:

$$AH_{(s)} \rightleftarrows AH_{(aq)} \rightleftarrows A^- + H^+ \quad (13)$$

$$S = [AH]_{aq} + [A^-] = S_0\left(1 + 10^{pH - pK_a}\right) \quad (14)$$

$$S_0 = [AH]_{(aq)} \quad (14a)$$

$$\log S = \log S_0 + \log\left(1 + 10^{pH - pK_a}\right) \quad (15)$$

and for a diprotic acid its equilibrium is given by:

$$AH_{2(s)} \rightleftarrows AH_{2(aq)} \rightleftarrows AH^- + H^+ \rightleftarrows [A^{-2}] + [H^+] \quad (16)$$

$$S = [AH_2]_{(aq)} + [AH^-] + [A^{-2}] = S_0\left(1 + 10^{pH - pK_{a1}} + 10^{2\,pH - pK_{a1} - pK_{a2}}\right) \quad (17)$$

$$S_0 = [AH_2]_{(aq)} \quad (17a)$$

$$\log S = \log S_0 + \log\left(1 + 10^{pH - pK_{a1}} + 10^{\left(2\,pH - pK_{a1} - pK_{a2}\right)}\right) \quad (18)$$

According to Equations 13 and 16, in a medium whose pH is above of the pK_a of the acidic solute, the solubility of the sample will be increased since the relatively low [H^+] forces the equilibrium to the right, making that more solid goes to aqueous form, increasing in this way the solubility. On the contrary, at pH much below of the pK_a, the molecules are entirely neutral, the solubility does not change even if the pH does. This solubility corresponds to the S_0 of the compound.

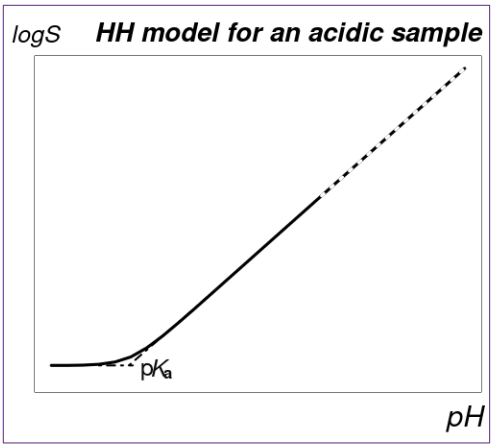

Fig 2: Solubility - pH dependent profile for a typical monoprotic acid.

The plot in Figure 2 represents the variation of *S* with pH, according to Equation 15 it shows two sectors where the flat one corresponds to the S_0 and the second one a straight line of slope 1 corresponding to the contribution ionised species to solubility. When both segments are intersected by each other, the crossing point corresponds to the pK_a of the molecule.

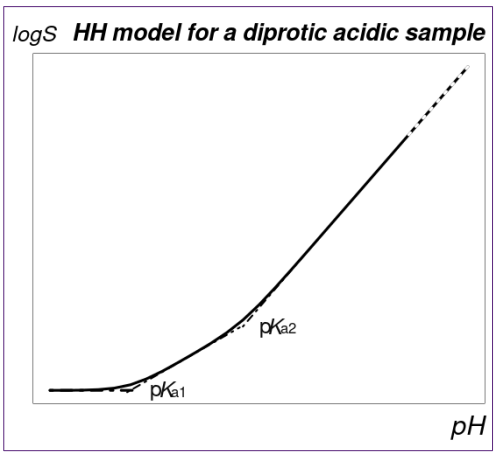

Fig 3: Solubility - pH dependent profile for a diprotic compound.

The plot in Figure 3 corresponds to a diprotic acid, where there are 3 expected sectors (Equation 18), the flat one correspond to S_0, the second segment between the two pK_a values of the sample has a slope of 1 and shows the first deprotonation of the sample, and the third sector – above of the second pK_a – has a slope of 2 and shows the

behaviour of the second deprotonation of the molecule. The mutual intersection of the corresponding segments let to predict the two pK_a values of the compound.

In a similar way, the Solubility equilibria for a monoprotic base can be described by Equations 19 – 21 and Figure 4. When pH is lower than the pK_a of the base, the [H^+] increases and the ionisation degree of the base will be higher because the equilibrium (Equation 19) is forced to the right increasing the solubility of the base. The S_0 can be obtained when the pH is much higher than the pK_a of the base (Equation 21).

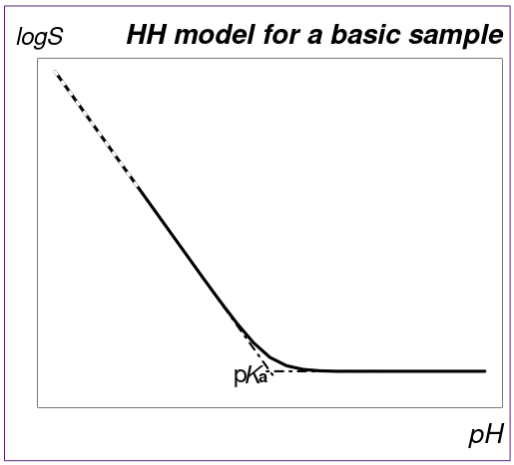

Fig 4: Solubility - pH dependent profile for monoprotic basic compounds.

$$B_{(s)} \rightleftarrows B_{(aq)} + H^+ \rightleftarrows BH^+ \quad (19)$$

$$S = [B]_{aq} + [BH^+] = S_0\left(1 + 10^{pK_a - pH}\right) \quad (20)$$

$$S_0 = [B]_{(aq)} \quad (20a)$$

$$\log S = \log S_0 + \log\left(1 + 10^{pK_a - pH}\right) \quad (21)$$

The model for an amphoteric compound is given by Equations (22 – 24) and Figure 5. Its behaviour is a combination of acidic and basic characteristics: in a range of pH lower than its basic pK_{a1}, the molecule will be more soluble because it will be protonated and positively charged, in the pH range within its two pK_a values, the compound will be neutral and less soluble and here will be its S_0; finally at pH range higher than its pK_{a2} value, the solubility will increase again because now it is deprotonated and negatively charged.

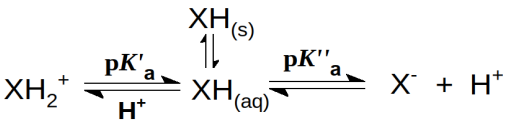

(22)

$$S=[XH_{(aq)}]+[XH_2{}^+]+[X^-]=S_0\left(1+10^{pH-pK_{a1}}+10^{pK_{a2}-pH}\right) \quad (23)$$

$$S_0=[XH]_{(aq)} \quad (23a)$$

$$\log(S)=\log(S_0)+\log\left(1+10^{pH-pK_{a1}}+10^{pK_{a2}-pH}\right) \quad (24)$$

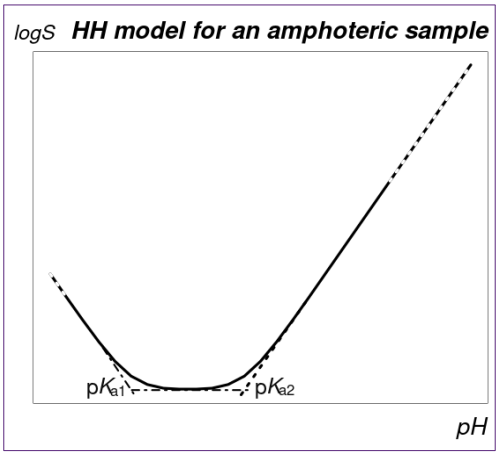

Fig 5: Solubility - pH dependent profile for amphoteric compounds.

Figures 2 to 5, are representations of Henderson–Hasselbalch (HH) models that are expressed by Equations (15, 18, 21 and 24) for monoprotic and diprotic acids, bases and amphoteric compounds, respectively. In these models the Solubility (*S*) of the compound is considered as the sum of the molar concentrations of the neutral and charged species of the compound in the solution.

In these mentioned HH models the solubility is only affected by the acid-base equilibria, and it is assumed that no other parallel or competing reactions are present. However, the buffer components that are used in the solubility studies, or the constituents of the body fluids, can interact with the sample or even the compound might interact with itself because of its chemical structure (for instance, aggregation reactions). For those cases of aggregate formation, there are adjusted models based on HH Equations, which consider the effect of other equilibria in the solubility process. Some of them are listed in Table 1.

Table 1: HH-like models exemplifying different aggregation reactions where: A for acids, B for bases and their respective charged states[12, 13].

Equilibrium Reaction	Model
$nAH \rightleftarrows (AH)_n$	$logS = logS_0 + \log(1 + K_a/[H^+] + n K_n S_o^{n-1})$
$nB \rightleftarrows (B)_n$	$logS = logS_0 + \log(1 + [H^+]/K_a + n K_n S_o^{n-1})$
$nA^- \rightleftarrows (A^-)_n$	$logS = logS_0 + \log(1 + K_a/[H^+] + K_a^n n K_n S_o^{n-1}/[H^+]^n)$
$nBH^+ \rightleftarrows (BH^+)_n$	$logS = logS_0 + \log(1 + [H^+]/K_a + [H^+]^n n K_n S_o^{n-1}/K_a^n)$
$nA^- + nAH \rightleftarrows (AH \cdot A^-)_n$	$logS = logS_0 + \log(1 + K_a/[H^+] + K_a^n 2n K_n S_o^{2n-1}/[H^+]^n)$
$nBH^+ + B \rightleftarrows (B \cdot BH^+)_n$	$logS = logS_0 + \log(1 + [H^+]/K_a + [H^+]^n 2n K_n S_o^{2n-1}/K_a^n)$

In these Equations the subscript *n* indicates that it is an aggregation process where *n* moles of reagent and product are involved, and these reactions occur with the sample itself.

Aggregations can be also produced when the sample interacts with any other component present in the solution, coming it from the buffer or from any other added reagent. Equations in Table 2 are applicable models to these situations.

Table 2: HH-like models exemplifying sample-sample/buffer components interactions, where A and B for acids and bases respectively, X for any component different from the sample[12, 13].

Reaction	Model
$nA^- + nAH \rightleftarrows (AH \cdot A^-)_n$ $AH + X \rightleftarrows [AH \cdot X]$	$logS = logS_0 + \log(1 + K_a/[H^+] + 2n K_n K_a^n S_o^{2n-1}/[H^+]^n + K_X)$
$nBH^+ + nB \rightleftarrows (BH^+ \cdot B)_n$ $B + X \rightleftarrows [B \cdot X]$	$logS = logS_0 + \log(1 + [H^+]/K_a + [H^+]^n 2n K_n S_o^{2n-1}/K_a^n + K_X)$

In the preceding Equations in Table 2, component *X* represents any compound used in dissolution assays different from the main sample[12, 13].

A graphical example of the aggregation processes is given in Figure 6, where the solid line (A) is for an hypothetical acid that follows strict HH behaviour. Meanwhile, the (B) line represents that the neutral form keeps its S_0 value unaltered suggesting the absence of interactions, but the ionic conjugate base

is involved in any type of interaction, producing an apparent pK_a value (p$K_{a\text{-app}}$), shiffted in relation to pK_a. The (C) line case in the same Figure 6, shows both S_0 ($S_{0\text{-app}}$) and pK_a (p$K_{a\text{-app}}$) displacements, indicating that both, the neutral and the ionic species of the sample are experiencing interactions with themselves or with any other medium component. These interactions can be seen as displacements to either left or right side of the theoretical HH curve, depending on the occurred type of reaction.

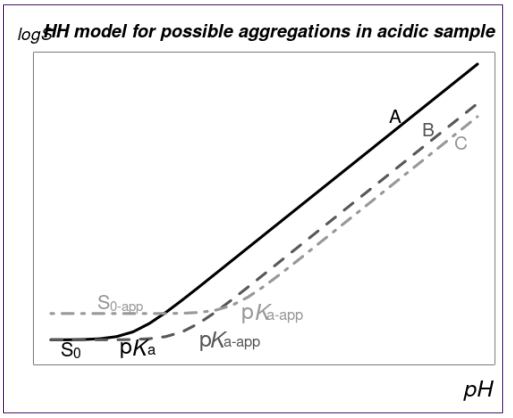

Fig 6: HH-like models where an acid has suffered two types of aggregations.

Another type of interaction is due to the charged state of the sample with opposite charged components in solution, leading to salt formation by ionic charge balancing. Usually, when the solution reaches a high concentration of ionic species, this is at pH << pK_a for basic compounds or pH >> pK_a for acidic substances, and when an excess of buffer counterion is present, the precipitation of the salt could occur, and its reaction is given in Equations 25 and 26.

$$E_X F_Y \rightleftarrows {}_X E^+ + {}_Y F^- \tag{25}$$

$$K_{sp} = [E^-]^X \cdot [F^+]^Y \tag{26}$$

where E^- and F^+ are the ionic components of the salt E_XF_Y and X and Y refer to the number of moles involved in the reaction respectively. In Equation 26 K_{sp} is the solubility product constant of this salt, which provide information about the ionic product concentrations causing the salt precipitation[14].

At a particular point four different equilibria could be present simultaneously: the solubility of the neutral form of the acid $\left(AH_{(s)} \rightleftarrows AH_{(aq)}\right)$, the acid-base equilibria of these solid forms $\left(AH_{(s)} + C^{+}_{(aq)} \rightleftarrows A^{-}C^{+}_{(s)} + H^{+}_{(aq)}\right)$, aqueous neutral forms $\left(AH_{(aq)} \rightleftarrows A^{-}_{(aq)} + H^{+}_{(aq)}\right)$, and the salt precipitation $\left(A^{-}_{(aq)} + C^{+}_{(aq)} \rightleftarrows A^{-}C^{+}_{(s)} + H^{+}_{(aq)}\right)$. As a result, due to the Gibbs constraint rule, as long as the precipitated salt and the solid form of the free acid coexist, the pH of the solution remains constant. This pH value is known as Gibbs pK_a $\left(\mathrm{p}\,K_a^{Gibbs}\right)$ or $\mathrm{pH_{max}}$[15–18].

Since pK_a^{Gibbs} makes reference to that specific value of pH of the solution in which the neutral form of the API (solid dissolved) is coexisting with the solid salt formed by API with other component, this is a point where the maximum solubility of the neutral species – acid in this example – is reached and also is the starting point of salt formation[18]. This salt will be formed with the conjugated base of this hypothetical acid and any other cationic species present in the medium, obtaining profiles like in Figure 7[19].

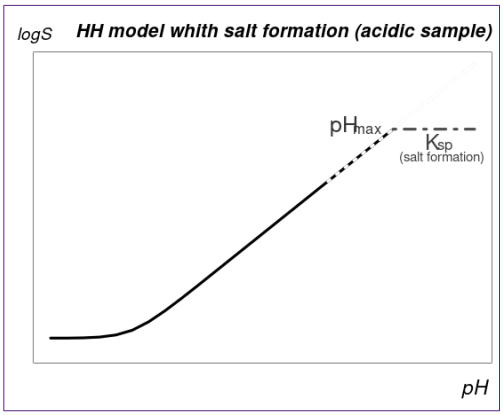

Fig 7: Example of HH model for an acidic molecule including pH_{max} when a salt can be formed.

1.3 Dissolution Rate

Drug Delivery Systems are those ways in which an active ingredient is released from the drug or medicament to the dissolution medium or fluids. Just as there are several pharmaceutical forms, there are also some different ways to liberate or release the API. In a cream for example, which is for topical use, the API starts to be delivered the moment in which the cream is decomposed by the action of enzyme in the subdermal space, and this happens only after the cream have crossed the stratum corneum of the skin.

Other example is that from a liquid suspension, where the API is not dissolved but it is suspended in microparticles (or nanoparticles, forming nanosuspensions), the drug is delivered in the instant when the suspension is broken (destabilized) by action of the pH in the stomach and the API starts its solubilisation process in the medium.

Meanwhile for solid forms, the API must be released from the pharmaceutical form to the bulk (in buccal mucosae, stomach, jejunum-ileum) by destruction, breaking or disintegration of the tablet or capsule.

In Figure 8 there is a schematic representation of the different steps of drug releasing, starting from the disintegration to the dissolution when a tablet (A) is used. The dissolution of the API can be done by many simultaneous ways where, the path A-B-C-D is the main process and the fastest one, and path A-D is the slowest. The disintegration, followed by deaggregation (disaggregation) and finally dissolution (see Figure 8), involves kinetic processes that can be very fast like in sublingual pills, or can be prolonged in time like in retarded release tablets. The selection of fast or slow delivery systems depends on how fast the API is needed to be available and consequently solubilized, to start the

pharmacokinetic (ADME) and pharmacodynamic processes of the drug[20–22].

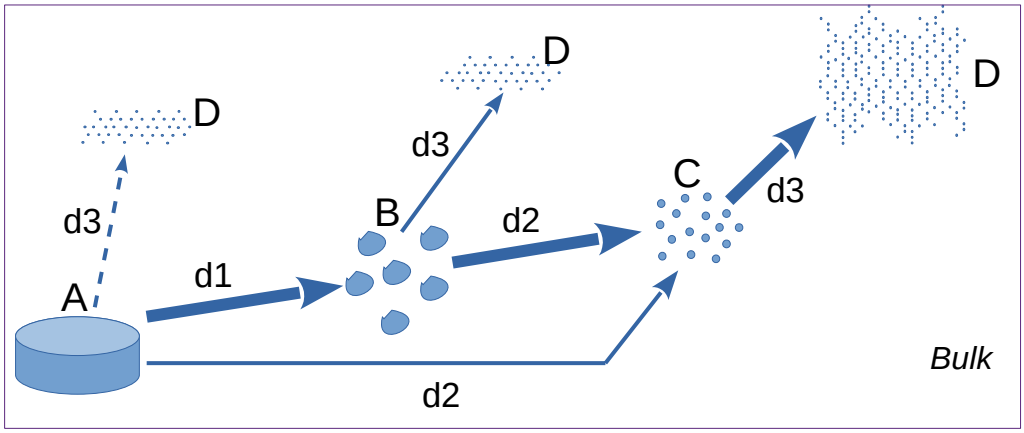

Fig 8: Releasing process of a drug from a tablet, suffering different processes: (d1) disintegration, (d2) disaggregation (deaggregation), (d3) dissolution.

The different delivery systems have their own way to be determined how fast release its API. Depending on the pharmaceutical form, these methods include some diffusional principles in many models (cylindrical, planar, spherical, and other geometrical models), diffusion mechanisms mediated by chemical reactions, passive pore diffusion and other models[23, 24].

Regarding to solid pharmaceutical forms for oral administration, the common model to measure the quantity of API released in a fixed volume of medium in a given time is based on the Noyes – Whitney[25] model expressed in Equation 27, where the velocity of dissolution or Dissolution Rate (DR) of a compound – variation of concentration per variation of unit of time – is directly proportional (constant K) to the difference between the saturated concentration C_0 and the concentration C_t in the bulk after a certain time:

$$\frac{dC}{dt} = K\left(C_0 - C_t\right) \tag{27}$$

This model was later updated by Nernst – Brünner[26] introducing other parameters to explain the constant *K* in Equation 27 and obtaining Equation 28[20]:

$$\frac{dC}{dt} = \frac{A \cdot D}{V \cdot h}(C_0 - C_t) \tag{28}$$

where *A* is surface area of the solid in contact with the liquid, *D* is the Diffusion coefficient of the dissolved sample, *V* volume of the bulk, *h* is the thickness of the diffusional layer or Aqueous Boundary Layer (ABL). ABL is the boundary zone formed between the solid surface and the bulk, and here is where the maximum concentration of the sample dissolved is found, what in turn corresponds to C_0 or the saturation concentration (thermodynamic solubility) of the sample, and C_t is the concentration after *t* time found in the bulk.

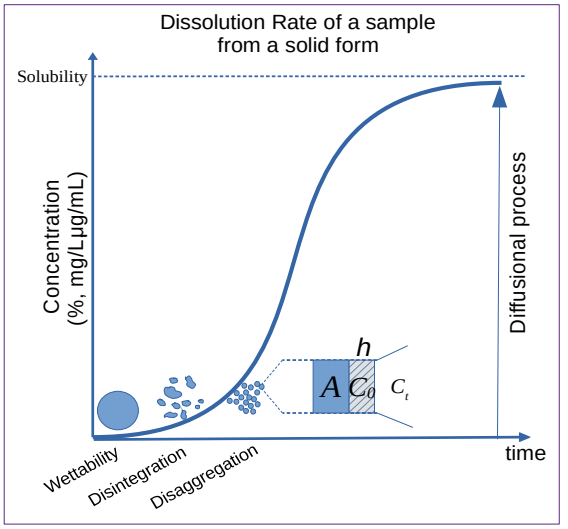

Fig 9: Scheme for the Dissolution process given by diffusional model. (adapted from Reference[30])

The C_t is continuously increasing while the sample diffuses from the ABL to the bulk. Once the sample ends its diffusional process, the sample reaches a concentration close to its solubility in the bulk, the DR will be constant and close to zero, as expressed in Equation 28 and Figure 9[27–30].

As pointed in Equation 28, the DR will be increased if *h* decreases and *A* increases, provided that *D* and *V* should be constant (*D* coefficient is inversely

proportional to the viscosity of the medium). On the other hand, it is desirable for C_0 to be as high as possible, and if the sample can form supersaturated solutions (kinetic solubility of high extension and duration) the DR will increase. Therefore, the better it is the solubility of a compound, the better it will be its DR. A good strategy to increase the solubility of the sample could be its introduction as an ionic form (ionic salt) in the formulation[10].

The solution of the Noyes – Whitney differential Equation (Equation 27) allows to obtain an exponential expression given in Equation 29. The concentration C_t after *t* time will be reached depending on how high or low is the solubility of the sample, and can be also calculated at any point of time[31]:

$$C_t = S\left(1 - e^{-k_d \cdot (t - t_0)}\right) \tag{29}$$

where *S* corresponds to the extrapolated solubility of the sample (at the given pH of the solution and infinite time), k_d is the rate constant for dissolution in $time^{-1}$ units, t and t_0 are time of assay and lag time (time to correction due to an instrumental delay), respectively. The product of $k_d \cdot S$ corresponds to the DR (at a certain point of time), and the maximum dissolution rate (DR^{max}) is achieved when $t = t_0$, i.e. when the difference between C_t and *S* is the highest. Since the DR is a change of concentration as a function of time (dependent on many parameters), the Intrinsic Dissolution Rate (IDR) is the ratio between the DR^{max} and the apparent Area of Surface Contact (A_{app}) of the particles (Equation 30).

$$IDR = \frac{DR^{max}}{A_{app}} = \frac{1}{h_{app}} D \cdot S \tag{30}$$

In the dissolution process, the particles in contact with the liquid are coming

from the disintegration of the surface of the tablet or from a capsule releasing its powder, in any case they will have an average particle size and therefore an apparent area of contact surface (A_{app}), and an apparent h of its ABL (h_{app}).

The general conditions to obtain the best IDR are that the particles in dissolution must be the most homogeneous and the smallest as possible, which let to obtain a high enough A_{app}. Controlling the agitation or stirring will produce h_{app} as low as possible, and thus the IDR will increase. Also controlling the pH of the media will avoid precipitation of the sample and will control its ionisation degree in case of molecules with acid-base properties[25, 32–36].

1.4 Biopharmaceutic and Developavility Classification Systems

The solid form is the most commonly used pharmaceutical form for oral use, and it is in charge of deliver and release the active ingredient in the gastrointestinal tract. This release process is driven by intrinsic factors of the pharmaceutical form, i.e. disintegration and dissolution rate. The latter is in turn driven by the solubility of the compound, and the solubility depends on the physicochemical properties of the API (pK_a, crystallinity state) and on dissolution media factors like pH, temperature, viscosity.

This allows to introduce the concept of ***Bioavailability***, which is defined as the highest quantity of drug available in blood, indeed, plasmatic concentration, enough to exert the pharmacokinetic and pharmacodynamic processes in the body, after the absorption process is completed. The absorption depends on the amount of compound dissolved, which in turn depends on the dissolution rate and solubility what are influenced by the factors early described.

Besides, once the compound is dissolved and has reached its highest possible concentration in the gastric or intestinal fluid, to be absorbed to the blood through the membrane cells in the intestinal wall, it is desirable for the compound to have the highest possible affinity for crossing these membranes, which is driven by the permeability of the molecule.

If both the solubility and the absorption are the highest possible, then the Bioavailability of the compound will be the best possible for that specific compound. Each molecule has their own capacity of getting dissolved and permeate through membranes, and in extreme cases they will have high solubility and high permeability or poor solubility and low permeability.

Ideally, an intravenous administered drug will be the 100% bioavailable because in this pharmaceutical form all the solute is completely dissolved, omitting thus the processes of dissolution and absorption. Meanwhile in an orally administered drug, its bioavailability always will be under 100% because not all of the sample is dissolved and even if all of the compound is dissolved, not all of this will be absorbed.

If the Bioavailability of the API administered orally is close to the bioavailability of the same API administered intravenously (100% available), it means that the oral pharmaceutical form is ***Bioequivalent*** with respect to the intravenous pharmaceutical form. These bioequivalent assays are made *in vivo* analysing the concentration of the drug in blood plasma for both, the intravenous and the orally administered medicaments, but some *in vitro* or *in silico* models have been proposed for the determination of the permeability and the bioavailability of the drug, and their results compared to those obtained for the same drug *in vivo*[4, 37–41].

The two parameters that most affect the bioavailability of the oral medicament, solubility and permeability, are used to classify the drugs or drug-candidates in the so-called **Biopharmaceutics Classification System (*BCS*)** that is a system in which the compounds are grouped in four classes[1, 42, 43]:

Class One: Drugs that have good permeability and good solubility, and therefore high bioavailability. In this case, it is no needed to demonstrate *in vitro – in vivo* correlation for the bioavailability, and the bioequivalence is close to 100%.

Class two: Compounds whose permeability is good and the solubility is poor, consequently the bioavailability is driven by the solubility (or Dissolution Rate) and its vehicles should be formulated to improve solubility. Studies of bioavailability *in vivo – in vitro* are needed to demonstrate the bioequivalence.

Class three: Substances showing sparing permeability but good solubility, the bioavailability (absorption, distribution) is not driven by solubility, and the vehicles for these cases should improve the permeability (absorption). Alternatively, the administration way could be parenteral instead of oral. A correlation of bioavailability *in vivo – in vitro* is not expected and studies of bioequivalence could not match, and thus *in vivo* studies are indispensable.

Finally, the fourth group is reserved for molecules that are poorly soluble and also have sparing permeability through the membranes. In these cases, oral administration is possible only if the vehicle improves considerably the solubility and permeability of the drug. Otherwise it would be better to formulate in vehicles for parenteral administration.

In recent years, this BCS system have been updated to a subdivision of the class II: a) *IIa* are molecules in which the bioavailability depends on the solubility and not on the dissolution rate and, b) *IIb* groups molecules that its bioavailability

depends on the dissolution rate more than the solubility. The particle size plays then a key role in the formulation.

The system now has been called ***Developability Classification System (DCS)*** (see Figure 10), which is a way to try to place the candidates to drug, in a point where the researchers can decide early if it is worth or not to continue the development of a drug with that new compound, then, manage resources in a better way[44].

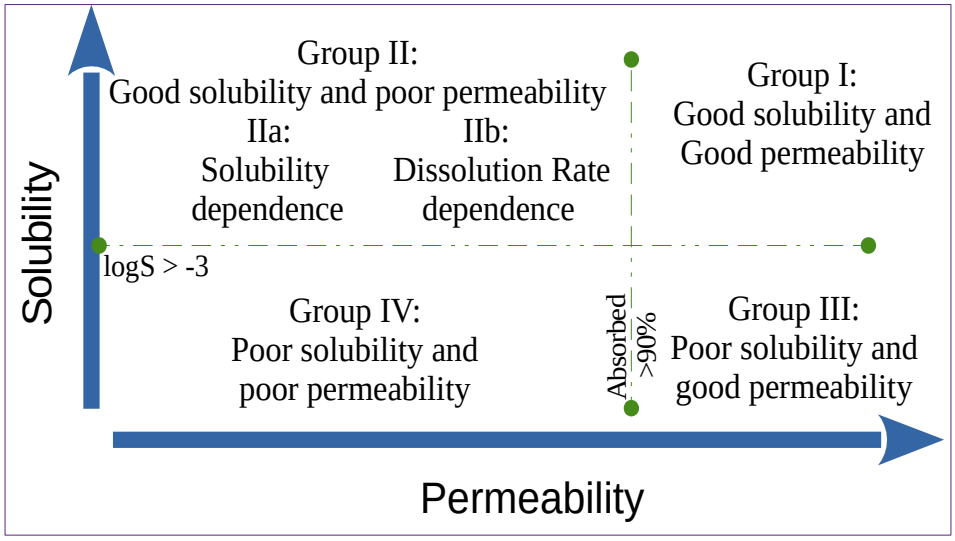

Fig 10: Developability Classification System.

The DCS updates the previous BCS improving some of its limitations, one of them concerning to the solubility. Regarding to BCS definition, the solubility for acidic compounds with pK_a lower than 5 corresponds to its solubility at gastric compartment (pH ~ 2), but indeed, these compounds are more solubilized at duodenal instances (pH ~ 6). Other limitation is concerning to the media used *in vitro* studies. The media proposed by BCS have higher buffer capacities than the *in vivo* media, which underestimates the self-buffering capacity of the compounds in the surface of the solid sample not yet dissolved.

This effect translates in a higher DR measured *in vitro* than the occurred *in vivo.* Moreover, in BCS media some bile components (bile salts, cholesterol, phospholipids like lecithin, etc.) are absent, which leads to underestimate values of solubility for lipophilic compounds compared to the solubility observed *in vivo*[45–47].

To control and/or attempt to mimic physiological conditions, some media have been developed, from simple phosphate buffer solutions which are widely used because they can be fixed at a pH value very similar to the physiological blood pH, until complex Biorelevant Dissolution Media (BDM) which are formulated mixtures of surfactants, salts, additives, enzymes and electrolytes in certain proportions to try to simulate gastric or intestinal fluids. In the present work, BDM called FaSSIFv2 and FeSSIF v2 were used.

FeSSIFv2 mimics the composition of the duodenal fluid in a fed state of pH 5.8, and FaSSIFv2 correspond to the fasted state of pH 6.5. The composition of both BDM includes lecithin and sodium taurocholate (surfactants), sodium oleate, sodium maleate (buffering species) and sodium chloride (ionic strength), in the respective proportions depending of the medium type.

These BDM are of paramount importance in physicochemical profiling of drug-candidates, because they not only allow to simulate physiological conditions, but let to understand the behaviour of the drugs under those conditions and how they interact with the medium. In this way, it is possible to obtain a better picture of the physicochemical fingerprint of the compound and how it can be affected during the preformulation, formulation and development of the pharmaceutical product[45, 48].

The excipients are all the needed substances to be combined with the API to

produce the final chosen pharmaceutical form under its formulation, and they are responsible for the physical properties of that given pharmaceutical form. A main function of the excipients, specially in solid forms, is the improvement of solubility and dissolution rate by disintegration and deaggregation. However, some other interactions in solution between excipients and active ingredients could be also possible. In this sense, BDM can play a relevant role improving the dissolution of drugs. Actually, BDM and excipients could be synergic components in the enhancement of the solubility and dissolution rate of the active compounds.

The process of prefomulation and formulation of a pharmaceutical form, requires the previous determination of several physicochemical parameters for the API, since they are affecting relevant properties for drug development (Figure 11).

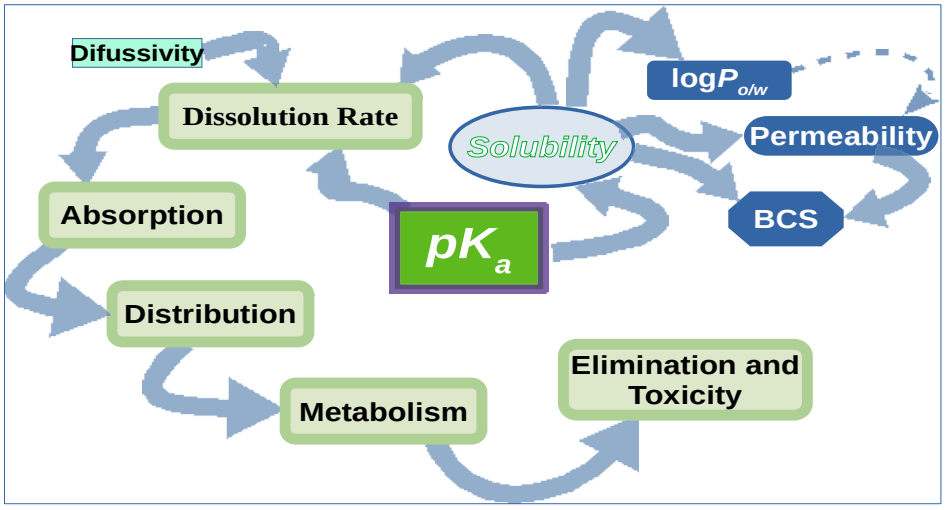

Fig 11: Relationship between physicochemical parameters of molecules and relevant properties for drug development interest.

1.5 Pharmaceutical forms and Excipients

1.5.1 Pharmaceutical forms

A pharmaceutical form is the physical manifestation of a product that contains the active ingredient(s) and/or inactive ingredient(s) (for example in placebo) that are intended to be delivered to the patient. Pharmaceutical forms are expected to provide stability and longest lifetime to the API, to be the vehicle for the API to safely enter to the organism, and to release the API at the appropriate time (immediate release to improve bioavailability, or retarded when necessary). Any pharmaceutical preparation has properties such as hardness (for tablets), viscosity (in liquid cases) or friability (in case of powders or tablets), defined boiling or melting point, or any other relevant property, depending on the type of pharmaceutical form.

There are many types of pharmaceutical forms but, based on its physical properties, they can be classified as: Solids, liquids (including suspensions and nanosuspensions), semisolids, aerosols, etc, and each one is developed to match perfectly with the requirements of the API and the administration way[49].

In this research, powders and tablets were chosen because they correspond to the most commonly used pharmaceutical forms around the world, as long as they are easy to take or administrate to the patient, relatively simple and of low cost production, and the raw materials are also simple of manage and produce.

1.5.1.1 Solid pharmaceutical forms: some definitions and classification

A solid pharmaceutical form is characterised by its hardeness, low friability (losses of weight by friction with production line machinery or conditioning material), defined size and geometrical form, among others. They can be

classified as tablets, capsules (powder for capsules), powders for suspensions, powders for aerosols, and other powders to be used to prepare another pharmaceutical form. These powders are binary or more complex mixtures obtained by grinding API(s) and excipient(s), with the aim of obtaining an homogenous solid product with the smallest possible particle size.

Methods like freeze-drying, colloidal grinding or others, allow to obtain nanosize particle of the powder, which is useful for nanosuspensions, inhalers or some injectable solutions, solving some trouble of solubility, dissolution, stability, precipitation (in suspensions), cohesion or compaction (in inhalers or powders to injectable forms), presents in these types of formulations.

Capsules are of cylindrical form and inside its body there is a powder made with API(s) and excipients, or could contain smaller tablets for different time-release action. The main reason of using the capsules is the protection of the powder or tablets from gastric fluids until they reach duodenum[1, 2, 50].

Tablets or pills

Tablet or pill is the most used pharmaceutical form[51], because it is easy to be administered, provides more stability to the active ingredient avoiding problems of chemical reaction with water or other liquids, it offers many sizes for use from paediatric to geriatric patients, good microbiological stability and ease to transportation. Its conditioning material (for transport, storage, dosage) is more simple than in other forms. Although solid-solid interactions may occur, they take place in the long term. In summary, tablets are more stable preparations and the manufacturing facilities are less complicated than those for other pharmaceutical forms.

There are some types of tablets such as: gastric resistant coated, sublingual fast

release (mucous release), chewable tablets, for controlled release by site and/or by time, effervescent (rapidly dissolve) etc. Each one can have its own size and geometrical form, and are made with different excipients that help to achieve the correct type of tablet.

The methods to fabricate tablets are by direct compression, humid compression, pre-compression and compression (or granulation). In all these cases, there is a machine exerting enough force in the previously prepared powder to compress it, and with help of moulds give it the final form and size to the tablet.

The forces applied to the solid components (API or excipients by separated) during the grinding process can alter its crystallinity, likewise the compression forces on the mixed powder (prepared from these milled components), as even the time of lying, temperature or humidity can alter the lattice structure of the single component[52–55].

Sometimes, interactions between the powders for tablets can be of such as impact on formulation, that some methods have been developed to try to classify these powders to anticipate its utility for tableting. Sun, Ch.[56] propose a methodology to try to predict if a binary mixture powder can be compacted and in what degree, which can be useful to avoid problems of changes of the properties of the components during the tableting process.

1.5.1.2 Excipients

As mentioned above, there is at least one excipient together with the API. For each type of pharmaceutical form, there is a certain group of excipients that intend a specific function in determined formulation. Thus, an excipient can be defined as the component of the pharmaceutical form that is different from the active ingredient and helps it to be stable in time, gives it a convenient

pharmaceutical form to safely administrate the API, it must be not reactive (be inert) with the API and must be innocuous, this is, must not cause any toxicological or allergenic reaction on patients[21].

Other characteristics of any excipient are: must have no bacterial charge, accomplishes pharmaceutical requirements under many manufacturing standards, should be inexpensive, commercially available and its production must assure reproducibility and purity, to secure its quality. All these characteristics can be measured under many parameters, which are found in standardized guides like USP, Phar. Eur., or similars[57, 58].

Functionality of excipients

The function of the excipient depends on the pharmaceutical form. In liquid forms, it can acts as agent of viscosity increasing the viscosity of the suspension but avoiding precipitation of the solid suspended. In solid pharmaceutical forms, an excipient has many more functions or roles since each excipient affects the physical properties of the powder to be used and the further tablet formed. The amount to be used of each excipient is calculated in percentage, based on the final desired size of the tablet and the final quantity (concentration) of the API that is needed in the tablet based on the dosage.

These functionalities or uses are[22, 59]:

Diluents: Provide a phase where the API will be diluted in a certain proportion, giving the overall necessary mass to obtain an acceptable size of the tablet. Therefore, diluents are specially needed when the API must be used in very small quantities. Examples of this type of excipient are lactose, carboxymethyl cellulose, polyvinylpyrrolidone, sodium laureate, etc. For final formulation they are used in range of 5-75% w/w.

Binders: When the powder is compacted, this type of excipient helps to bind together the granules of the powder, producing a better compaction and obtaining tablets with high hardness. Common binders are: corn starch, hydroxypropylmethyl cellulose or any other modified cellulose. They are used in a concentration below than 25% w/w, since excessive binder in formulation can cause sticky tablets of too much hardness.

Lubricants and glidants: Compounds used to allow a better flow of the powder through the hopper, dies and punches of the tablet-machine, by reducing the friction, also the granules flow better between them. These excipients avoid loosing material during the compressing process. Typical example is talc, solid laureate or stearic salts.

Anti-adherents: Sometimes the powder for tablets tends to stick to the wall of the containers, or to hopper, cavities, punches and dies of the machinery, or sometimes after the compression the tablet can suffer adhesion to the wall of the cavity of the mould, to avoid this, substances like talc are used.

Colourants: Substances that give a desirable colour to the tablet, sometimes are substance that can be also used in food and alimentary industry. Like any other excipient, must be not reactive with the API and must be not allergenic or not cause any toxicological response in patients. These are compounds usually of pharmacopoeial grade and are not used in more than 0.01% w/w of the final formulation.

Edulcorants or sweeteners: The purpose of this excipient is to mask the taste or any disgusting flavour of the other excipients or the API, which are usually substances with acid, metallic, bitter or any other characteristical taste that are not always well accepted or tolerated by the patients. In a typical formulation, an

edulcorant is not used more than 1% w/w. The most used are: sucralose, sucrose, lactose, maltose, sorbitol, and others.

Disintegrants: Used to destroy the tablet when it sinks into fluids in the gastrointestinal tract (GIT), it induces that the surface of the tablet in contact with the liquid disaggregate in small granules. It is maybe the more important type of excipient to use, because the smaller the particle disintegrated, the better the contact area between the solid and fluid. This will cause a major quantity of API dissolved in the absorption place, and better opportunities of the drug to pass through biological barriers like cell membranes, especially in GIT.

Modified polyvinylpyrrolidone like Explotab®, Kollidon®, other Plasdones like S630, various methylcelluloses modified like Klucel®, some cyclodextrins like Captisol® or Cavasol®, etc, are the most used disintegrators in the pharmaceutical industry and, like diluents, can be used up to 75% w/w of the final formulation.

An ideal disintegrant should be of good solubility and high hydration or wettability, poor capacity of gel formation, high compressibility, do not form complex with API and, should not be mixed with many others disintegrants to avoid problems of flow of powder or losing compression[60]. The disintegrants used in this work are described as follow.

Polyvinylpyrrolidone

Chemically this is a pyrrolidone ring joined to a vinyl group, which is the bridge for the next group, *n* numbers of these groups form the polymer. Also, different radicals R can be placed either in ring or vinyl group, this *R* gives the polymer different hydrophilic degree. Those used in this work were Kollidon® PF17 and Plasdone S630. Kollidon is a polyvinylpyrrolidone (Figure 12-A),

whereas Plasdone S630 is a mix between polyvinylpyrrolidone and polyvinylacetate (Figure 12-B). In both cases, *n* gives the grade of polymerization and therefore the different denominations of these compounds.

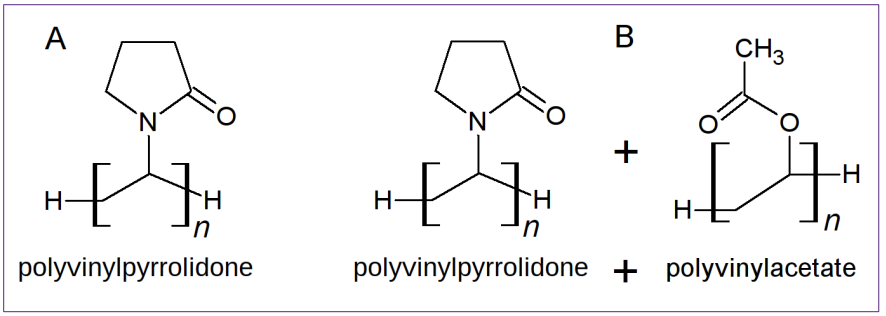

Fig 12: (A) Kollidon and (B) Plasdone S630 chemical structures.

Cyclodextrins

A cyclodextrin is a cyclic structure based in modified glucoside groups, obtained from starch. The size of the cycle depends on the number of the glucoside groups, which are connected usually by etheric bonds given by a hydroxyl from the sugar. Each cyclodextrin (CD) is formed by n number of glucoside groups, where for α-CD $n = 6$, for β-CD $n = 7$ and γ-CD $n = 8$ (see Figure 13). In addition, some other hydroxyl groups can be modified by adding more functional groups *R*, which will modify the CD behaviour in solution. The used

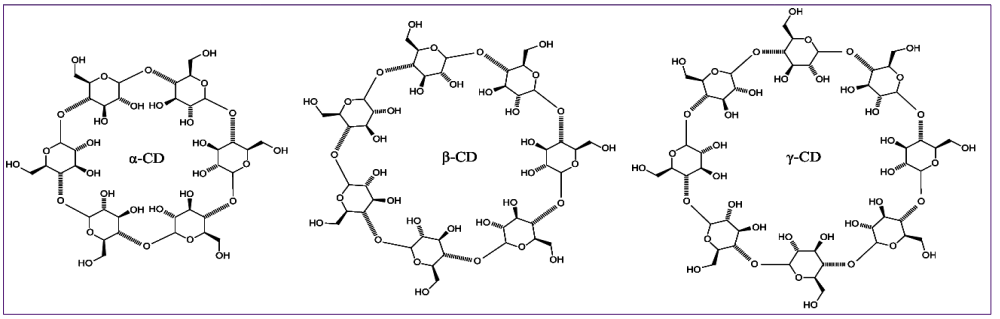

Fig 13: Structures of a, β, γ cyclodextrins (left to right)(image licensed by Creative Commons Attribution-Share Alike 3.0 Unported license, no modifications were made. License on https://commons.wikimedia.org/wiki/File:Cyclodextrin.svg and image is on https://upload.wikimedia.org/wikipedia/commons/5/51/Cyclodextrin.svg)

CD in this work were Captisol® (CAP) and Cavasol®W7M (CAV), which are β-CD type but CAP has sulfonic functional groups and CAV has hydroxypropyl groups.

Figure 14a shows the upper side view of these CD. The side view (Figure 14b) reveals that CD can adopt a toroidal formation (vessel-like form), which creates an internal cavity of high lipophilicity. The size of this cavity depends on the type of CD, where α-CD usually are smaller and γ-CD are bigger, whereas β-CD are intermediate due to *n* polymeric number as pointed before. Due to their cavity size the last ones are the most used in pharmaceutical formulations. The inner cavity can be modulated by modification of the *R* groups. For example, sulfonic groups in CAP are having mutual repulsion which enlarge the entrance of the cavity, whereas in CAV its hydroxyl groups (from its glucoside or hydroxypropyl groups) are more closer each other with less repulsion, making the size of the cavity smaller respect to CAP[60–64].

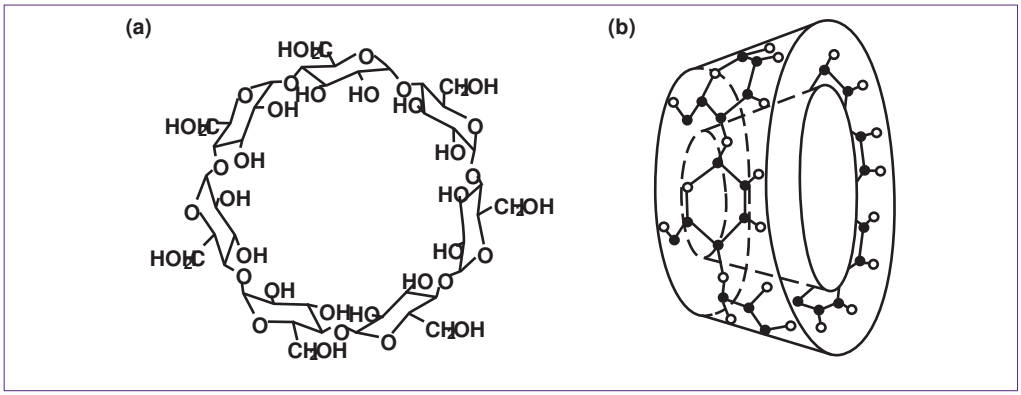

Fig 14: β-cyclodextrin: (a) upper view, (b) side view of its toroidal form. (adapted with permission from S. Jambhekar, P. Breen, DDT (21)2, p 356-362, 2016[64])

Cellulose modified

The cellulose is a natural polymer that shows many hydroxyl groups which can

be bonded to different radicals like a methyl, propyl, hydroxymethyl, hydroxypropyl, or even to a carboxylic group, forming for example, the methylcellulose (MC), or hydroxy-methylcellulose (HMC), hydroxipropyl-methylcellulose (HPMC), hydroxypropylcellulose (HPC), carboxymethylcellulose (CMC), etc. Depending on the size of the polymer some commercial variations are found like Klucel® which is a variation of HPC (Figure 15).

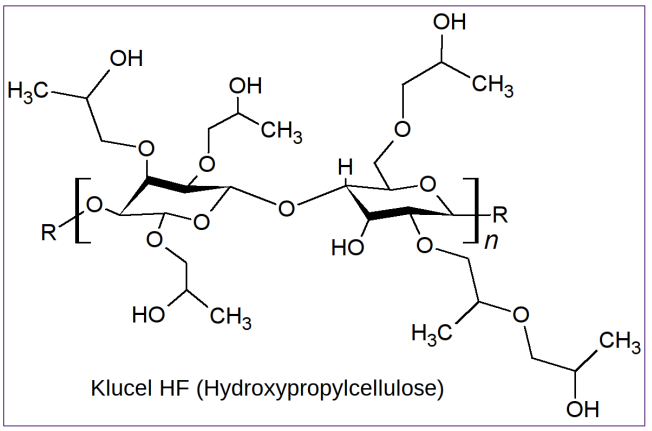

Fig 15: Structure of Klucel, where n will determine the type of Klucel

All the previously mentioned excipients have similar affinity for water, although cellulose-based excipients have a tendency to form gels in low concentrations (<5% w/w).

1.6 Analytical methods to determine physicochemical parameters of drugs

In this section it will be described the methods used to the study of physicochemical properties or parameters of different compounds of medical interest. Those methods are for pK_a determinations, solubility and dissolution rate measurements, including some complementary methods based in different analytical techniques that help in the characterization of solids.

1.6.1 Methods for pK_a determinations

Potentiometric Methods

In pK_a determinations there are some options for applicable methodologies based in potentiometric and spectrophotometric techniques. The first option is a potentiometric one, because this reliable method is based on a primary technique like potentiometry, which measures directly the response of the analyte in the media, using a conventional combination glass electrode.

The method is based in a classic acid-base titration that can be performed in aqueous media or aqueous – organic solvents mixtures (to improve solubility of the sample). The information of the protolytic equilibria of the acid or base used, the amount of sample and the data of the pH response during the titration, are used to calculate the pK_a of the sample.

There are instruments that allow the automatic performance of the titration. In many of them the pK_a is determined by means of Bjerrum function plot, which represents the average number of bound protons per unit of analyte concentration ($\bar{n}$) versus pH. The value of pH in which the 50% of the molecules have the ionisable group protonated corresponds to the pK_a value of the molecule (see Figure 16)[65, 66].

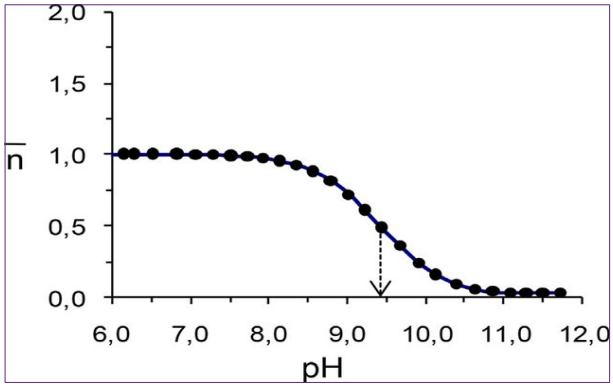

Fig 16: Bjerrum plot for pK_a determination of a sample, the arrow indicates the pH value corresponding to pK_a (with permission from [67]).

Potentiometric method is useful for compounds enough soluble in water, at least up to 10^{-5}M. For sparingly soluble substances, the use of organic co-solvents is also suitable, and the pKa must estimated through the appropriate approach. The time to complete an assay is relatively short, the amount of sample needed

is low and the volumes of titrants and solutions are quite low, making this technique reliable and low-cost.

Spectrophotometric Methods

When the substances have very low solubility, ***a Spectrophotometric Method*** can be a better option than potentiometry, because the spectrophotometrical signal can be acquired at lower concentrations of analyte. The method also allows the determination of extreme pK_a values (close to 2 or 11). Nevertheless, for applying this method the substance must have a chromophore group near to the ionisable group and the spectra of the different species must be different enough. Experimentally the method is based on the measurement of the absorbance at different pH values near to the pK_a value. The absorbance can be measured at one specific wavelength, but there are computer programs that let to treat with multiwavelength spectrophotometric data, making the measurement of pK_a more reliable[66].

The method can be easily automatized through a spectroscopic titration where the sample solution is titrated with a standardized strong acid or base. At a defined stage of the titration, the pH is measured and the absorbance at a specific λ – or complete spectra – is acquired. Some instruments have together an immersion probe coupled with a Deuterium lamp for emission in UV/Visible spectrophotometric range and a combination glass electrode, allowing the pH measurement at the same time that the spectral data is collected. The spectrophotometric data collected in function of pH, combined with Target Analysis Factor, allow to calculate the pK_a values of the sample. The advantage of this method with respect to the potentiometric is the low-demand of sample, where its needed quantity is not above of 1 or 2 mg, and thus it allows to work with substances of sparingly aqueous solubility[19, 67, 68].

1.6.2 Methods for Solubility determinations

Potentiometric CheqSol® Method

The CheqSol® method, based on a Chasing Equilibrium approach, is a potentiometric performing developed by Sirius Ltd.[69] which allows the Intrinsic Solubility determination. The method begins with the titration of an ionisable compound until precipitation appears. At the beginning of the titration the compound must be completely dissolved, this is, if the sample is an acid, titration starts at pH higher than its pK_a. Then a strong acid is added until the free acid (neutral species) precipitates. The detection of the precipitation is achieved by an optic fiber immersion probe. Thus, the probe is used as turbidimetric sampler.

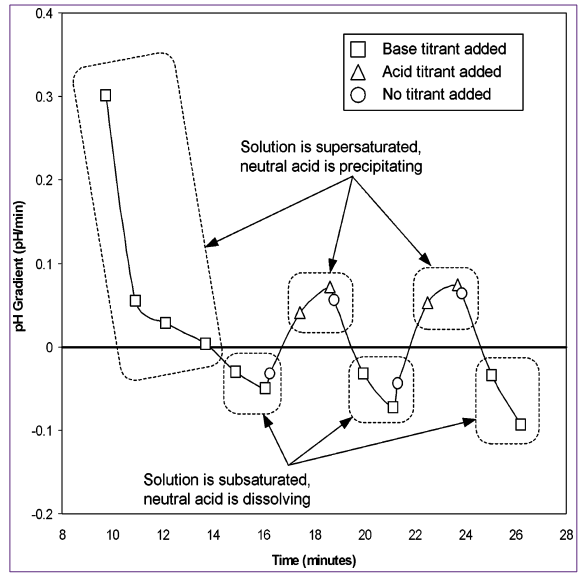

Fig 17: Example of Cheqsol titration where the pH-precipitation changing cycles are shown (with permission from [70]).

When the first precipitation is detected, small volumes of the strong acid titrant are still added to ensure the presence of sufficient precipitate whereas the pH is continuously measured. The addition of titrant is stopped when the pH starts to increase smoothly due to losing of H^+ in the medium, which means that the sample is trying to reach the equilibrium by formation of precipitate that is the neutral form of the acid.

Once the pH gets a constant change in time, the next step consists on the addition of small volumes of strong base titrant to dissolve a minimum quantity

of the formed precipitate. When this happens, the pH spontaneously decrease because the dissolved free acid in equilibrium with its conjugate base, is releasing H^+ to the medium. Then, an aliquot of acid titrant is added to promote the precipitation of the acid, which causes a change in the pH variation trend (the precipitation of the neutral form of the acid increases the pH of the solution as previously mentioned). Again the base titrant is added, the cycle is repeated and the system is continuously changing from supersaturated to subsaturated solutions as can be seen in Figure 17.

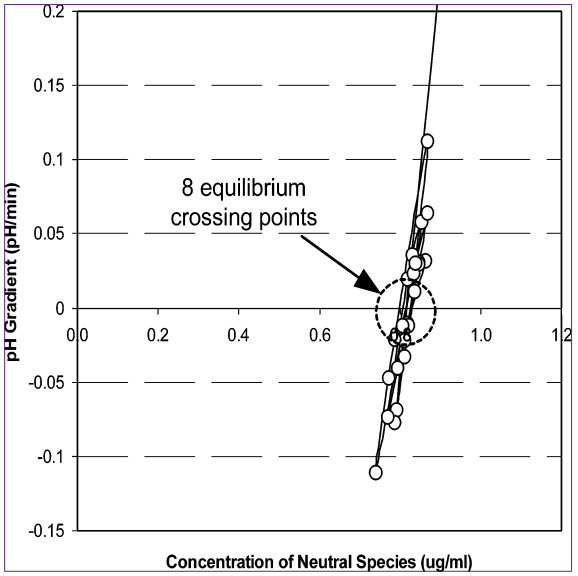

Fig 18: pH gradient of the titration of an acidic sample in front of its calculated neutral species concentration. (with permission from[70])

Applying mass balance principles, the concentration of the neutral species can be calculated at each point of the graph (Figure 18). At the crossing points, where the slope of pH-gradient is zero, the system would be at equilibrium. These points are named **cheqpoints**. Then, the intrinsic solubility of the acid is determined as an average of the concentration of the neutral species at the cheqpoints[35, 69–71].

This method provides information about possible changes in the crystalline configuration of the solid formed during the precipitation process. This is reflected in behaviour changes during the titration steps. Compounds can be classified in three groups according to their general titration behaviour: a) Chasers, b) Non-chasers and c) Special cases.

Molecules with a behaviour as in Figure 19 are known as chasers, as described by Box, K. et al.[72] in 2006. A crystalline chaser form precipitates and follows clearly these cheqpoints, (right-bottom segment in Figure 19, crossing points in Figure 18). Nevertheless, not all chasers show exactly the same behaviour, particularly regarding to the supersaturation. Thus, the supersaturation capability can be also determined in extent and duration (peak in Figure 19), and linked with this is the Kinetic Solubility (S_K) of the samples. High kinetic solubility and supersaturation could affect positively the dissolution, absorption and bioavailability of the drug.

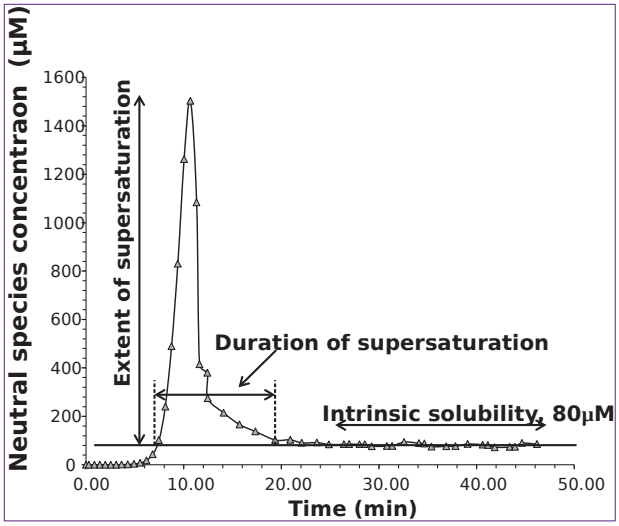

Fig 19: Example of a chaser class compound (with permission from[90]).

On the other hand, a non-chaser compound cannot redissolve again once it precipitates, and therefore no cheqpoints are observed. Finally, the third group consists of molecules that start the precipitation process as chasers and after a while their behaviour change to non-chasers, or vice versa. This change from one behaviour into another is not necessarily reversible. In fact, the stability of the crystal forms is linked to its precipitation behaviour, and the more stable the crystal form, the lower the solubility and therefore more easily it precipitates.

Summarizing, this method allows not only the determination of S0 but also SK and the identification of a compound as a chaser, non-chaser or special behaviour, which in turn is linked to its capacity to supersaturate solutions.

Shake-Flask for Equilibrium phases

Shake-Flask (SF) methodology allows to reach equilibrium phases between solid and aqueous forms of a certain compound. This is performed under controlled stirring or shaking speed, temperature and constant control of pH in the medium.

General consensual conditions for an optimal work with SF methodology are given by Avdeef et al.[73], among them, keeping the solution under stirring or shaking at least by 24 hours, and other 24 hours of resting of the solution. To ensure the equilibrium, the pH of the solution should be controlled during both the stirring and resting periods. After this 48 hours period time, the supernatant is collected and the concentration of the compound of interest in the solution is determined by any analytical technique, such as HPLC or UV/Vis spectrophotometry.

In order to avoid sample lose, centrifugation is recommended to assure the separation of the solid phase from the liquid. In a filtration process the analyte could be adsorbed by the material of the filtering device, or in case that the pores of the filter are bigger than some small particles of the compound, those particles could remain in the liquid phase.

Once the supernatant is obtained and analysed by adequate means, the remaining solid can be characterised with the aim of studying possible changes that might have happened during the SF process. The solid can be dried under suitable conditions, and techniques like X-Ray Diffraction or Differential Scanning Calorimetry (DSC) can help to identify the solid obtained.

1.6.3 Additional analytical techniques used

X-Ray Diffraction.- This technique is based on the capacity that the crystals of a compound have to change the direction of a high energy-light beam, like X-Ray, because of its lattice structure. According to the type of crystal, the crystalline lattice is different and hence the way in which this beam is diffracted is different for each compound, obtaining a characteristic diffraction pattern for each crystalline form.

First the intensity of a X-Ray beam is measured as blank, and then it is measured again with the sample placed between the X-Ray source and a suitable detector. Since the X-Ray beam is diffracted in many different directions, the detector is placed in several angles – respect to the plane of the sample – which changes in a certain range of time. The intensity measured in function of the angle provides a *Diffractogram* that is unique to each sample[74].

Differential Scanning Calorimetry – DSC.- The DSC allows to identify any thermic process that the solid can undergo as a function of temperature or time under a certain temperature. The energy (heat) that a sample needs to change its crystalline form or to melt and change its state, is measured against a reference, which gives a differential of heat flow in function of temperature between the sample and the reference, plotting the differential heat flow allows to obtain a *Thermogram*. This tool allows to identify, among other characteristics, differences between polymorphs of the same compound, because each crystal form of the same sample suffer thermal processes on its own way.

2 OBJECTIVES

The drug development implicates many tasks in order to obtain a product of proved effectiveness, secureness and ease of administration. The initial steps in the drug development require a detailed study of the characteristics of the Active Pharmaceutical Ingredient (API). In this field, the physicochemical properties of the compound candidate to drug are a key base for the understanding of its behaviour under the conditions given by the different *in vitro* and *in vivo* assays. The results obtained during these assays are of paramount importance for the success of a drug candidate to become a marketable active pharmaceutical ingredient. The obtention of reliable results are ensured only if the previous physicochemical parameters are correctly measured. The pK_a, Solubility and Dissolution Rate are some of the most important physicochemical parameters that must be measured with high precision and accuracy. Consequently, the factors that directly affect these parameters, like pH, presence of enhancers (excipients) and nature of dissolution media, should be extensively studied in order to determine their effects.

The scope of this work is emphasised in the determination of the effect that the dissolution media and the excipients exert on the Solubility and Dissolution Rate of different APIs, especially of acidic compounds.

Three acidic molecules with different physicochemical properties, i.e. benzthiazide, isoxicam and piroxicam, will be chosen in this study. Their diverse pK_a values will lead to different ionisation degrees along the pH range corresponding to the gastrointestinal tract (GIT). The selection of these compounds should allow studying the following aspects:

- The ionisation effect on Solubility and Dissolution Rate of these APIs through the GIT. The study will be carried out at three pH values that are representative of different parts and/or conditions of the GIT: pH 2.0

accounts for the pH in the stomach, and pH 5.8 and 6.5 mimic the pH conditions in the small intestine in fed and fasted states, respectively.

- The effect of the addition of excipients on the Solubility and Dissolution Rate of the APIs. Two cyclodextrins (Captisol W7 and Cavasol) and three polymeric excipients (Klucel HF, Kollidon 17PF and Plasdone S630) will be tested at pH 2.0, 5.8 and 6.5, and at different percentages excipient:API. This will allow to study not only the enhancement effect of the excipients on the dissolution of the API, but also their effectiveness depending on the ionisation degree of the drug.
- The Solubility and Dissolution Rate in two Biorelevant Dissolution Media mimicking the small intestine fluid in fed and fasted states (FeSSIF and FaSSIF). The results for the APIs and their mixtures with the excipients will be compared with those obtained in aqueous medium.

Since the dissolution of compounds with acid-base properties depends on the ionisation degree, an accurate and reliable determination of the pK_a values of the studied APIs will be needed. In addition, the techniques and methodology used for Solubility measurements are not always applied in an adequate performance, or their capabilities are not fully described. Then, before addressing the main scope of this work, a previous study will be conducted on the accurate determination of Solubility by the shake-flask and the potentiometric CheqSol methods, exploring the complementarity of these two approaches. For this study, three drugs with different acid-base behaviour will be selected, which are expected to show distinctive solubility-pH profiles: glimepiride as an acid, pioglitazone as an ampholyte, and sibutramine as a base. Additionally, the influence of the nature of the starting solid (free species or salt) in solubility measurements will also be studied.

3 EXPERIMENTAL SECTION

This section describes the different samples, solutions, reagents and instruments to be used during the experimental work. Procedures are also described and any particularity about the methodology is emphasised when needed.

3.1 Molecules, reagents and consumables.

The drugs glimepiride (Glm), pioglitazone (Pio), sibutramine (Sib) and the hydrochloride salts of Pio and Sib were provided by "Unitat de Calorimetria" from *CciT-UB*, with >99% of purity. Benzthiazide (Bzt), isoxicam (Iso) and piroxicam (Pir) were obtained from Sigma-Aldrich Chemie GmbH (Steinheim, Germany) with no less than 99% of purity.

Regarding the excipients used, Captisol (CAP) (Sequoia Research Products, Pangbourne, United Kingdom), Cavasol (CAV) (Wacker Chemie AG, München, Germany), Klucel (KLU) (Ashland, Columbus, USA), Kollidon (KOL) (BASF SE, Ludwigshafen, Germany) and Plasdone S630 (S630) (ISP International Specialty Products, Köln, Germany), all of them were products of pharmaceutical grade.

Solutions of KOH and HCl 0.5M were used as titrants in the spectrophotometric and potentiometric-CheqSol methods. They were prepared from standardized Titrisol® solutions from Merck KGaA (Darmstadt, Germany).

The FaSSIFv2 and FeSSIFv2 are preformulated powder mixtures which both contents bile salts and lecithin but differing in their concentration. These were purchased from Biorelevant (London, United Kingdom).

Chromatography grade methanol (MeOH) used as cosolvent and organic modifier was from Chem-Lab NV (Zendelgem, Belgium), while

dimethylsulfoxide (DMSO) of 99% of purity was used as solvent and it was from Merck KgaA (Darmstadt, Germany).

Buffers and other solutions for spectrophotometric measurements are consisting of:

- The Ionic Strength Adjustment buffer or ISA water is prepared dissolving 11.184g of KCl in 1L of purified water (low total organic carbon <3ppm, with a resistivity equal or better than 18.2MΩ·cm), resulting in a solution with 0.15M of ionic strength.
- Buffer pH 1.6 (Ac/P): where 1.701g of KH_2PO_4 are weighed together to 1.701g of Sodium Acetate trihydrate and both dissolved in 50mL of purified water, then pH is adjusted with HCl 0.5M and made up to 100mL in a suitable flask. This solution is 0.125M of ionic strength.
- Buffer Potassium Phosphate monobasic (BPP): 0.051g of KH_2PO_4 are weighed and dissolved with ISA water in a 25mL flask. This solution is 0.015M of KH_2PO_4.
- 80% MeOH/KCl solution: 5.592g of KCl are weighed and dissolved with 50mL of purified water and 200mL of MeOH with constant stirring by around 30min up to totally dissolved. This solution is made up to 1 L with a previously prepared solution of 80%w/w of methanol with purified water. This solution is used for pK_a determinations in several %w/w of MeOH/water mixtures.
- Solutions of 10mM in DMSO of the studied compounds to be used for pK_a determinations by spectrophotometrical methodology. These solutions are prepared in volumetric flasks of 1 or 2 mL to avoid waste

of samples.

For shake-flask (SF) solubility determinations some buffers and biorelevant media solutions were used. The preparation for each one is described as follows:

- Buffer Ac/P: previously described in solutions for pK_a determinations.
- Buffer maleic acid/maleate (MM) is prepared using a 1L flask: 3.27g of NaOH are added to 6.39g of maleic acid and 7.33g of NaCl to be dissolved with 900mL of purified water, then pH is adjusted to 5.8 using NaOH or HCl 1M and then made up to 1L with purified water. This buffer solution is also used to prepare FeSSIFv2 solutions.
- A variant of MM is prepared as follows: in around 0.9L of purified water, add 1.39g of NaOH, 2.22g of maleic acid and 4.01g of NaCl. Adjust the pH at 6.5 using same NaOH or HCl 1M and make up to volume (1L) with purified water. This buffer is also used to prepare FaSSIFv2 solutions.
- FaSSIFv2 medium preparation: weigh 1.79g of FaSSIFv2 powder and dissolve it with MM (pH 6.5) until complete dissolution. Make up the volume (1L) using same buffer solution at room temperature.
- FeSSIFv2 medium preparation: weigh 9.76g of FeSSIFv2 powder and dissolve it using 900mL of MM (pH 5.8) until complete dissolution under stirring. Make up the volume up to 1L with same buffer solution at room temperature.
- Solutions of FeSSIFv2 and FeSSIFv2 were used for both SF and Dissolution Rate assays, and both of them are stable only for 48h. These

solutions should be used only at least after one hour of their preparation.

- The consumables needed for SF assays are listed as follows: Pasteur-type glass pipettes, plastic tips for calibrated quantification pipettes, 2mL glass-vials for HPLC, 5mL volume glass test tubes with caps.
- Column 1: a 1.7 μm, 50 × 2.1 mm Waters (Milford, MA, USA) Acquity BEH C18 column, was employed to quantify Glm, Pio and Sib.
- Column 2: a 5 μm 150 × 4.6 mm Gemini C18 and a 4 × 3.0 mm guard cartridge from Phenomenex (Torrance, CA, USA), used for quantification of Bzt, Iso and Pir.
- Combination glass electrode from Sirius Analytical (Forest Raw, UK).

When solid characterization was conducted, the consumables needed were:

- Aluminium pans of high capacity (up to 70mg) with leads, used for DSC and TGA analysis.
- Nitrogen and Helium 5.0 grade as carrier gases for DSC and TGA analysis.
- Low absorption films for PXRD.
- Plastic tubes of 2mL of volume with cap, for solid collection.

3.2 Instrumentation

Due to the variety of the analytical techniques used to measure the different samples, some instruments were needed to perform a characterization and quantification for all of the analytes. These different instruments are described as follows:

- Instruments used for pKa, potentiometric intrinsic solubility and dissolution rate determinations:
    - GlpKa automated titrator from Sirius Analytical Instruments (Forest Raw, UK) equipped with a dip probe optic fibre D-PAS from Hellman Analytics (Mülheim, Germany) with 10mm optic pass and deuterium lamp to cover UV/Vis range, including a combination glass electrode for pH measurement in situ, in a sampler for many positions. Controlled by computer running Refinement Pro 2.2 software for instrument manage and data collection and processing.
    - PCA200 automated titrator from the same company, with siilar features as GlpKa but with the exception that PCA200 have a single position sampler.
- For SF samples treatment:
    - Brand micropipettes model Transferpette® S (Wertheim, Germany), calibrated and for different volumes.
    - Rotatory shakers from P-SELECTA, model MOVIL-ROD (Abrera, Spain), for shaking of the samples.
    - DINKO DC90 (Barcelona, Spain) vacuum pump.
    - A GLP 22 potentiometer from Crison (Alella, Spain) with Sirius Analytical combination glass electrode, calibrated with standard aqueous buffer solutions of pH 4.01 and 7.00 at 25 °C (Hach Lange GmbH, Düsseldorf, Germany), for pH measurement of buffer solutions and samples.

- Rotanta 460RS centrifuge with temperature control (Hettich Lab Technologies, Tuttingen, Germany) fixed at 3500 rpm and 25 °C for separation of phases in the samples.

- For the analysis of the different liquid phases from the SF samples, two liquid chromatographers were used, consisting on:
  - Shimadzu liquid chromatographer (Kyoto, Japan) model Nexera UPLC system, consisting of two LC-30AD pumps, a DGU-20A5 online degasser, a SIL-30AC autosampler, a SPD-M20A diode array detector, a CTO-10ASvp oven at 25 °C, and a CBM-20Alite controller.
  - The second system consisted in a Shimadzu (Kyoto, Japan) liquid chromatograph, composed of two LC-10ADvp pumps, a SIL-10ADvp auto-injector at 25 °C, an SPD-M10Avp diode array detector, a CTO-10ASvp oven at 25 °C and a SCL-10Avp controller.
- For solid characterization, where:
  - The instrument used for PXRD was a PANalytical X'Pert PRO MPD θ/θ diffractometer of 240 millimetres of radius in transmission configuration, using Cu Kα1+2 radiation (λ = 1.5406 Å) with a focusing elliptic mirror and a PIXcel detector.
  - Thermal characterization was made using DSC and TGA instruments: Mettler-Toledo DSC-822e calorimeter (Greifensee, Switzerland) for analysis of Glm, Pio and Sib and their derivatives, and a Perkin Elmer DSC 7 with controller TAC/7DX (San Francisco, USA) including software for instrument control and data

processing Perkin Elrmer DSC Scan 2.0 running in a computer, used for excipient:API solid mixtures. The Mettler-Toledo TGA-851e thermobalance (Switzerland) was used for thermogravimetric analysis.

3.3 Software

Software used for solubility data treatment, to construct solubility – pH profiles was pDisol-X^{TM} (*In-Adme Research*, New York, USA).

RefinementPro v2.2 (Sirius Analytics, East Sussex, United Kingdom) is used to control GlpKa and PCA200, and for data collection, treatment and export.

Liquid chromatography systems are controlled by Shimadzu LC solutions software (Kyoto, Japan).

T3 software (Sirius Analytical, East Sussex, United Kingdom), which is used to data treatment for obtention of dissolution rate profiles.

ACD/Labs/Percepta v10.2 (release 2020.1.2, biuld 3382, 18 June 2020) and ACD/Labs/Chemsketch v2019.1.3 (file version C05E41, build 111302, 27 August 2019) were used for prediction of physicochemical parameters and chemical structure drawing respectively. Both software are provided by Advanced Chemistry Development, Inc. (Ontario, Canada)[75].

R version 3.6.3 (2020-02-29) -- "Holding the Windsock" © 2020 The R Foundation for Statistical Computing. Platform: x86_64-pc-linux-gnu (64-bit), used for chart and plots drawings.

Microsoft Word 10 v14.0.6023.1000 (32 bits) for text processing.

LibreOffice Version: 7.0.3.1, Build ID: 00(Build:1), 64 bits. The Open

Document Foundation © 2000-2020, used for spreadsheet calculations.

3.4 Procedures

3.4.1 Spectrophotometric pK_a determinations

Since the thesis work is focused on Solubility and Dissolution Rate, it is imperative to perform an accurate previous measurement of the pK_a of the samples, provided that these values are needed for solubility and dissolution calculations. The studied compounds have as common characteristic that they are poorly soluble in aqueous media, and this is why the spectrophotometric methodology was selected instead of a potentiometric pK_a determination. This spectrophotometric method allows to work with low concentration solutions in order of 10^{-5} to 10^{-6}M, with good sensitivity and low sample consumption.

From 10mM stock solutions in DMSO, between 50 to 100µL of sample are placed in a vial with 250µL of BPP. Then ISA water is added up to complete 10mL in the vial. The assays can be started using KOH or HCl as titrants for acids or bases, respectively, under thermal control at 25°C. The assays for pK_a determinations were started at basic pH for acids and acidic pH for bases, adjusting this initial pH with the same titrant solutions. This is to ensure the complete dissolution of the samples in its ionic species.

The instrument used was the previously described Sirius GlpKa. Its deuterium lamp allows to cover a significant part of the ultraviolet and visible region of the spectrum, which allows an accurate measurement of the absorbance and thus the quantification of neutral and charged species of the sample, at any particular pH value, obtaining a very complete spectral information of the sample.

The range of pH for these titrations is usually setted from pH 11 to 2 or vice versa, depending on the acidic or basic nature of the sample. Each pH point is measured by the electrode and to obtain the titration curves the instrument is programmed to add titrants even in μL steps if needed, and with a maximum $0.005\,\Delta\,\mathrm{pH}\cdot\mathrm{min}^{-1}$ units for stabilization until next titrant addition. At each pH step the spectrum is collected, and with the spectral data from all pH points a Target Factor Analysis (TFA) is performed to calculate the pK_a values for the sample. The data obtained can be exported in a suitable format for further use, as well as the graphics.

In case of the pK_a determination for Glm, solutions of 80%w/w MeOH/KCl conveniently diluted with ISA water were used. The instrument doses the programmed volume of these solutions to reach mixtures settled from 15 to 50% of MeOH. A titration is performed at each percentage of MeOH, then a Yasuda-Shedlovsky extrapolation is performed to obtain the aqueous pK_a[71, 76].

3.4.2 Shake-Flask determinations.

The solubility of Glm, Pio and Sib and their respective hydrochloride salts was determined without any excipient added. Powders of Bzt, Iso, Pir and their mixtures with excipients were used without any previous treatment except the grinding needed to get a homogeneous solid mixture. These mixtures used for either solubility or dissolution rate assays, were prepared at ratios 3:1, 1:1 and 1:3 of Excipient:API, respectively.

The protocol recommended in in Avdeef et al.[73] was applied. Samples were precisely weighed in vials of 5mL of capacity. The amount needed depends on the sample and must be enough to ensure presence of precipitate. Then, 3mL of the respective aqueous or biorelevant media were placed and the vials were

closed. The shaking process using rotatory shakers was carried for 24h. After 4h of shaking started, pH was measured and adjusted if needed. To correct the pH to a nearest initial value, solutions of HCl or NaOH 1M were used as recommended The samples were after leaved to rest for a further 24h period. At the end of this second period the pH was measured prior to the centrifugation. During shaking and resting periods, the samples were kept at 25±1 °C.

The centrifugation process was performed also at 25 °C during 30min at 3500 rpm. After centrifugation the supernatant was collected using glass pasteur-pipettes, to fill suitable glass HPLC-vials and avoiding solid collection. By its side, remanent solids were dried by vacuum filtration for about 30min, using glass-fibre funnels and 25mL glass flasks, coupled to a vacuum pump. Dried solids were collected in 2.0mL plastic tubes for further analysis.

Liquid phases from Glm, Pio and Sib were injected in the Nexera UPLC system, whereas the collected supernatant from Bzt, Iso and Pir were injected in the other Shimadzu liquid chromatograph, both early described. The experimental conditions were as follow:

Waters Acquity BEH C18 column was employed to analyse Glm, Pio and Sib. In addition, the Gemini Column was used for analysis of Bzt, Iso and Pir.

Mobile phases: for Glm, Pio and Sib was a phosphoric acid solution at pH 3 mixed with methanol as organic modifier, at a flow rate of 0.5mL·min^{-1} and injection volume of 0.2µL. Another mobile phase formed by aqueous solution of ammonium hydrogen carbonate 0.1M pH 8.0 and methanol as organic modifier was used for Bzt, Iso and Pir analysis. Specifically MeOH was used at 50% v/v for Bzt analysis and at 45% v/v for Iso and Pir. The applied flow rate was 1.0mL·min^{-1} and injection volumes were set to 10µL.

Detection: Wavelengths used were 319, 349 and 355nm for Bzt, Iso and Pir respectively. In case of Glm, Pio and Sib, the used wavelength was 254nm.

The data obtained after HPLC quantification of supernatants was processed using pDisol-X^{TM} software for solubility profiles charts drawing and to calculate the solubility and aggregation parameters. Using the introduced experimental information and calculating a theoretical titration curve from a known value of concentration of HCl (or any other strong acid) as acid titrant, the software calculates the concentration of all possible species of the sample until pH ~0, followed by counter-titration with strong base (for example NaOH or KOH of known concentration) until pH ~13, calculating the concentration of the species (ionic, neutral, etc.) of the sample on each programmed pH point, to estimate the exact solubility on each possible point.

Once each calculated value per pH point is found, a nonlinear-least squares analysis is performed to found the minimum value of difference between the calculated values and the experimental data. When the minimum is reached, it is because the model fits in the better possible way to the experimental data, obtaining information from the molecules about their intrinsic and apparent solubilities, aggregates formation, product solubility constants, etc., and therefore the solubility – pH profiles.

3.4.3 CheqSol Determinations

This potentiometric method required pure samples weighed in a range from 3 to 30 mg depending on the solubility of the compounds. Samples are placed in glass vials of 25mL, then 10mL of ISA water of 0.150 M of ionic strength are added. The instrument used was a Sirius PCA200, which is programmed to start at basic pH when sample is an acid or at acidic pH when sample is a base, due

to the same reasons as exposed in pK_a determinations. In this case, the D-PAS is used as turbidimeter to detect the formation of precipitate, meanwhile the electrode measures the pH during the titration[77].

For example, for an acidic compound the initial pH fixed is usually 11.0, and the titrator adds enough strong base to reach that value. If sample is not completely dissolved, an external agitation with ultrasound-bath for a few minutes can be used to complete the dissolution of the sample. Then, titrator adds strong acid in controlled steps until precipitate is formed, which is detected by turbidimetry. At this point the solution has changed from supersaturated to subsaturated state. The instrument now adds few microlitres of base to redissolve just a few part of the precipitate formed. This re-dissolution can be detected because the pH decreases slightly but steadily due to the protons releasing, when it gets stable – linear relationship between slope ($\Delta pH/\Delta t$) vs time is reached – the instrument adds acid again and precipitate is formed again, which can be detected because the pH now rises slightly but sustainedly due to the protons from solution are captured to form the neutral solid. The slope vs time is linear again – but of opposite sign respect to the previous slope – and the process is repeated. There must be a point where the precipitate and redissolved sample should be in equilibrium, this moment is where the pH does not change in the time $\Delta pH/\Delta t=0$, at this point the concentration of neutral species found corresponds to the intrinsic solubility (S_0).

These steps of changing the direction of pH between the precipitation (subsaturation state) and redissolution (supersaturation state), are called crossing-points. These potentiometric solubility determinations are performed with at least 8 of these crossing points, the assays in this work were performed with 12 to 30 crossing-points.

Software RefinementPro v2.2 provided with the instrument was used to titrator control, data acquisition, calculations and some charts drawing. Solubility calculations with this software can be done using crossing-points (described above process) or by curve fitting approaches. This second one is more applicable when experimental points full-fit the theoretical precipitation curve (non-chasers). Moreover, data can be exported for further treatment with any other suitable software needed.

3.5 Dissolution Rate determinations

For dissolution rate assays, APIs or their solid mixtures were weighed directly. To prepare the solid mixtures a grinding process was needed to obtain homogeneous mixtures, using mortar and pistil until particle size and colour were visually clear and homogeneous.

About 10mg of API or the corresponding amount of powder of the solid mixtures are weighed directly inside the miniaturized discs kits, to form the tablets which are 3mm of diameter after compression, to ensure constant surface during the assays. The compression is made applying 918N (100kg-force), using a manual press machine, to fabricate pills with high enough resistance avoiding to destroy them only by stirring forces[32]. The discs with the coupled tablets are placed into the 25mL vial, to this, 1.5mL of buffer Ac/P are added and instrument fills the vial with 13.5mL of ISA water (0.150 M ionic strength). The assay starts when pH is stabilised at the fixed value, then the dip probe collect spectral data every 30 seconds and keeps collecting data until the end of the assay. The collected data at each point is used to calculate the concentrations of neutral and charged species of the samples by application of Lambert-Beer law using the previously determined molar absorptivity

coefficients. Constructed charts with this concentration in $\mu g \cdot mL^{-1}$ (or another suitable units) as a function of time are the Dissolution Profiles for each sample, which are fitted to a first order kinetic model, that allow to calculate the Dissolution Rate (DR) of the samples.

A group of samples were measured during 120min at fixed pH values, i.e. 2.0, 5.8 or 6.5; while other group were measured at two pH sectors values, i.e. 2.0 – 5.8 and 2.0 – 6.5, by 30min in first sector and 120min at the second pH stage. The value of pH and time selected in each sector for the different arrangements, are according to the needed conditions to simulate drug circulation through gastrointestinal tract. For single pH sector studies, mixtures API:Excipients are prepared at ratio 1:1, whereas for two pH sectors assays, samples are prepared at ratios 3:1, 1:1 and 1:3 of API:Excipient respectively.

3.6 Powder X-Ray Diffractometry

The analysis and characterization of all the solids collected under SF assays, were conducted under PXRD, using external Scientific and Technological Centre (*CCiT-UB)* services from University of Barcelona. A PANAlytical XRD was setted at maximum active length of 3.347° for the detector, with a convergent beam with a focalizing mirror and a transmission geometry with flat sample sandwiched between low absorbing films, measuring from 1 to 40° in 2θ, with a step size of 0.026° and a measuring times of 75 or 300 seconds per step.

3.7 Thermal characterization

For solid analysis from Glm, Pio and Sib samples and its derivatives, DSC was carried out using Mettler-Toledo instruments (before described). Experimental

conditions consisted in the use of aluminium pans of 40µL volume, atmosphere of dry nitrogen at 50mL·min^{-1} flow rate, and heating rate of 10°C·min^{-1}. The calorimeters were calibrated with indium of 99.99% purity.

Besides, DSC was also used to characterize solid mixtures API:Excipients (ratio 1:1), to explore if there was any solid-solid interactions between drugs and excipients. The conditions applied were 5min steady temperature at 25°C, then heating ramp from 35 to 285°C, at 5°C·min^{-1} of heating rate, using N_2 as carrier gas at flow rate of 25 mL·min^{-1}.

Moreover, TGA was performed on an also Mettler-Toledo system (TGA-851e thermobalance early listed in section 3.2). The experimental conditions were: alumina crucibles of 70µL volume, atmosphere of dry nitrogen at 50mL·min^{-1} flow rate, and heating rate of 10°C·min^{-1}. This technique was applied to characterise the solids formed during SF assays.

4 RESULTS AND DISCUSSION

4.1 Chemical nature of the studied molecules

Five Active Pharmaceutical Ingredients (APIs) were studied: benzthiazide (Bzt), glimepiride (Glm), isoxicam (Iso), pioglitazone (Pio), piroxicam (Pir) and sibutramine (Sib). The hydrochloride salts of Pio and Sib were also used.

Their pharmacological action is very varied, Bzt is a diuretic compound, indicated to the treatment of arterial hypertension, Glm and Pio are anti-diabetic agents that help in transport of glucose, Iso and Pir are non-steroidal anti-inflammatory molecules and Sib was used as anti-obesity (anorexygenic) drug until 2010, when it was withdrawn from the market because of cardiac side effects[79].

Chemically, Bzt is a derivative from thiazides, Glm is a sulfonylurea-based drug, Pio comes from thiazolidinediones, Iso and Pir are modified molecules from group of oxicams, and Sib is a derivation from chlorophenyl-cyclobutyl amine[78]. Their chemical structures are shown in Figure 20.

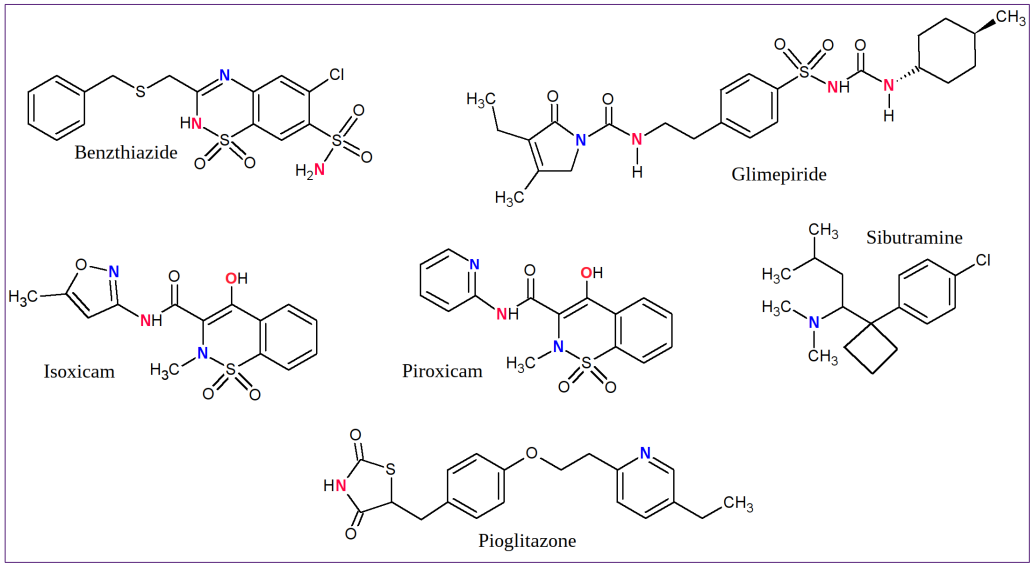

Fig 20: Chemical structures of the studied molecules. Atoms in red and blue are acidic or basic-expected behaviour, respectively.

Table 3: Some calculated molecular properties for studied compounds.

Compound	Molecular weight (g/mol)[b]	Melting point (°C)	H donors	H acceptors	Freely rotatable bonds	Polar Surface Area (PSA) ($Å^2$)	Polarizability (Pol) ($x10^{-24}$ cm^3)‡	Molar volume V_M (cm^3)‡
Benzthiazide	431.94	231-232[a] 238-239[b] 210-211[c]	2+	7+	5+	161+	41.21	259.0 ± 7.0
Glimepiride	490.62	207[b]	3*	9*	6*	133†	51.30	378.8 ± 5.0
Isoxicam	335.34	265-271[b]	2+	7+	2+	121+	31.83	211.0 ± 3.0
Pioglitazone	356.44	183-184[b]	1*	5*	7*	93.6†	38.93	282.7 ± 3.0
Piroxicam	331.35	198-200[b]	2+	6+	2+	108+	32.97	211.9 ± 3.0
Sibutramine	279.85	191-192[b]	0*	1*	5*	3.2†	33.20	271.3 ± 3.0

a reported in [82], **b** Merck Safety-Data Sheets (https://www.merck.com), **c** reported in [79], ‡ ACD/ChemSketch [80]. †ACD/Labs Software v11.02 embedded in SciFinder [75]. + Computed by Cactvs 3.4.6.11 (PubChem release 2019.06.18 in https://pubchem.ncbi.nlm.nih.gov, accessed in April 11 of 2020 [81].

In Table 3 are shown some calculated molecular properties for the studied compounds like melting point, molecular weight, number of H donors/acceptors, freely rotatable bonds, Polar Surface Area (PSA) and Polarizability (Pol). PSA is the molecular surface associated with heteroatoms (mainly nitrogen and oxygen) and polar hydrogen atoms[83]. PSA is a popular descriptor for aqueous solubility and membrane permeability, used for example in oral absorption. Solvation of polar groups increases solubility, and their desolvation is needed when drug molecules diffuse from an aqueous extracellular environment into lipophilic membranes. As a general rule for drugs showing only passive diffusion, molecules with PSA > 140 $Å^2$ are poorly absorbed[84]. The Polarizability of a molecule characterizes the ability of the electronic system to be distorted by an external electric field. An electric field can be generated, for instance, due to the proximity of a charged species. Polarizability is determined by the strength of the attractive interaction between electrons and atomic nuclei, and thus larger polarizabilities are expected for molecules with large number of electrons and diffuse electron distribution. This molecular property seems to have a strong impact on chemical–biological interactions, particularly in the binding of drugs with body fluids or cells and their passage through biological membranes[85]. Polarizability is expected to favour solubility, due to interactions with polar water molecules, and hinder to some extent the gastrointestinal absorption.

All of the substances presented in Table 3 have at least one ionisable functional group with acidic or basic properties, depending on its capability of releasing protons or donating electrons, respectively. The acid strength depends on the polarity of the bond to which the acidic hydrogen atom is attached. The hydrogen atom should have a positive partial charge and the heteroatom

(typically oxygen or nitrogen) a negative one. The more polarized the bond, the more easily the proton is removed and the greater the acid strength. The polarity of the bond not only depends on the particular heteroatom bonded to the hydrogen atom, but also on the surrounding atoms bonded to the heteroatom, that could stabilise the electrons of the ionisable functional group due to, for instance, the electronic cloud created by the aromaticity of the rings and the π bonds close to the ionisable functional groups. Besides, rotatable bonds can also have a certain influence in the electronic cloud of the molecule.

As an example, Figure 21 (left panel) shows the map of electrostatic potential of Bzt. There are two acidic hydrogen atoms (indicated with arrows) with a low electronic density giving a partial positive charge, bonded to the nitrogen atoms of sulfonamide groups with higher electron densities and partial negative

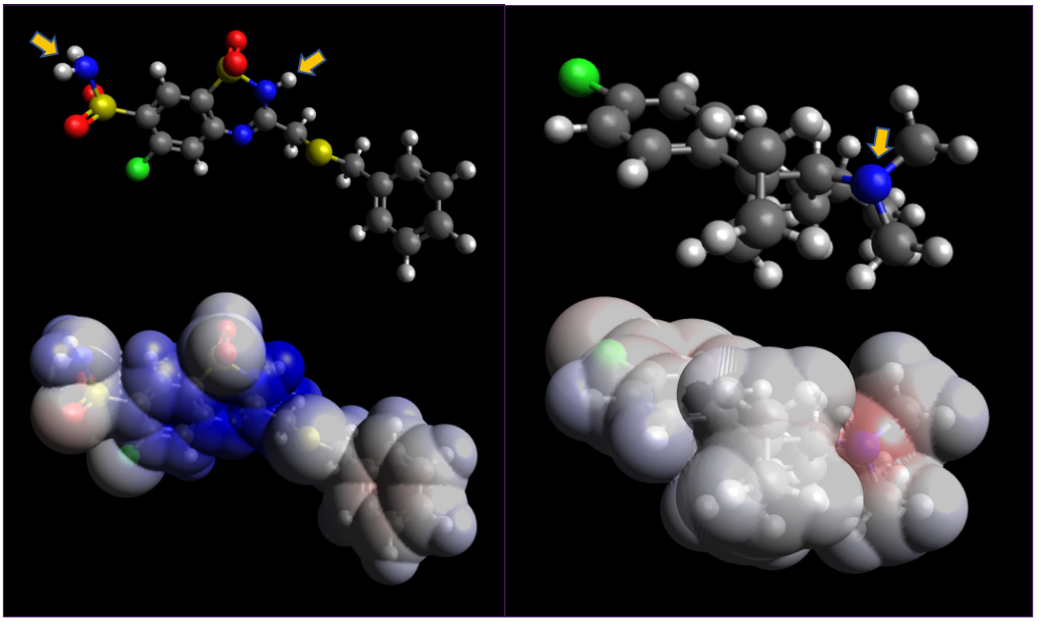

Fig 21: Calculated electrostatic-potential map of Benzthiazide (left panel) and Sibutramine (right panel). 3D structure computed by Chem3D (Perkin Elmer), version 20.0.0.41, using a MM2 algorithm, and the map was calculated by Avogadro, version 1.2.0, http://avogadro.cc/. High electron densities are shown in red and low densities are shown in blue. Arrows show acidic protons and basic nitrogen.

charges. The basic strength in turn, depends on the electronegativity of the heteroatom acting as electron donor (or hydrogen acceptor). Nitrogen is normally more basic than oxygen, since the latter is more electronegative and holds more tightly to its lone pair of electrons than nitrogen. Sibutramine, for instance, shows one basic nitrogen (Figure 21, right panel).

Many oxygen and nitrogen atoms of the molecules shown in Table 3 can be, in principle, proton donors or acceptors. In Figure 20 these atoms have been highlighted in red colour to indicate that it could be a proton donor (releaser), or in blue colour for the possible proton acceptor (or electron donor). They show different degrees of acidity or basicity, depending on the considerations above exposed. Five of the six studied compounds could show acidic or basic properties, or both simultaneously (amphoteric behaviour). If the free rotatable bonds can also influence in this behaviour, it is expected that some H donors/acceptors sites can be more active than others for each molecule, except for Sib which have only 1 H-acceptor and none H-donor, expecting that this compound should have basic behaviour only.

The melting point of the compounds studied, by its side, ensures their stability during the formulation processes. Moreover, melting point can be used as criterium of purity and it is correlated with other physicochemical properties, particularly with the solubility with which is strongly correlated because, in general terms, the solubility decreases with the increment of melting point[86].

4.2 Determination of pK_a

Several programs allow to estimate the acidity constants of molecules with functional groups susceptible to be acidic or basic. Table 4 shows calculated pK_a values using different modules of the ACD/Labs – Percepta® software[75, 87],

which allows to realise what to expect about the acid-base behaviour of the studied compounds when planning the experimental procedure for pK_a determination. In this table only pK_a values between 1.8 and 12.5 have been considered, since this includes the most common range of weak acids and bases in aqueous solution and, additionally, represents the limits of the potentiometric or spectrophotometric determinations of acidity constants. In this Table, (A) refers to the possibly acidic functional group and (B) for a basic one.

Table 4: Assigned pK_a values for the studied compounds using the ACD/Labs software

	ACD/Labs – Percepta®*	
Compound	***Galas***	***Classic***
Benzthiazide	(A) 6.0±0.5 (A) 10.0±0.4	(A) 5.9±0.5 (A) 9.7±0.2
Glimepiride	(A) 5.2±0.4	(A) 5.1±0.1
Isoxicam	(A) 4.0±0.4	(A) 4.5±1.0
Pioglitazone	(B) 5.3±0.4 (A) 6.4±0.4	(B) 5.5±0.2 (A) 6.3±0.5
Piroxicam	(B) 2.4±0.4 (A) 5.5±0.4	(B) 3.5±0.1 (A) 4.5±1.0
Sibutramine	(B) 8.6±0.4	(B) 9.7±0.5

***** Software by ACD/Labs[75]. (A) acidic-expected (B) basic-expected. (predicted values below 1.8 and above 12.5 are excluded, due to those values are not in the experimental range of the method used)

The differences observed in the pK_a values obtained with the Galas or Classic modules of the software are due to the different algorithms used in each one. On the one hand, the Galas algorithm is a multi-step procedure involving the estimation of pK_a microconstants for all possible ionisation centers in a hypothetical state of an uncharged molecule. Then the software corrects these initial pK_a values according to the surrounding of the reaction center, including the influences of ionised groups to the neighboring ionisation centers. On the other hand, the Classic algorithm uses Hammett-Taft-type equations and

electronic substituent constants to predict pK_a values for ionisable groups[75, 87, 88]. Figure 22 highlights the functional groups assigned to the respective pK_a values.

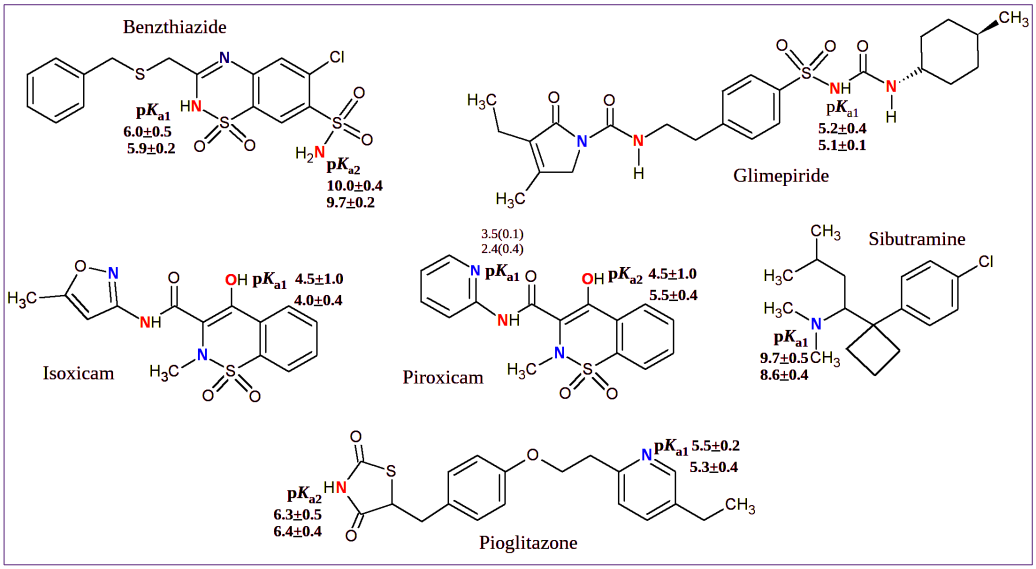

Fig 22: Assigned pK_a values for the studied compounds (from table 2). (red) atoms with acidic expected behaviour. (blue) basic expected behaviour atoms.

According to Table 4 and Figure 22, excepting Sib, which is considered as monoprotic basic compound, the other molecules do not have same number of pK_a values and/or not the same type of ionisable groups. Although Bzt, Glm and Iso have more H-acceptors than donor groups (Table 3), and according to Table 4, they are expected to be acidic compounds. This is because the predictions by the software are considering structural conditions that could reduce the probability of activation of one or more H-donor/acceptor. In addition, Pio and Pir are of amphoteric-behaviour expected, which confirms that at least one of its H-donor and one of its H-acceptor will be probably active. Despite that these two compounds have the least amount of H-donor/acceptor, they show more active ionisable functional groups than the other four compounds, due to their chemical structure differences.

The predictions from computational methods are only for guidance and experimental planning. An experimental determination is mandatory to obtain accurate and precise values of pK_a, which in turn will be useful to confirm the capacity of prediction of these types of software and principally for further work.

In the experimental context, because of the poor solubility of the studied compounds, the pK_a values were determined by a spectrophotometric method, which allows working at a lower concentration than the potentiometric one. Moreover, for glimepiride the aqueous pK_a was obtained from Yasuda-Shedlovsky extrapolation[70] from pK_a values obtained in different methanol/water mixtures. Table 5 lists the obtained experimental values together with those reported in the bibliography.

Table 5: Experimental and literature values of pK_a for the studied compounds. The experimental was made under 25°C and 0.15M of ISA water.

Compound	***Experimental pK_a***	***Literature***
Benzthiazide	(A) 6.64±0.03[a]	6.0[b];
	(A) 9.22±0.04[a]	8.1[c], 9.6[c]
Glimepiride	(A) 5.41±0.06	8.07[d];7.26[d],5.62[e] 6.30[f]
Isoxicam	(A) 3.79±0.02	3.80[g]
Pioglitazone	(B) 5.67±0.09	5.8[h]; 5.63[i]
	(A) 6.60±0.09	6.4[h];6.63[i]; 7.24[f]
Piroxicam	(B) 1.89±0.07	2,12[g]; 3.95[h]; 1.87[j];
	(A) 5.31±0.04	5.31[g]; 5.27[k]; 5.98[l]; 5.29[j]
Sibutramine	(B) 8.74±0.12	

Reported values in literature: **a** in [93]. **b** in [98]. **c** in [94]. **d** in [89] by two different methods. **e** in [91]. **f** in [90]. **g** in [96]. **h** in [97]. **i** in 16. **j** in [72]. **k** in [95]. **l** in [92]. (A) Acidic, (B) Basic. Values are reported with ± SD.

As predicted by ACD/Labs (Table 4), two pK_a values were previously found for Bzt by our research group[93], corresponding to the two H-donors (highlighted in Figure 21). The first one agrees with the reported in Hennig et al.[98]. The slight

difference can be attributed to the use of 20% of ethanol by Henning, since the presence of organic solvent (ethanol in that case) can rise the pK_a of acidic molecules[99] (and thus the need of an extrapolation to aqueous solution).

The fact that only one pK_a value (6.0) was determined by Henning et al. could be due to the methodology applied. They used the conventional spectrophotometric technique described by Albert and Sergeant[100], whereas we used a dip-probe absorption spectroscopy (D-PAS) multi-wavelength spectrophotometric technique, which allows the pH control directly *in situ* making more accurate pH and spectrophotometric measurements[68].

Maren[94] reported two pK_a values for Bzt (8.1 and 9.6) determined by a potentiometric method. The first one very different to the one reported in this work (6.44) and by Henning[98], and the second one closer to the one determined in our research group. No details about the experimental procedure are reported by Maren making it difficult to compare the results.

Figures 20 and 22 indicate that Glm has three potentially acidic hydrogens bonded to nitrogen atoms, but only one can be clearly expressed, whose experimental pK_a value is 5.41±0.06. The other two could be too strong or too weak acidic groups that cannot express themselves under the working conditions.

Figure 23 shows the spectral information (left panel) for Glm. Although the acidic (red) and basic (blue) spectra for the respective species seem to be very similar, there are enough differences in the molar absorptivity that let to quantify them in the solution. Then the right panel in same figure can be obtained, where the distribution of species as function of pH is shown. Figure 23 agrees with monoprotic acidic profile, confirming at least one pK_a for Glm.

As it was pointed before, due to the low solubility of Glm, its pK_a value was obtained by Yasuda-Shedlovsky plot (see Figure 24).

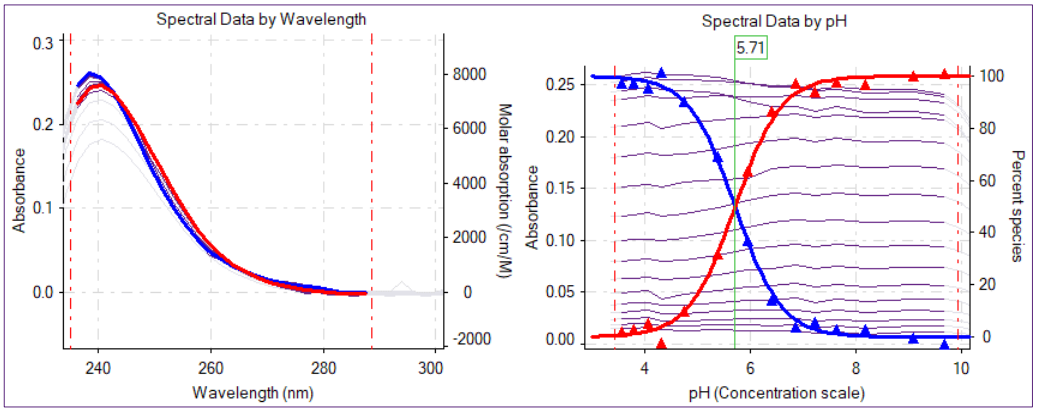

Fig 23: Spectrophotometric absorption (left) and distribution of species (right) for Glm.

The pK_a value is in agreement with that reported by Lakshmi[91] (5.62), who used the same methodology. At time, ACD/Labs approach is close to the experimental value found in this work. The discrepancies with the values by Grbic[89] can be explained by the methods used, where the disagreement in their spectrophotometric pK_a value (7.26) is not only attributed to the presence of 10% of ethanol, but also in the pH working range (7.4, 7.8 and 8.0), which is far from the pK_a values detected in this work. The other pK_a value of 8.07 reported in her work was obtained from solubility determinations.

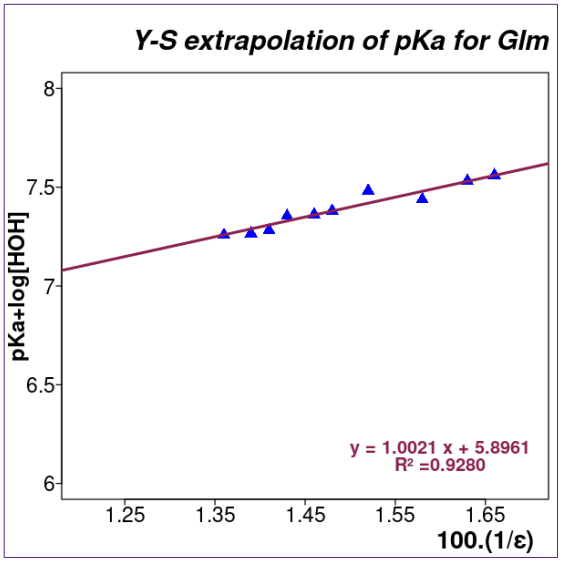

Fig 24: Yasuda-Shedlovsky extrapolation for aqueous pK_a calculation for Glm in methanolic solutions.

This value could correspond to an apparent pK_a, because if there were interactions between the molecule and solution components, or maybe intermolecular interactions, the pK_a could be displaced.

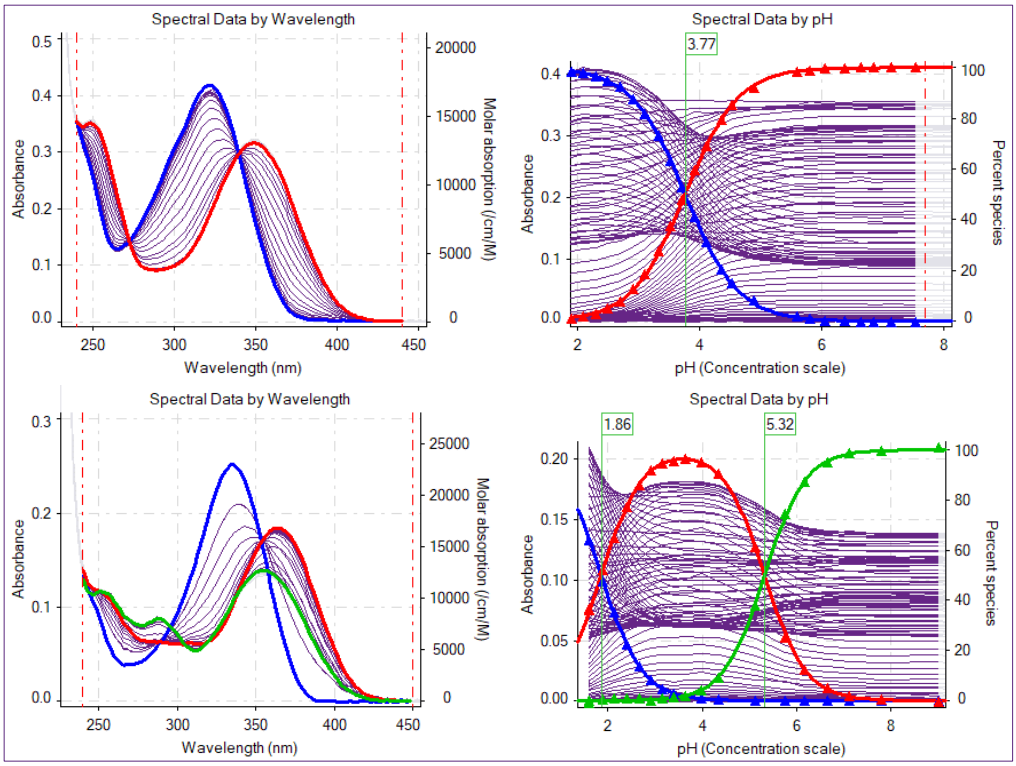

Fig 25: Spectral information for Iso (left-up side) and Pir (left-down side). Distribution of species for Iso (right-up side) and Pir (right-down side) as function of pH.

As predicted by ACD/Labs, one and two pK_a values were detected experimentally for Iso and Pir, respectively. Figure 25 shows the spectrophotometric profiles by pH for Iso (left-up) and for Pir (left-bottom) with their respective distribution of species showed at the right of each one in same figure.

In case of Pir, the low basic pK_a (see Table 5) can be determined because spectrophotometric method can detect pK_a values around 2 when the

chromophore is different enough from the neutral to protonated molecule. The experimental pK_a values for isoxicam and piroxicam are strongly consistent with those reported in literature[72] (1.87 and 5.29), where the same methodology was applied. Moreover, they also agree with the ones determined by CE (Pir 2.12, 5.31; Iso 5.80)[96]. However, the pK_a values reported by Demiralay (Pir 5.98)[92], which are obtained from Yasuda-Shedlovsky extrapolation from titrations in several acetonitrile/water (from 30% to 45%), does not agree with the others.

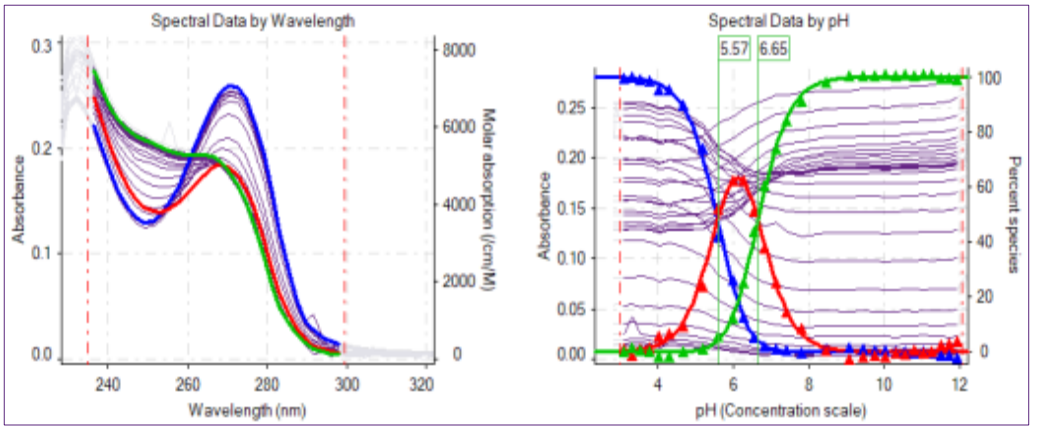

Fig 26: Pio distribution of species as function of pH (right) and UV absorption spectra (left).

As can be seen in Figure 26, the spectrophotometric method allowed to determine two pK_a values for Pio (right panel), which are similar to those predicted by the software (see Tables 4 and 5). Moreover, the values obtained agree with the bibliographic ones, except for the single pK_a value reported by Seedher et al. (7.24)[90], which is far from the second pK_a. The lack of experimental details about how the authors determined the acidity constant makes the comparison difficult.

For Sib the value predicted by Galas module is close to the experimental determined pK_a, but the value given by Classic algorithm differs in almost one

unit respect to the latter (see Tables 4 and 5). Figure 27 shows the spectrophotometric pK_a for Sib, whose relatively high variability can be attributed to the existing distance between the ionisable functional group and the chomophore, which reduces the spectral differences between the ionised and neutral species. Although the spectra are similar, they are different enough to quantify their concentrations and obtain the species distribution diagram.

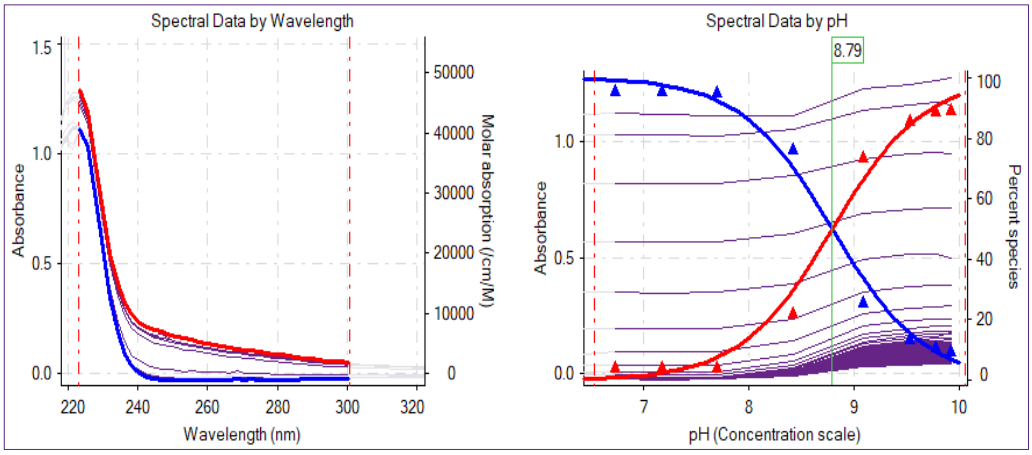

Fig 27: Sibutramine distribution of species with pK_a (right) and spectral absorption (left).

4.3 Comprehensive study about Solubility Determinations

The solubility determinations can yield some different results for the same substance due to many different reasons. This variability can be attributed to the different methodology and/or technique used, the experimental conditions, raw material, working process, etc., that can be sources of aleatory and systematic errors that can affect the results. Nevertheless, even if all of these situations are controlled, that variability could be produced because of the deficient or not enough knowledge about the use, application, limitations and scope of the technique and methodology used.

As has been mentioned in the introduction, the Shake-Flask (SF) is a widely recommended method to conduct these studies, but it needs to be implemented following some consensual recommendations, and even some common practices under this methodology need to be standardized in the daily work to guarantee confident results.

On the other hand, potentiometric methods, like CheqSol, are developed not to replace other methods, but to improve the assay time in solubility studies, especially in early stages of drug development, but its many usages are not completely elucidated, as well as its limitations.

Thus, this section focuses on two parts. In the first one a comparison of the Shake – Flask vs potentiometric method is formulated for solubility studies. Three molecules of different acid-base properties, glimepiride (Glm), pioglitazone (Pio), sibutramine (Sib) and the hydrochloride salts of these last two are studied. The second part is focused on the study of solubility of three compounds, i.e. benzthiazide (Bzt), isoxicam (Iso) and piroxicam (Pir), in different media like aqueous buffers or Biorelevant Dissolution Media (BDM). In addition, some excipients are added to the media to determine their effect on the solubility property.

4.3.1 Comparative: Shake – Flask vs Potentiometric CheqSol®

Ageneral idea about a possible behaviour of the substances in terms of solubility, will help for a better experimental planning. There are some computational programs that allow the prediction of intrinsic solubility and/or the solubility at different pH values, usually assuming Henderson-Hasselbalch model. Then, an estimated Solubility – pH profile of the studied molecule can be obtained. These commercial software include many proprietary algorithms,

which allow to obtain some models and plots for the solubility of the compounds.

In this work, ACD/Labs-Percepta®[75] and *pDisol-X*™[101] software are used to predict theoretical solubility – pH dependent profiles for Glm, Pio and Sib, which are shown in Figure 28. At first sight, the shape of models from both software are the same for the respective compound and, although both of them show the presence of salt formation and similar pK_a^{Gibbs} zones (values) for the respective molecule, pDisol-X draws more specific profiles in the sectors where the precipitation of a salt is expected.

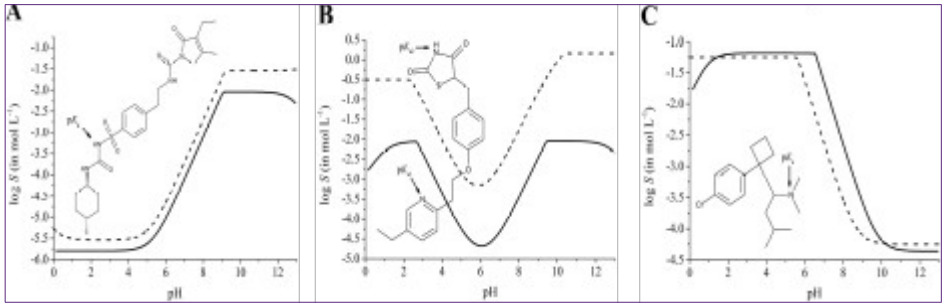

Fig 28: Solubility – pH dependent profiles proposed for: (A) glimepiride, (B) pioglitazone and (C) sibutramine, which are obtained using ACD/Labs-Percepta (dashed line) and pDisol-X (solid line).

ACD/Labs tends to show profiles of higher solubility values than pDisol-X, specially in profile for Pio, where the expected solubility by ACD/Labs differs in more than one logarithmic unit respect to that predicted by pDisol-X. The difference in Sib profiles is due to the pK_a value predicted, which differs in about one pH unit depending on the software used. For that substance, ACD/Labs predicts lower solubility values in the zone where the molecule is ionised.

4.3.1.1 The Shake Flask method

Buffer and pH considerations

As mentioned in the introduction, the experimental conditions used for Shake-Flask determinations were the recommended by Avdeef et al.[73]. The buffer selected was a Mass Spectrometry-friendly Minimalist Universal Buffer (MS-MUB), which has a good buffering capacity over a wide range of pH values (8.3mM/pH between pH 3 and 11) and maintains almost constant the ionic strength (average ionic strength of 96mM between pH 2 and 12), avoiding the use of salt-formers like the phosphate anions in its composition.

In addition to the use of buffering agents, periodical control of pH during both the stirring and resting time periods is required. A change in pH can be observed depending on the solubility of the API at working conditions and its formulation. It is recommended to measure the pH after 4 hours of stirring started and, if it is necessary, re-adjust the pH to its original value with concentrated acid or base to avoid dilution. After the resting period and before the phase separation process the pH must be again measured.

The pH variation after 4 hours of stirring compared to the initial pH values (in a pH range from 2 to 12) is shown in Figures 29 to 31 for Glm, Pio and Sib, respectively. The variations observed for the hydrochloride salts are included as well.

In the case of solubility assays involving Glm (free neutral acid), at first 4 h pH-measurement no considerable changes of pH were detected in the solutions up to pH 5.5 (close to its pK_a). In solutions of initial pH between 6 to 9.5 the pH slightly decreased after 4 h of stirring, but at pH above 11 it changed about 1 pH unit (see Figure 29, left panel).

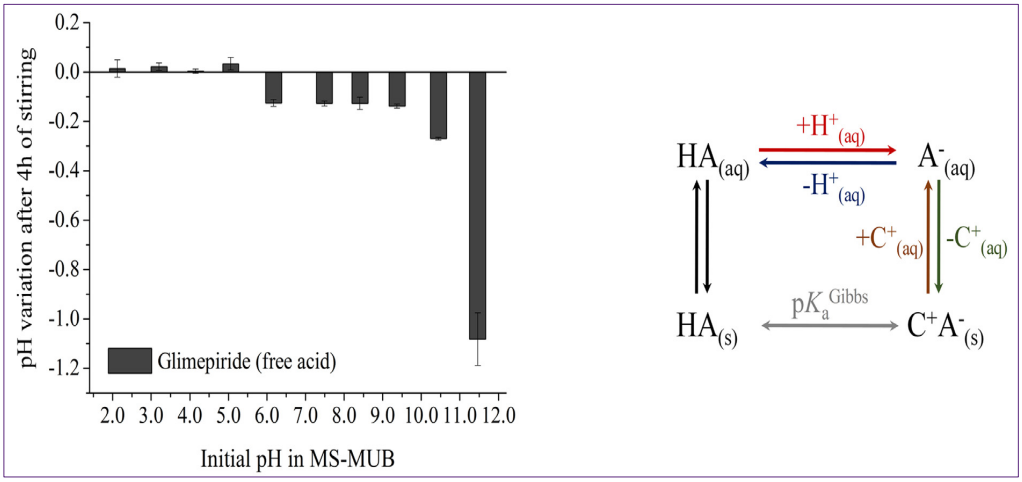

Fig 29: In left panel is shown the pH variation in Glm samples after 4 hours of stirring. In right panel are proposed the equilibrium reactions between different species of Glm.

This behaviour in 3 differentiated sectors could be attributed to the presence of different species of Glm in each one. In the first range, since the pH is lower than its pK_a, the solid and aqueous forms of the compound are both neutral (uncharged), and these are not reacting with any other component from the buffer solution. Thus the pH remains unchanged.

In the second range, where the pH is higher than the pK_a, the solid form remains as neutral acid, whereas in solution the sample is ionised and it is releasing protons. However, the pH decreases slightly because the low solubility of the sample makes that the released amount of protons is low enough to not affecting the pH of the solution, where its buffering capacity keeps stable the pH.

At pH much higher than the pK_a, the concentration of the conjugate base of the acid (A^-) could be high enough to react with an appropriate quantity of any other positive charged species present in the solution (C^+), forming a precipitating salt (C^+A^-) by charge balance. The formation of this type of salt

reduces the available ionised sample in the solution (A^-), which forces the equilibrium $(HA \rightleftarrows A^-)$ to the right (see Figure 29, right panel). At the same time, more solid (HA) is solubilised and immediately ionised (pH >> pK_a) releasing more protons and decreasing the pH, which in turn will be stable only until all the possible formed salt (C^+A^-) will be in equilibrium with the remaining solid (HA).

The pH variation for Pio (both free base and hydrochloride salt) can be seen in Figure 30, where this ampholyte showed negligible changes of pH in the studied range when the free base was used as starting solid (black bars). On the contrary, when the hydrochloride salt (grey bars) was used, the pH decreasing behaviour was significant (up to one unit). The slight increasing of pH for the free base in the range below its basic pK_a (pH < 5.6) is attributed to the protonation of the molecule $(HX \rightleftarrows H_2X^+)$, and therefore the pH increases because the molecule is capturing H^+ from the solution. Meanwhile in the neutral zone of the molecule (pH values within its pK_a values) the pH change is negligible. Above its second pK_a (pH > 6.6) the pH decreases because the

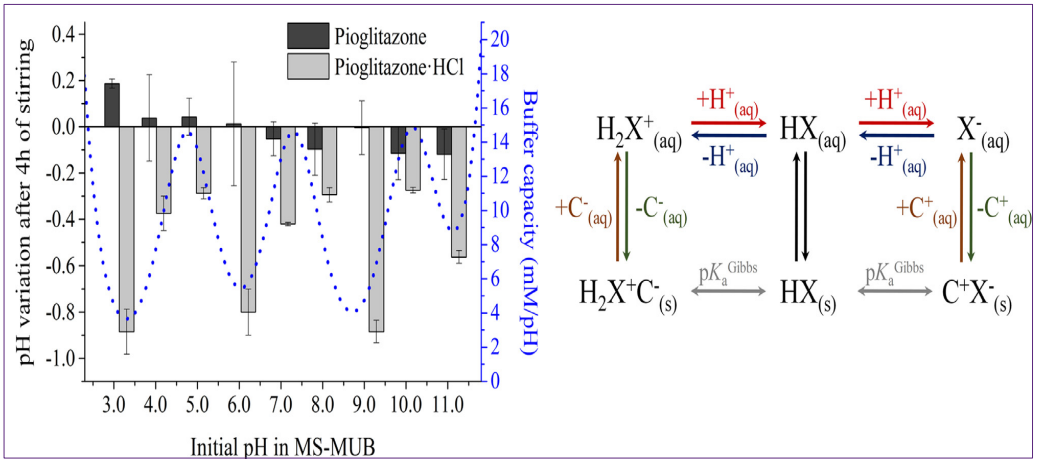

Fig 30: In left panel, pH variation for solutions with Pio (black bars) and its hydrochloride salt (grey bars). In right panel, equilibrium reactions between different charged states.

molecule is deprotonated releasing H^+ and acidifying the solution $(HX \rightleftarrows X^- + H^+)$.

The difference in the pH changing behaviour between the free neutral form (HX) and the salt ($H_2X^+Cl^-$) can be explained taking into account that the solid collected was always the free base, disregarding the initial solid (either neutral form or salt). When the salt is weighed, there is a portion of HCl included, which is released to the solution when the salt gets solubilized. Thus, the pH drops because of the presence of H^+ coming from the hydrochloride salt (grey bars in Figure 30). This effect of hydrochloride salt on changing the pH of the solutions is evidenced by the declining buffering capacity of the MS-MUB, which is dropping to one-fourth (right blue axis of left panel in Figure 30) just right at pH 3, 6 and 9 where the biggest pH changes are observed. The more the salt is dissolved, the higher the concentration of added HCl, affecting the buffering capacity.

The Sib case is very interesting because of the pH variation found and the different solids collected during solubility assays, which are dependent on the solid initially used. The pH increases in solutions below pH 7 when the free base (B) was used as starting solid (see black bars in Figure 31), and the highest increment was observed at pH 2 where the change was of 3 units. At this point, the free base is highly protonated, decreasing the H^+ concentration in solution and consequently increasing the pH. Besides, the formation of enough protonated base may lead to the formation of a salt by charge balancing, displacing the equilibrium to the left (see Figure 31, right panel), reducing the concentration of protonated base in solution and forcing the solubilisation of more neutral solid, which is newly protonated increasing the pH again.

In solutions of pH above of 7 with free base as initial solid, the neutral form of the compound is predominant, and thus no salts can be formed and neither H^+ are bonded to the molecule nor the pH change.

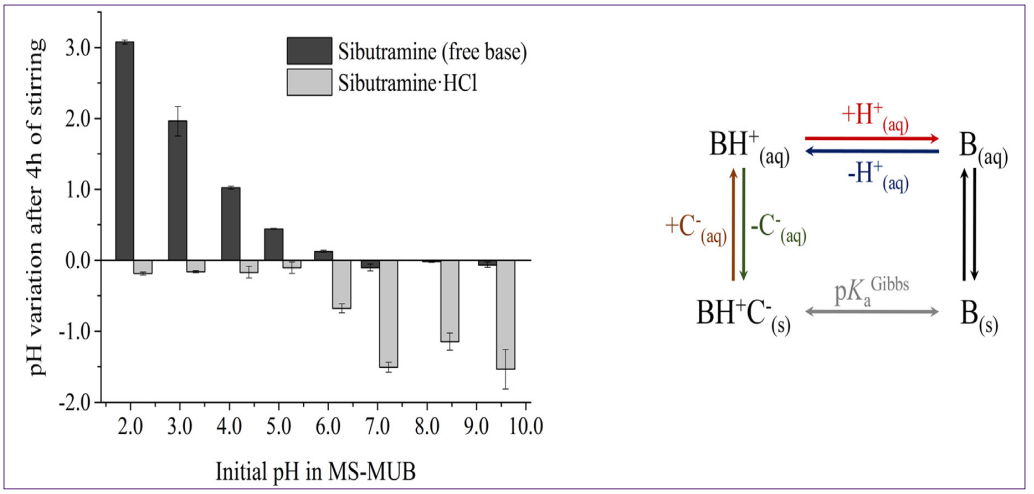

Fig 31: (left panel) Sib and its hydrochloride salt pH variation, (right panel) equilibria reactions proposed.

The contrary tendency was found when the hydrochloride salt was used as initial solid. The pH decreases when the pH of the solution is 6 or higher, because in this occasion the neutral form is precipitating, releasing HCl and therefore decreasing the pH. At pH below 6, the variation of pH is negligible because the solid introduced and the precipitating species found were of the same nature $\left(BH^{+}_{(aq)} \rightleftarrows BH^{+}C^{-}_{(s)}\right)$.

Solids Characterization

In the introduction section was pointed the importance of collecting the solids after the resting period, because solids can transform into another form, and the solubility will correspond to the form in equilibrium with the solution. Then, the solids collected from the solutions after resting period were characterised using Powder X-Ray Diffractometry (PXRD) as well as the starter solids. All

these samples were also characterised using Differential Scanning Calorimetry (DSC) and Thermogravimetry (TGA).

In case of Glm, at pH below 9, the solid in equilibrium was always its pure Form I, which is the most insoluble form of Glm[102, 103] and it is the same as the initial weighed solid for the experiments. Around pH 10 and above the analysed solid presented a diffractogram different from Form I and also from other forms reported in the literature[102, 104–109]. Due to the buffer composition, the solution for pH adjustment and the ionic species of Glm present at pH > 10, we attribute this new form to the sodium salt of Glm. The diffractograms of Glm Form I and its new crystallographic phase are shown in Figure 32. The characterization of the salt (DSC, TGA and peak list of diffraction angles information) can be found in the Appendix (Table A1, Figures S1, S2 and S3).

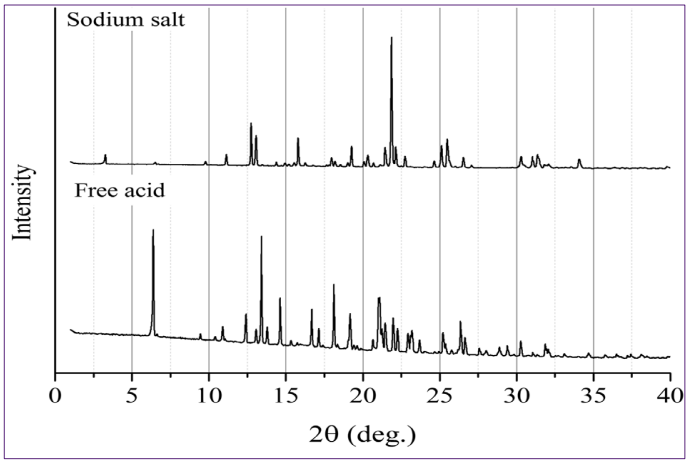

Fig 32: Diffractograms for neutral form and sodium salt of glimepiride.

Furthermore, in Figure 33 can be appreciated the diffractograms for the neutral form and the hydrochloride salt of Pio (left panel) and for Sib and its salts (right panel). These diffractograms help to confirm the starting solid used and describe the formed solids in the distinct assays for both compounds. In the Pio study the solid collected in all the pH range was always its neutral form, independently of the starting material used (free form or hydrochloride salt). In

case of Sib, disregarding the initial solid, above pH 5.8 the collected solid was the neutral form of Sib, but below that pH none of the solids found were the pure neutral form or the pure hydrochloride salt.

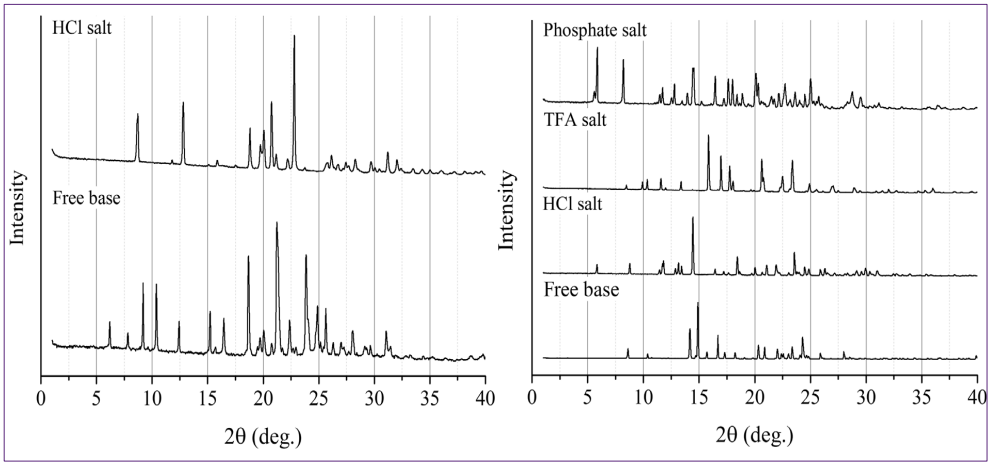

Fig 33: Diffractograms for: neutral form and hydrochloride salt of Pio (left) and for neutral Sib and its salts (right).

Interestingly, to the best of our knowledge, the salt formed between sibutramine and trifluoracetic acid was a solid never characterised before (see Figure 33, right panel). The protonated base reacts with the conjugate base of that acid, forming a new entity whose peak list of diffraction angles, DSC and TGA thermograms are in the Appendix (Table A2, Figures S4, S5, S6 and S7).

Solubility – pH dependent profiles

After the resting period, when the solids were collected for their respective analysis, liquid chromatography assays were also conducted with the supernatant of each solution to determine the concentration of the substances in the liquid phase. The concentrations found in all the solutions, together with the solid analysis results, allowed to establish a Solubility – pH dependent profiles for each compound.

Glimepiride

The solubility, expressed as logS, found for Glm at each pH point is presented in Table 6 together with the respective solid collected when was available. Figure 34 shows the representation of these values in front of pH, i.e. the solubility – pH profile, where the squared black points represent the logS values whose collected solid was Form I of Glm. The red points show the logS values where the solid collected was the sodium salt of Glm plus its Form I. Triangles in the same Figure correspond to measured log*S* values where the solid was not collected.

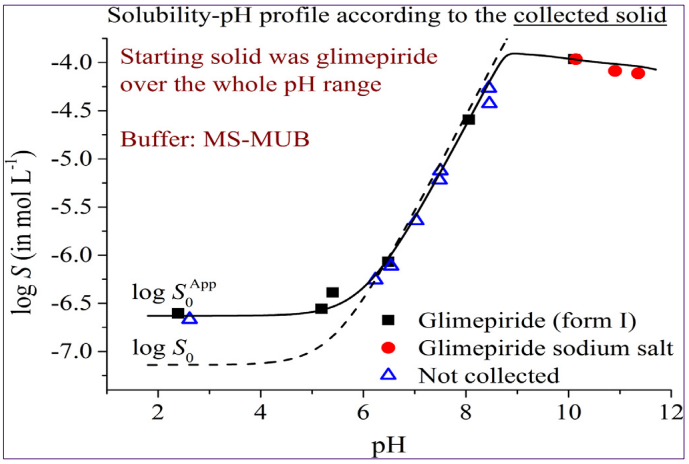

Fig 34: Glimepiride Solubility-pH dependent experimental profile (solid line), theoretical H-H model (dashed line). Solid was not collected (△).

The experimental points from Table 6 seem to follow a HH behaviour, and thus this model was first applied. Although, the segment of slope 1 between pH 6 and 9 (see Figure 34) is suggesting that ionised form of the substance is not suffering interactions in that range of pH, this model reveals a displacement of the pK_a in around 0.5 units respect to the potentiometrically pK_a previously found. This suggests the presence of parallel reactions[73] involving only the neutral form of Glm.

Table 6: Glm solubility and solid type collected at different pH.

***pH*[a]**	**logS[M] [b]**	***Solid collected***
2.39	-6.60	Form I
2.61	-6.60	Form I
5.19	-6.56	Form I
5.40	-6.39	Form I
6.23±0.05	-6.26±0.18	–
6.49±0.02	-6.07±0.15	Form I
6.54±0.04	-6.11±0.11	–
7.03±0.04	-5.64±0.04	–
7.49±0.03	-5.22±0.03	–
7.50±0.03	-5.12±0.01	–
8.06±0.06	-4.59±0.06	Form I
8.45±0.04	-4.27±0.04	–
8.46±0.08	-4.43±0.23	–
10.02±0.01	-3.97±0.02	Form I
10.14±0.02	-3.96±0.01	Form I + sodium salt
10.90±0.02	-4.09±0.04	Form I + sodium salt
11.35±0.06	-4.11±0.02	Form I + sodium salt

a pH measured at the end of sedimentation step.
b Values presented with standard deviation are the average of replicates made at similar pH values (SD<0.1).

In the pH range above 9, where the solid collected pointed out the salt formation, the ionised form of Glm is forming a new solid entity, which is attributable to the sodium salt. In fact, at these pH values the only cationic component present in the solution that can react with the anionic form of Glm is the Na^+, that comes from the NaOH used to adjust the pH of the MS-MUB buffering system.Considering these situations, a corrected model was proposed (solid line in Figure 34) which includes a neutral aggregate formation and salt formation constants (Equations 31 and 32 respectively):

$$logS = logS_0 + \log\left(1 + K_a/[H^+] + 2\,K_2^{A_2H_2} S_0\right) \quad (31)$$

$$K_{sp} = [Glm^-]\cdot[Na^+] \quad (32)$$

where $K_2^{A_2H_2}$ corresponds to the formation constant of a dimeric neutral aggregate of Glm, which is more soluble than the monomeric neutral form.

Thus, the difference between the intrinsic solubility of the monomeric species obtained from the fitting (S_0) and the apparent intrinsic solubility (aggregates, S_0^{app}) is around 0.5 logarithmic units. The neutral aggregates found in Glm are explained because sulfonylurea derivatives (like Glm) can suffer self-assembling due to its sulfonamide and urea groups, in which there are active H-donor/acceptor sites (as described in the previous pK_a chapter), that could lead to a stable union through interactions between these acidic/basic groups[102, 104, 110].

Figure 34 shows fitted model (solid line given by Equation 31) and the corrected HH model (dashed line, Equation 15) based on the fitted S_0 from the aggregation model. The values of S_0, S_0^{app}, $K_2^{H_2A_2}$, and K_{sp} for Glm are shown in Table 7. In the same table are listed the fitted values for these parameters, calculated with the proposed model (Equation 31) using solubility data reported in previous studies by different authors. The respective fitted models are shown in Figure 35.

Table 7: Experimental and fitted solubility values taken from different sources for Glm.

$logS_0$	$logS_0^{app}$	$logK_2^{H_2A_2}$	K_{sp}	*comments*
-7.14±0.02	-6.63	7.18±0.21	5.35 ± 0.01	This work
-6.76±0.07	-4.72	8.49±0.09	–	pH 2.0 – 9.5, 0.05M glycine; centrifuged, then filtered[a]
-7.21±0.03	-5.47	8.65±0.06	–	pH 4.5–8.2, 0.2M phosphate; filtered [b]
-7.29	–	–	–	pH 6.5 (I = 0.15M)[c], 37 °C value corrected to 25 °C[e]
-7.83±0.10	–	–	–	pH 3; centrifuged 3 times[d]; 21 °C corrected to 25 °C[e]

a in [90]; **b** in [89]; **c** in [113]; **d** in [112]; **e** in [111]

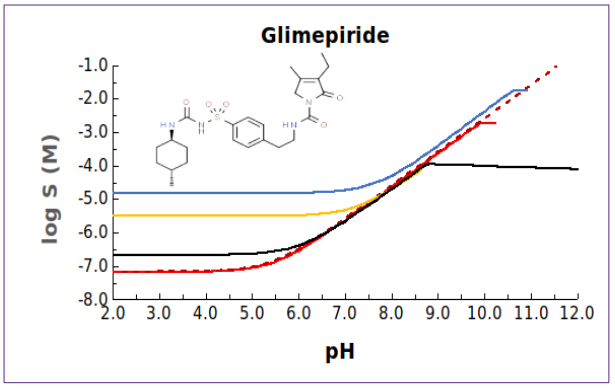

Fig 35: Fitted models for Glm: (dashed line) HH model, (solid line) proposed model in Eq. 31, (black) this work, (yellow) from Grbic data [89], (blue) from Seedher & Kanojia data [91], (red) from Taupitz data [111].

Although the differences observed in the neutral zone of the profile (Figure 35), the calculated S_0 from each data set is in agreement with the value reported in this work (Table 7). These fitted results are also in accordance to a dimeric aggregation formed by neutral Glm.

The $\log K_2^{H_2A_2}$ calculated with the data from Seedher & Kanojia[90] or Grbic et al.[89] are almost one unit higher than the $\log K_2^{A_2H_2}$ found in our work. Maybe this could be attributed to a supersaturation in the solutions used in the referenced works, where shaking period is performed during 24h but no sedimentation process is reported. Additionally, the $\log S_0$ value of -6.06 given by Taupitz[113] at pH 6.5 is in good agreement with our result at the same pH. The value given by Bergström[111] is the lowest reported, and this could be due to the triple centrifugation of the supernatant made by the researchers, followed by a filtration step that might lead to losing sample by adsorption of the solute on the filtering material.

Pioglitazone

The solubility values determined with both the neutral form of Pio and its hydrochloride salt as starting solids are listed in Table 8, where can also be observed the type of solid collected after the sedimentation period. The precipitated solid was always the neutral form of Pio disregarding the type of

the starting solid used, and no significant differences in solubility were observed in the studied pH range (Figure 36).

Table 8: Solubility of Pioglitazone determined in MS-MUB buffer.

pioglitazone			***pioglitazone hydrochloride***		
pH	***logS*** $[M]$	***Solid collected***	***pH***	***logS*** $[M]$	***Solid collected***
1.98	-3.43	Free base	2.04	-3.16	–
2.03	-3.34	Free base	2.06	-2.94	Free base
2.18	-3.31	Free base	2.16±0.03	-3.51±0.03	–
3.19±0.10	-4.06±0.09	Free base	2.36	-3.13	–
3.46±0.01	-4.37±0.04	–	2.96	-4.31	–
3.6	-4.71	–	3.11	-3.48	–
4.08	-4.96	Free base	3.12±0.08	-4.50±0.14	–
4.18±0.01	-4.97±0.03	–	3.56	-4.77	–
4.22±0.01	-5.19±0.01	Free base	3.86±0.11	-5.03±0.09	–
5.06±0.01	-5.62±0.04	–	4.04±0.07	-5.08±0.07	Free base
5.01±0.02	-5.29±0.05	–	4.97±0.03	-5.20±0.12	–
6.13±0.01	-5.59±0.07	–	6.07±0.04	-5.54±0.08	–
7.00±0.04	-5.67±0.22	–	7.04±0.05	-5.62±0.14	–
7.92±0.02	-5.18±0.07	Free base	7.46±0.01	-5.17±0.07	–
8.04±0.01	-5.76±0.02	–	7.94±0.01	-5.52±0.05	–
9.19±0.01	-4.45±0.02	–	7.94±0.07	-5.36±0.06	–
9.25	-4.16	Free base	9.11±0.04	-4.42±0.04	–
9.87±0.01	-3.79±0.04	Free base	9.28±0.09	-4.31±0.11	–
10.96±0.05	-2.74±0.06	Free base	9.93±0.03	-3.56±0.05	–
11.04±0.02	-3.07±0.02	–			

Results shown with SD correspond to the average of at least three replicates.

The solubility – pH profile corresponds to the amphoteric nature of the drug. As in Glm, both series were fitted with a model that suggests the aggregation of neutral species of Pio (solid line in Figure 36), given by Equation 33.

$$\log S = \log S_0 + \log\left(1 + K_{a1}/[H^+] + [H^+]/K_{a2} + 2K_2^{H_2X_2}\cdot S_0\right) \qquad (33)$$

In same Figure 36, the dashed line correspond to the HH model obtained with the fitted $\log S_0$ from Equation 33. The apparent solubility of neutral Pio $\left(logS_0^{app}\right)$ is around one unit higher than the fitted intrinsic solubility of monomeric species. The pK_a values used for these calculations were previously spectrophotometrically determined, as reported in chapter 4.2.

Although the applied model considered the formation of neutral aggregates, the apparent higher solubility of Pio could be also due to formation of nanoparticles or colloids[114, 115]. In the profile of Figure 36, the left and right sloped segments of the lines do not show evidence of salt formation, and the fitted and HH models matches in these segments (slope 1). This confirms that the ionic species of Pio do not interact with themselves or any of the buffer components in the studied pH range.

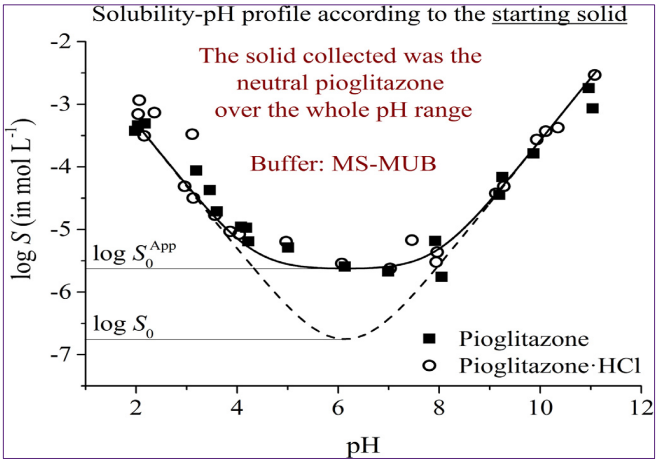

Fig 36: Solubility-pH dependent profile for pioglitazone: (solid line) fitted profile, (dashed line) HH model

Sugita[116] and coworkers reported some solubility values in the pH range 1.2 – 6.8, to which the same model of Equation 33 was applied, obtaining a similar $logS_0$ value that agrees with ours. Similar situation was found using the values reported by Seedher and Kanojia[90] in the pH ranges of 1.8–3.9 and 7.4–9.5, using glycine based buffers, where the calculated solubility value was highly consistent with the present results.

The solubility – pH profiles from the above mentioned works are represented in Figure 37, where solid lines correspond to the reported values (the black solid line is from this work) and, the dashed line is the theoretical HH model using the estimated $logS_0$ found in this work. The fittings of literature data to Equation 33 are summarized in Table 9.

The $logS_0$ value reported by Tanaka et al.[97] seems to be too low respect to the other values in Table 9. This low solubility (-7.36) could be due to the relatively short shaking period reported by the authors (3 h), which could not be long enough to reach the equilibrium between phases despite it took place at 37 °C. Other relevant fact could be that samples were filtered instead of centrifuged, which could led to lose of sample by absorption on the filtering material.

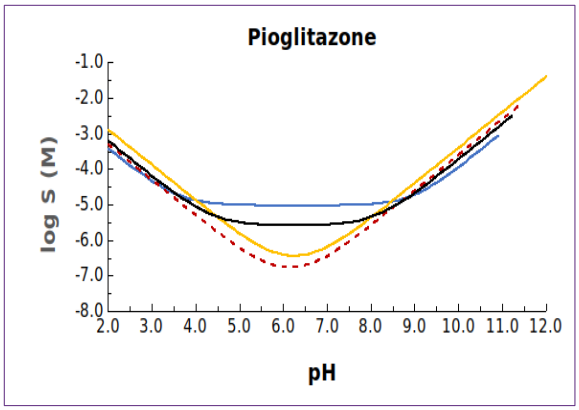

Fig 37: Literature fitted models compared to the model calculated in this work: (yellow) Sugita et al.[116], (blue) Seedher et al.[100], (black) This work, (dashed line) HH model.

Table 9: Experimental and fitted solubility values from this work and the literature for Pio.

$logS_0$	$logS_0^{app}$	$logK_2^{H_2X_2}$	*comments*
-6.98±0.04	-5.70 ± 0.05	7.98 ± 0.12	this work
-6.63±0.05			in [a]
-6.86±0.16		9.05 ± 0.15	hydrochloride salt, pH 2 – 9.5, 0.05 M glycine, centrifuged then filtered[b]
-7.36			pH 2.4, 0.05M phosphate, 3h incubation then filtered [c], corrected to 25°C [d].

a in [116]; **b** in [90]; **c** in [97]; **d** in [112]

Sibutramine

The study for Sib was the most extensive among these three compounds because of the implications with its solid phases. In first instance the solubility of neutral and charged species of Sib were measured in a wide range of pH. Table 10 lists the *logS* values found for this compound in MS-MUB, and Figure 38 shows the corresponding solubility – pH profiles. Above pH 5 the

experimental points seem to follow a normal HH behaviour for basic compounds, and below that pH the points lose that behaviour due to the salt formation.

Table 10: Sib and Sib hydrochloride salt solubilities in MS-MUB.

sibutramine [a]			***sibutramine hydrochloride*** [a]		
pH	***logS*** $[M]$	***Solid collected***	***pH***	***logS*** $[M]$	***Solid collected***
2.12	-1.91	TFA salt	1.98±0.08	-1.76±0.09	TFA salt
2.24	-1.86	TFA salt	2.95±0.08	-1.78±0.02	TFA salt
3.33	-1.68	TFA salt	3.83±0.03	-1.50±0.09	Freebase + TFA salt
3.70±0.09	-1.54±0.02	TFA salt	3.99±0.07	-1.71±0.12	TFA salt
4.28±0.03	-1.61±0.10	TFA salt	4.75	-1.77	TFA salt
4.41	-1.64	TFA salt	4.81±0.04	-1.58±0.08	TFA salt
4.52±0.02	-1.07±0.08	Free base and TFA salt	5.84±0.04	-2.65±0.03	–
4.76±0.20	-1.69±0.05	Free base and TFA salt	7.04±0.07	-3.76±0.04	Freebase
5.12±0.01	-1.71±0.03	Free base and TFA salt	7.39±0.09	-4.17±0.11	Freebase
5.14±0.07	-2.13±0.10	–	8.49±0.09	-5.12±0.27	–
5.29±0.02	-1.87±0.03	Free base and TFA salt	8.51±0.12	-5.08±0.11	Freebase
6.00±0.01	-2.72±0.05	Free base	9.40±0.12	-5.27±0.15	Freebase
6.99±0.03	-3.75±0.03	Free base			
7.24±0.06	-4.09±0.05	Free base			
8.01±0.11	-4.93±0.11	Free base			
8.22±0.01	-5.16±0.03	Free base			
8.52±0.12	-5.18±0.16	Free base			

a When the SD is indicated, the values are the average of at least three replicates.

Considering this, a model based on HH but that includes a salt formation was proposed, obtaining the solid line observed in Figure 38, where the black squares and white circles correspond to the points where free base or the hydrochloride salt, respectively, were used as starting solids. The salt formation was confirmed by solid characterization with PXRD (as previously discussed), which is also indicated in Table 10.

Interestingly, the precipitating salt at acidic pH range does not correspond to the sibutramine hydrochloride. It means that the protonated Sib is interacting with any buffer constituent and/or pH-regulator solution present in the medium. Since MS-MUB is a relatively complex buffering system, SF assays were performed with solutions of isolated components from this buffer, this is, trifluoroacetic acid or acetic acid, in order to identify the formed salt.

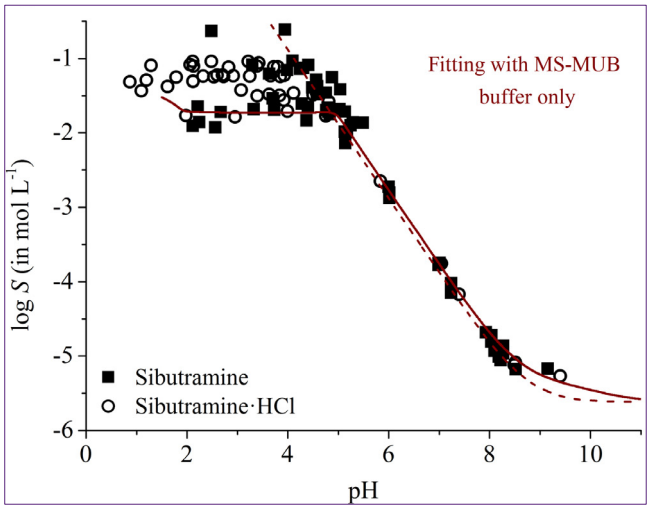

Fig 38: Sib solubility profile according to the starting solid: (black squares) Free base, (white circles) hydrochloride salt.

The analysis of the collected solids demonstrate that, disregarding the starter solid of Sib (free base or hydrochloride salt), the Sib – trifluoroacetate (Sib – TFA) salt was always formed. This was the main salt present at pH 4.4 and below, whereas at pH 4.5. – 5.5 a mixture of this salt coexists with the neutral solid form, and above pH 5.5 the solid collected was always the neutral base.

Experiments using solutions of hydrochloric acid or phosphate were performed in order to test a possible formation of more salts of Sib. The use of the mentioned solutions also let to the formation of hydrochloride and phosphate salts of Sib. The new series of points are represented in Figure 39, where in the left and right panels are plotted the points by the type of solid obtained and the points by the solubility media used, respectively.

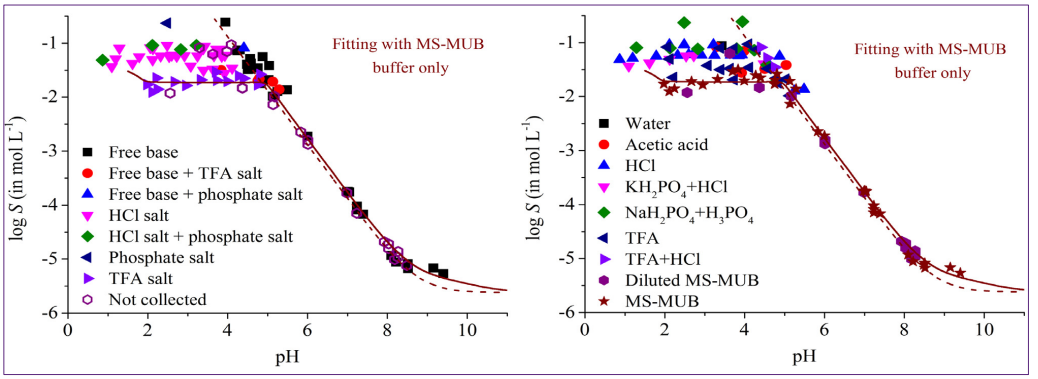

Fig 39: left panel: Profile by collected solid. Right panel: profile by buffering species.

Thus, the MS-MUB induces the formation of the TFA salt at acidic region with a determined pK_{sp} of 3.23 ± 0.03. When the hydrochloric acid was used as dissolution media, the precipitated solid was the hydrochloride salt with a pK_{sp} of 2.37 ± 0.01, being it more soluble than the TFA salt. When the starting solid is the hydrochloride salt, it is easier to precipitate this one because of the relatively high concentration of Cl^- arising from the initial sample weighed, or the hydrochloric acid used to adjust the pH of the sample solution. When the phosphoric acid is used, the respective phosphate salt is precipitated, showing that the protonated Sib can virtually react with any anionic species present in the media (phosphoric acid is well known as salt former).

In the region around pH 4.5 and 5.5 in Figure 39, the formed salts from protonated base were found together with some neutral solid Sib. This is suggesting that the pK_a^{Gibbs} of Sib is around the mentioned pH range, what in turn matches with the model of this profile.

The experimental points match quite well with the HH model (dashed lines in Figures 38 and 39) with the exception of points in the sector within pH 9 – 10 that barely lose this adjustment. Then, another model was proposed to include

the interaction of the neutral form of Sib with a buffer component (solid line in Figure 39). This interaction could be attributable to the complexation of Sib with ethylenediamine (EDA), that comes from MS-MUB. This correction shows a better fitting with the experimental points at pH ~9.5. The constant formation for this aggregate is $\log K^{agg}_{Sib.EDAH^+} = 1.54 \pm 0.28$, where at that pH range (considering that both species have pK_a around 9), the molar fraction of both the neutral Sib and protonated EDA is above of the 80%, making possible the formation of this entity. The apparent solubility given by the fitted model seems to be almost the same as the intrinsic solubility given by HH.

Table 11 summarises the experimental solubility results found in this work for Glm, Pio and Sib when SF is used.

Table 11: Solubility values determined in this work for the three studied compounds by SF.

Compound	$logS_0$	$logS_0^{app}$	$logK^{agg}$ †
glimepiride	-7.14±0.02	-6.63	7.18±0.21
pioglitazone	-6.98±0.04	-5.70±0.05	7.98±0.12
sibutramine	-5.62±0.02		1.54±0.28

† in Glm and Pio, the log*K* is given for the respective neutral dimeric aggregate, in Sib, the log*K* is given for the neutral form of Sib interacting with a protonated specie of EDA

Compounds like Glm and Pio are molecules with many acceptors and donors of protons that could lead to form hydrogen bonds, which explains the capability of these two compounds to form neutral aggregates between themselves. On the contrary, the very limited hydrogen-bonding capabilities of Sib hinders self-aggregation, but this is not an obstacle to form aggregates between the neutral form with protonated species from buffer. In addition, the basic ionisable group of Sib allows the formation of salts when it is positively charged.

4.3.1.2 Potentiometric CheqSol® method

The $\log S_0$ values for Glm, Pio and Sib were also determined by CheqSol® methodology, starting with the same raw material used in SF experiments. The obtained results are listed in Table 12, where these values are the average from several replicates made with different starting solids (free base or hydrochloride salt) for each compound. In the potentiometric CheqSol method the titration is started when the sample is fully ionised and completely dissolved, as described in the introduction chapter, expecting only neutral species forming the precipitate.

Table 12: *Intrinsic solubility determined by CheqSol method* for the studied compounds.

Compound	***pK$_a$***	***logS_0[M]***	***literature***
glimepiride	5.41±0.06	-6.31±0.12	-6.44[a]
pioglitazone	5.67±0.09, 6.60±0.09	-5.81±0.24	-6.16[b]
sibutramine	8.74±0.12	-5.33±0.13	–

a in [91]; **b** [117]

The experimental values are close to those reported in bibliography (Table 12), which were conducted in both cases under the same potentiometric method than our work. On the other hand, the $\log S_0$ obtained by CheqSol are very similar to the $\log S_0^{app}$ obtained by SF method (see Table 11). It means that CheqSol method cannot differentiate if neutral aggregations in solution are formed or not. In fact, the algorithms of CheqSol do not include the formation of aggregates in its base-model. Therefore, the $\log S_0$ reported by Cheqsol corresponds to the apparent one $(\log S_0^{app})$ for these cases.

However, as before described (in section 1.6.2), this method can distinguish between *chasers*, *non-chasers* or *special case* compounds, and evaluate the possible supersaturation of the solutions.

The following paragraphs are to describe the characteristics found for each

molecule using the obtained profiles of neutral species-concentration vs time and Bjerrum graphics from the potentiometric titrations.

Glimepiride

Glimepiride because of its acidic nature, was titrated starting at basic pH to ensure solubility of the sample. Then, acid was added until precipitation appeared and chaser behaviour was produced, determining the intrinsic solubility. Figure 40A shows the theoretical Bjerrum function curves for the solubilised and precipitated sample, together with the experimental titration points. Figure 40B in turn shows the neutral species concentration as a function of time during the titration, where can be appreciated the Kinetic Solubility (S_K) and the extent and duration of the supersaturation. Both graphs are representative profiles corresponding to a chaser compound.

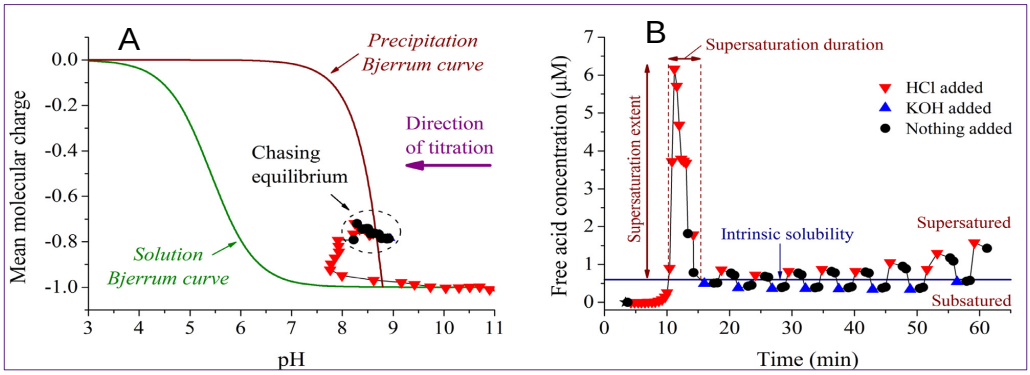

Fig 40: Potentiometric solubility of glimepiride: (A) mean molecular charge for Bjerrum function of solubility, including precipitation curve and experimental titration points. (B) neutral species concentration – time profile.

The supersaturation of Glm in the solution remains around 6±1 minutes with a $R_S = 124 \pm 23$ when S_K is reached, it means that the concentration of the sample reached at this point is more than 120 times higher than its solubility, keeping this supersaturation for a few minutes. When the precipitate appears (concentration falls in Figure 40B), the sample keeps its crystalline form

unaltered during the time of the assay, maintaining the chasing process relatively constant over time (black points in graphs of Figure 40).

Pioglitazone

The amphotheric nature of Pio allows to start the titration from acidic or basic pH. However, at pH 1.8 the solubilisation was not complete and thus, the titration was started at pH 11.5 where the sample was completely ionised and dissolved. The experimental points match the first segment of the Bjerrum theoretical solubility curve (Figure 41A, red points) until pH around 9.

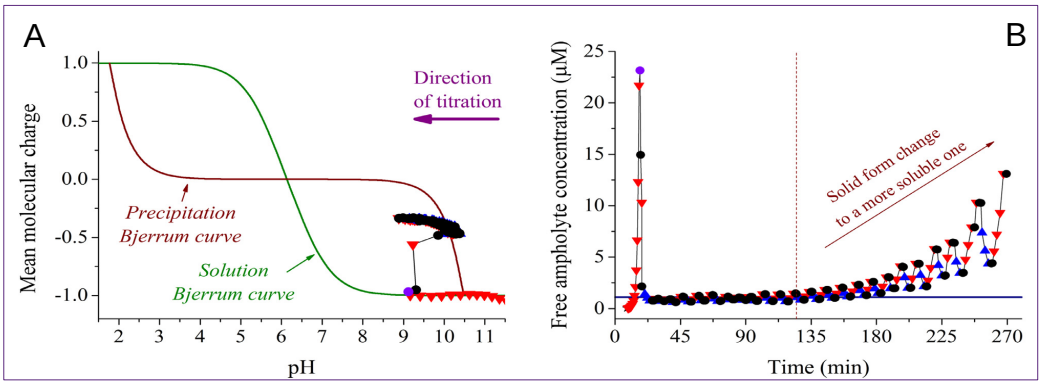

Fig 41: Bjierrum plot (A) and chasing conditions (B) for potentiometric determination of solubility of Pio.

When the precipitate appears the experimental points match now the theoretical precipitation curve (group of black points), where these points are moving in a narrow range around pH 10. However, about 130 minutes after the beginning of the assay the behaviour of the titration slightly changes, and after around 180 minutes the titration pH range increases, covering almost two pH units (Figure 41A). This indicates that the solid form of the Pio is changing into another form, making that the concentration of the neutral species of Pio progressively increases.

Figure 41B denotes the typical chaser behaviour of Pio which can supersaturate the solution in $R_S = 10 \pm 2$ with duration of 7 ± 2 minutes. The difference in R_S between Pio and Glm is in accordance to the parameters of hydrogen bonding capabilities (H-donors/acceptors), PSA and Pol of these molecules, where Glm have higher values for these parameters respect to Pio (see Table 3).

Sibutramine

The titration of Sib started at acidic pH, where the molecule is completely solubilised and ionised. For this molecule different behaviours can be appreciated (Figure 42). The first observed behaviour of this sample is that of a typical non-chaser compound, where once a precipitate appears, the experimental points follow the theoretical precipitation curve (Figure 42A, blue points). This behaviour remains until pH ~10 and after about 60 minutes the sample changes and its neutral species concentration increases, reaching its maximum value (Figure 42B). After this point, the concentration falls drastically and this new behaviour takes around 20 minutes to stabilize between the non-chaser and chaser forms (red points in Figure 42B). When the sample has mostly been converted into the *chaser form* (around 90 min after the beginning of the assay), the titration now follows the typical behaviour for this

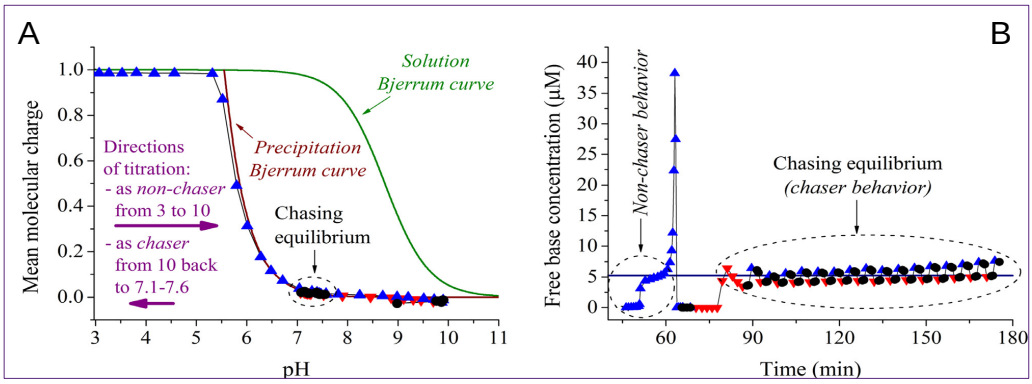

Fig 42: Cheqsol titration for Sib: (A) Bjerrum curves for precipitation and solubilisation, (B) Concentration of neutral species as a function of time.

form, as can be seen in the group of black points in Figure 42.

During the stabilisation time between the non-chaser and chaser behaviours, the calculation of the concentration is very difficult because, in this transition zone, the molecular charge is close to zero. The stability observed during the process of chasing equilibrium (chaser form) is indicative that, at least during this time of assay and experimental conditions, this process of change from a non-chaser to a chaser form is not reversible for Sib.

The intrinsic solubility $(\log S_0)$ calculated from the non-chaser form is −5.28 ± 0.06 using a curve fitting approach to Bjerrum precipitation curve, whereas that calculated from the chaser form applying the crossing points method is −5.37 ± 0.14. The $\log S_0$ from chaser form is consistent with the non-chaser result, and it is also consistent with the solubility found by SF (see Table 11). This is why the reported value of solubility in Table 12 is the average from the non-chaser and chaser forms results.

4.3.2 Study of the effect of some solubility enhancers

This section is focused on the use of some excipients, particularly Captisol (CAP), Cavasol (CAV), Klucel (KLU), Kollidon (KOL) and Plasdone S630 (PS630), to measure their effect on the solubility of benzthiazide (Bzt), isoxicam (Iso) and piroxicam (Pir), assayed by Shake Flask (SF) methodology. Different dissolution media are also used to simulate the pH conditions of several zones of GIT, thus, buffer solutions of Acetate/Phosphate (Ac/P) or Maleic/Maleate (MM), as well as FeSSIFv2/FaSSIFv2 as biorelevant dissolution media (BDM), are also applied in the presence of the APIs with or without excipients.

The selected APIs have acidic properties with pK_a values (see Table 5)

relatively close to the pH values studied. The chosen pH values, i.e. 2.0, 5.8 and 6.5, are of physiological interest. The first value is approximately the pH at stomach, but also it allows the S_0 determination of the compounds (except for Pir where its S_0 is determined at pH~3.5). The pH 5.8 is the pH at duodenal stage when it is in fed state conditions, whereas the physiological pH of a fasted state in duodenum is 6.5. These last two pH values correspond to FeSSIFv2 and FaSSIFv2 biorelevant media, respectively.

Acetate/Phosphate (Ac/P) and Maleic/Maleate (MM) buffers were used to prepare the different solutions. Ac/P buffer is selected because it is widely used in solubility studies and has a good buffering capacity in the working pH range. Moreover, no salt formation with phosphate is expected[73]. The MM buffer was selected because it is the buffer used for FeSSIF and FaSSIF media preparation, and its buffering capacity covers the pH range of interest. As Ac/P buffer, the components of MM buffer are of acidic nature and no ionic interactions with the selected APIs are expected, such as salt formations.

In the appendix (Table A3) are listed the solubility values obtained for each API at the different aqueous media used.

4.3.2.1 *The effect of pH on solubility*

In first place, the experimental solubility values obtained in the different aqueous buffer conditions (Ac/P and MM) were evaluated. For the stirring SF period, no change in pH of the solutions was observed after 4 hours of stirring due the low solubility of the compounds and the good buffering capacity of the buffers used. The PXRD performed on the solids collected (see Appendix, Figure S8) at the different pH values were the same as the raw materials, where Bzt and Iso are their phase I and Pir is mainly the monohydrate. Anhydrate of

Pir is also present in less than 10%, but the difference in the solubility of both forms is negligible, and the presence of the anhydrate does not improve the solubility of the drug[118].

Measured $\log S$ values were used to establish solubility-pH models for the compounds, that allow not only the prediction of solubility at any pH value, but also to evaluate which equilibria in solution (i.e., acid-base, aggregations) are affecting the solubility. For the three studied compounds a Henderson-Hasselbalch (HH) model, which only considers the acid-base dissociation equilibria as the one that can affect to solubility, was first tested. When this model did not fit to the experimental values, other models were tested. Table 13 shows the fitted and bibliographic solubility values, and Figures 43 – 45 show the $\log S - pH$ profiles obtained.

Table 13: Fitted and bibliographic values of solubility for the studied compounds. $(\log S_0)$ *intrinsic solubility,* $(\log S_0^{app})$ *apparent intrinsic solubility,* $\log K_2^{A_2H_2}$ *aggregation constant. GOF goodness of fit. Solubility values in mol·L^{-1}.*

Compound	***pK$_a$***	***logS$_0$***	***logS$_0^{app}$***	***logK$_2^{A_2H_2}$***	***GOF***	***logS$_0$ literature***
Bzt	6.54 9.22	-5.03±0.01	--	--	4.9	-4.84±0.22[a]; -4.83±0.01[b]; -4.89±0.09[c]; -5.13[d]
Iso	3.84	-6.70±0.02	-5.68±0.02	7.39±0.05	1.0	-5.61±0.14[c]; -5.75[e]
Pir	1.89 5.31	-4.63±0.03	--	--	1.8	-4.80±0.02[f], 4.68[g] -4.72±0.003[g], -4.75[h]

a in [120]; **b** in [122]; **c** in [93]; **d** in [121]; **e** in [77]; **f** in [122]; **g** in [123]; **h** in [119].

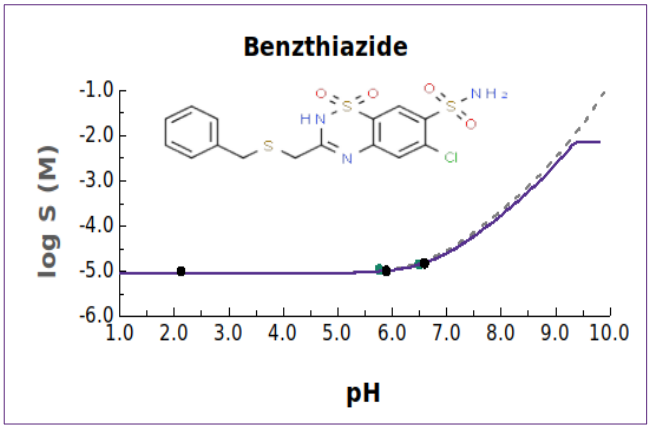

Fig 43: Benzthiazide: (solid line) fitted model, (dashed line) HH theoretical model. (green points) Ac/P buffer. (blue points) MM buffer

Benzthiazide seems to follow a simple HH behaviour. Figure 43 shows the HH fitted model (solid line) together with the theoretical one (dashed line) built from the intrinsic solubility and the spectrophotometrically determined pK_a values. Even the lack of experimental points at pH > pK_a, the HH fitted model matches the experimental values. The adjusted $\log S_0$ = -5.03 ± 0.01 agrees with the reported by Avdeef[120] in his $wiki-pS_0$ data base, where the solubility values were evaluated and processed, when necessary, to obtain S_0 at 25 ºC. This value includes the CheqSol determinations by Fornells[93] and Llinás[122]. Although the value reported by Igo et al.[121] is lower, it is not far from the one obtained in this work. These last authors also reported $\log S$ values in phosphate buffered saline solutions, which are also lower than the predicted by the theoretical HH model. This could indicate the formation of aggregates and to confirm this hypothesis, more solubility values should be determined above pH 6.5.

The HH model does not match the experimental points of Iso (Figure 44). Then, a model considering dimeric aggregates formed by neutral species is proposed and good fit is obtained. The fitted model corresponds to the model for neutral aggregates for an acidic compound given in Table 1, in the introduction chapter. The apparent solubility obtained $\left(\log S_0^{app}\right)$ is around 1.2 times higher than the intrinsic solubility determined from the fitted model and, it agrees with the

obtained value by CheqSol method. Given that the theoretical HH model and the fitted model matches in the sloped segment (Figure 44), then the aggregation capacity of Iso is not promoted by its ionic species, whereas the neutral species of Iso are interacting to form the self-aggregate.

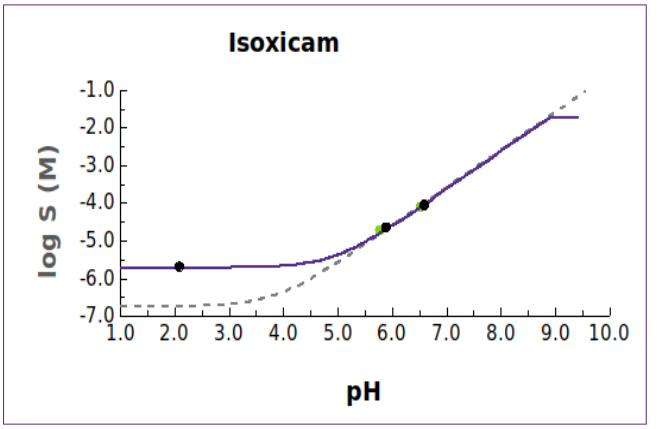

Fig 44: Isoxicam model of solubility: (solid line) calculated aggregation model. (dashed line) HH theoretical model. (green points) Ac/P buffer. (blue points) MM buffer.

As can be seen in Figure 45, Pir shows the HH behaviour of an amphiprotic compound and no evidence of aggregates is found. The $\log S_0$ determined in this work agrees with the values reported in literature either by SF or CheqSol methods.

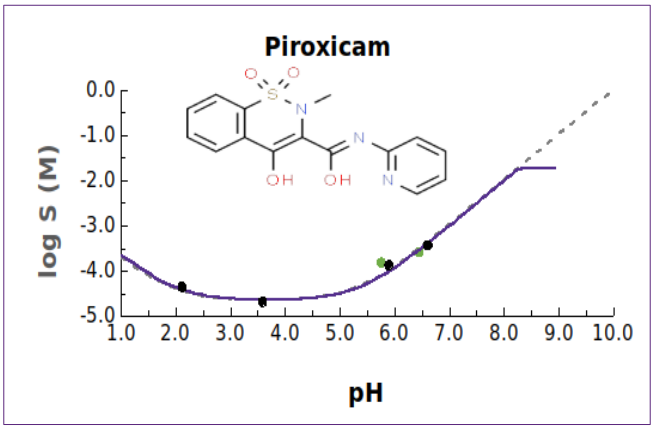

Fig 45: Pir solubility models: (solid line) calculated model, (dashed line) HH corrected model. (green points) Ac/P buffer. (blue points) MM buffer.

Table 14 and Figures 43 – 45 show the experimental solubilities obtained at the different worked pH values in both aqueous buffer solutions, Ac/P or MM. At pH 5.8 and 6.5 the respective solubility values obtained by buffer type show non-significant differences between them, which confirms the same solubility

behaviour of the studied APIs in both buffers. Therefore, average values from these results can be calculated and settled as aqueous reference values. For each compound, the solubility increases with pH increment, because of the ionisation degree, and the higher the concentration of ionised species of the compound in the solution, the higher its solubility value.

Table 14: Experimental log*S values in two aqueous media at different pH.*

	logS(exp)			
	pH 2	**pH 3.5**	**pH 5.8**	**pH 6.5**
		Bzt		
Ac/P	-5.00±0.00	--	-4.99±0.03	-4.82±0.01
MM	--	--	-4.96±0.05	-4.84±0.01
average			-4.97±0.02	-4.83±0.01
		Iso		
Ac/P	-5.68±0.03	--	-4.63±0.07	-4.04±0.03
MM	--	--	-4.71±0.08	-4.09±0.03
average			-4.67±0.08	-4.07±0.04
		Pir		
Ac/P	-4.35±0.03	-4.68±0.03	-3.87±0.04	-3.48±0.01
MM	--	--	-3.81±0.02	-3.44±0.02
average			-3.84±0.04	-3.46±0.03

4.3.2.2 *The effect of the addition of excipients on aqueous solubility*

The effect of the addition of several excipients on the solubility of Bzt, Iso and Pir in aqueous media was studied at different pH values. Five excipients were selected, two from group of cyclodextrins (CAP and CAV), and three from polymeric composition group (KLU, KOL and S630). Their characteristics or properties are described in “Functionality of excipients” (*section 1.5.1.2*).

The solubility values obtained in presence of excipient were compared with that obtained without excipient. In order to check if the solubility enhancement is significant, the limits to determine this significance were established using twice the standard deviation as upper and lower limits, this is logS±2SD. However, because of the small experimental SD obtained in some cases, the

limits adopted were consisting on using a SD of 0.05 at each pH studied for the lonely API solubility. This SD value corresponds to an average standard deviation obtained in our laboratory for SF solubility measurements, that is in agreement with the recommended one when SF method is properly performed[73, 124]. Then, any obtained solubility within these limits can be considered as statistically non-significantly different from the respective reference value.

Usually the solubility of acids increases with pH because of the increment in the ionisation degree of the substances, but the addition of excipients generates different behaviours depending on the API and/or the enhancer, changing the solubility in different degree.

Table 15: variation of $\log S$ *according to the charged state of the APIs in aqueous media.*

Charged state	Enhancer	$\Delta logS$		
		Bzt	**Iso**	**Pir**
Neutral form	CAP	0.46	0.42	0.41
	CAV	0.22	0.76	0.31
	KLU	0.10	1.03	0.57
	KOL	0.24	0.38	0.48
	S630	0.32	0.99	0.62
pH 5.8	CAP	0.37	0.19	-0.06
	CAV	0.18	0.12	0.11
	KLU	0.12	0.27	0.25
	KOL	0.33	0.37	0.27
	S630	0.48	0.46	0.35
pH 6.5	CAP	0.20	0.01	-0.02
	CAV	0.15	0.12	0.18
	KLU	0.16	0.29	0.40
	KOL	0.34	0.22	0.46
	S630	0.51	0.40	0.55
Cationic form	CAP	–	–	0.51
	CAV	–	–	0.11
	KLU	–	–	0.50
	KOL	–	–	0.38
	S630	–	–	0.48

The average experimental log S values can be observed at Appendix (Table A4) and Figure 46. Table 15 shows the variations of these aqueous log S obtained for each API in presence of excipients (formulated at 50% w/w respect to API), with respect to the aqueous solubility of the API alone at the different pH values studied, and grouped by the charged state of the samples. The results are evaluated by excipient-type order, this is cyclodextrins and polymeric type enhancers, to compare results between similar additives.

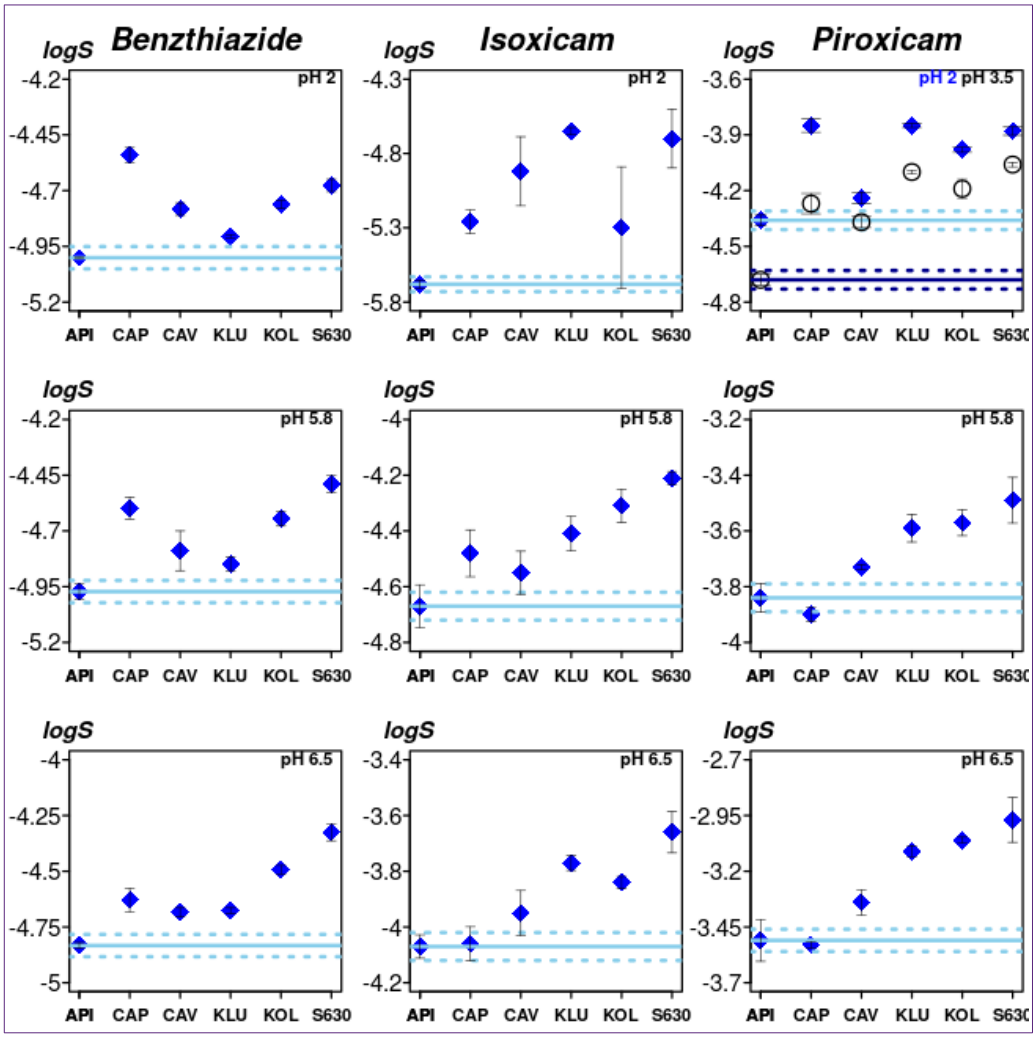

Fig 46: Solubility of the three studied compounds in aqueous media with and without excipients. (o) pH 3.5

Cyclodextrins in the solubility enhancement

Solids collected in the presence of CAP and CAV are mainly the same than those collected for the three API when no enhancer is used. This is Bzt and Iso showing their respective phase I forms and Pir is in its monohydrate form. Only when CAV is used a minimal presence of anhydrous form of Pir is detected which, as we appointed before, it does not have any influence in the enhancement of solubility. Then, at same pH stage studied, the increase in solubility of the compounds can be explained by the presence of the cyclodextrin in solution. As observed in Figure 46 and Table 15, when the three compounds are in neutral form, this is at pH 2 for Bzt and Iso and pH 3.5 for Pir, the main expected interactions are from hydrophobic type, driven by the inclusion of the molecules inside of the cavity of the CDs. Nevertheless, CAP and CAV do not act in the same way respect to the API.

Although CAP and CAV are both β-cyclodextrins, their cavities have different sizes, particularly at the entrance. The sulfonic groups in CAP are repulsing each other and the cavity gets enlarged, whereas in CAV the –OH groups in the limits of the entrance are closer each other, and thus the size of its cavity is smaller. This could cause difficulties for the molecules to be introduced into the cavity of CAV due to steric impediment, reducing their hydrophobic interactions with CAV. This effect can explain why the use of CAV enhances the solubility of Bzt and Pir in a lesser degree than CAP. Nevertheless, CAV behaves in a better degree with Iso. This could be because Iso in its neutral form can interact with CAV by formation of hydrogen bonds (HB) between the hydrogen of the external groups of the CD and the isoxazole ring from Iso[60, 61], producing in this way a better enhancement of the solubility of this compound when CAV is used respect to the other two molecules. This electrostatic

interactions could be in a very lesser degree in Pir respect to Iso (both are oxicam derivatives), because the piridinic ring of Pir has only one HB acceptor heteroatom, whereas two of them are present in the isoxazole ring of Iso.

When pH increases from 2.0 to 5.8, the effect of CAP is almost the same for Bzt, but its activity decreases with Iso and Pir. Similar situation is observed with CAV. This can be caused by the different ionisation degree of the drugs, where Bzt is less than 15% ionised, Iso is fully deprotonated and Pir is more than 70% negatively charged, influencing in a different way their interaction with these excipients. Hence, the hydrophobic interactions between Bzt and CAP are mostly present, but in case of Iso and Pir the hydrophobic interactions are significantly reduced and in addition, their increased negatively charged species could cause repulsion with the sulfonic groups of CAP. This reduced effect is more evident in Pir than in Iso (see Table 15), probably due to the presence of electrostatic interactions between Iso and the external functional groups of the excipient. Whereas in CAV, its external hydroxyl groups do not cause electrostatic repulsion with the negatively charged species of the drugs.

When pH is 6.5 the activity of CAP is reduced for Bzt but still working, because Bzt at this pH is still around 60% neutral. Meanwhile, for Iso and Pir the effect of CAP is almost negligible, since they are both fully ionised and electrostatic repulsions with sulfonic groups are expected. For CAV, when pH increases no significant changes in the solubility behaviour are observed for the three APIs in reference to pH 5.8.

At pH 2, where Pir is close to 40% protonated, the enhancer effect from CAP is higher than that with CAV, since CAP could interact with both, neutral and protonated species of Pir, by hydrophobic and electrostatic interactions respectively. The negatively charged sulfonic groups in CAP could be balanced

with the protonated Pir. In case of CAV, the interaction with protonated Pir seems to be negligible, and the effect of CAV on solubility of Pir at this pH is due to the hydrophobic interactions only. Then the variation in solubility is lower than that at pH 3.5, where Pir is fully neutral (see Table 15).

In summary, the solubility-enhancer effect from CAP or CAV is reduced with the increase of the ionisation degree of the compounds, due to the fact that the principal interactions between APIs and excipients are of hydrophobic type. The low solubility enhancement observed at pH 5.8 and 6.5, could be attributed to the ionisation of the APIs, which reduces the extent of hydrophobic interactions and increases the electrostatic repulsions with the polar groups of the external surface of the CDs.

Polymeric excipients and its behaviour in the solubility enhancement

Polyvinylpyrrolidones (PVPs) and their copolymers with vinylacetate are hydrophilic excipients. Their functionalisation make them show a good affinity for water and they will tend to be dispersed through the solution helping the dispersion of the APIs. The difference between the used PVPs is the presence of vinylacetate groups in S630 respect to its absence in KOL, making S630 more hydrophilic than KOL (see section 1.5.1.2), which in turn causes a difference in the HB acceptor capability. Thus, S630 seems to have a better interaction with molecules with HB donors than KOL.

In its neutral form the three studied molecules have at least one HB donor, which can interact with the HB acceptors from PVPs. The HB formation abilities of Bzt could be lower than those in Iso and Pir, and thus, the solubility of Bzt is less increased by these PVPs with respect to Iso and Pir. On the other hand, PVPs especially S630, could interact in higher degree with Iso due to HB

interactions with its isoxazole ring. Nonetheless, the $\log S$ values measured for Iso at pH 2.0 in different replicates in the presence of S630 or KOL show high variability, which could level off the improvement observed for the S630. A slight enhancer effect in solubility can also be detected for Pir at pH 3.5 when S630 is used as excipient. Figure 46 and Table 15 show the differences of $\log S$ obtained for the three APIs applying these PVPs.

When pH is increased up to 5.8, the effect of PVPs on the solubility of Bzt seems to be slightly better. On the contrary, the solubility of Pir when pH increases seems to decrease with PVPs (see Table 15). Although the ionisation degree of Bzt increases with the pH, it is not even close to 15% at pH 5.8, and then the HB interactions remains almost the same because there are more neutral species of Bzt than ionised. In opposite, at pH 5.8 the ionisation degree for Pir is more than 70% deprotonated thus, the enhancer effect of PVPs is lower because of losing HB interactions due to increased concentration of ionised species.

When pH is 6.5, there are not significant changes in solubility of Bzt or Iso in presence of PVPs. At this pH value, the ionisation degree of Bzt is about 40%, the enhancer effect remains the same because there is still more neutral phase of Bzt than ionised, whereas Iso is fully ionised as in pH 5.8. Regarding to Pir, which at pH 6.5 it is now at least 90% ionised, surprisingly the solubility enhancement seems to be slightly better at this pH value than the variation observed at pH 5.8, and very similar variation than that at pH 2.0. At this latter pH value, the positively charged Pir (>40%) could interact with any electron donor site of polymeric excipients, especially S630, increasing its solubility. At pH 6.5 the few remaining neutral form of Pir (<10%) and its negatively charged species could be involved in some type of interactions with the excipients,

which are not present with Iso at the mentioned pH, slightly improving its solubility.

At difference from PVPs, KLU is a hydroxypropylcellulose (HPC) characterised for being a HB donor. Comparing the enhancement made by KLU on neutral Bzt respect to the other two polymeric excipients, KLU is less active because of the low HB acceptor capability of Bzt. This capability remains similar even when pH changes, because of the low ionisation degree of Bzt (<50% at pH 6.5), as discussed previously. Hence, the HB relationships are the same between Bzt and KLU at different pH values. The overall effect of KLU represents a change of only around 0.12 $\log S$ units, which can be seen in Table 15 and Figure 46.

The enhanced solubility of neutral form of Iso and Pir caused by KLU through HB seems to be better than the effect produced by the other polymeric excipients, being it around 1.03 $\log S$ units for Iso and 0.57 units for Pir (see Table 15). The interaction between KLU and Iso is affected when the pH changes from 2.0 to 5.8, probably due to the difficulties of KLU to be reactive in front of the deprotonated species of Iso. However, some HB interactions are still present, giving to KLU still some capacity to enhance the solubility of Iso at this pH value. This characteristic remains stable when pH changes to 6.5. On the other hand, KLU seems also to have better interactions with neutral and protonated Pir species, whereas the interaction with the deprotonated form seems to show another behaviour not very well defined (like in PVPs). For this last part, a more extensive study of the solubility – pH profile could be needed, although, the enhancer capacity of KLU is clearly present.

4.3.3 The effect of Biorelevant Dissolution Media (BDM) on the solubility

This section is focused on the solubility of APIs by the usage of BDM (FeSSIFv2 and FaSSIFv2), compared against the results in aqueous media at pH 5.8 and 6.5. Besides, the mixtures made with excipients and APIs (1:1 ratio) were also studied using these BDM solutions. In first instance, each API was tested in BDM and contrasted with its solubility in aqueous medium. Afterwards, excipients were added and the variation on solubility was contrasted with respect to the solubility of pure API in BDM. The experimental *logS* values obtained under these conditions are listed in Appendix (Table A5).

FeSSIF and FaSSIF are both intestinal fluid simulators for different feeding states. The differences between them are not only the pH value in solution, 5.8 in FeSSIF and 6.5 in FaSSIF, but also in the concentration of their components, principally in taurocholate and lecithin. Their higher concentration in FeSSIF allows the formation of micelles, which in turn are not expected in FaSSIF. Then, neutral compounds can be introduced inside the micelles and ionic compounds could interact with the surface of the micelle, depending on the external charge of the latter. Moreover, drugs could also interact with the free components of the biorelevant media in solution.

Table 16 shows the variations of $\log S$ for the three studied drugs at pH 5.8, corresponding to FeSSIF, where Bzt is more than 85% neutral, Iso is nearly 100% ionized and Pir is about 25% in its neutral state. Under these conditions, the neutral species of the samples could partition into the FeSSIF micelles, and since Bzt is the only highly neutral, it shows the highest variation of solubility in this BDM (around $0.5 \log S$ units). In case of Iso and Pir, since they are similar in structure, a resembling interaction with FeSSIF is expected, although

the effect on Pir seems to be better. The presence of some portion of neutral form of Pir in solution possibly allows the API to partition into the micelle, together with some electrostatic interactions of the ionised species with the charged external face of the micelle. The minimal increment on solubility present for Iso could be only due to the interactions of its ionic species with the micellar external face.

Table 16: Variation of $\log S$ *between aqueous and BDM values for the studied compounds.*

	API	$logS_{(aq)}$	$logS_{(BDM)}$	$\Delta logS$
in FeSSIF (pH5.8)	Bzt	-4.97±0.04	-4.49±0.03	0.48
	Iso	-4.67±0.08	-4.50±0.01	0.17
	Pir	-3.84±0.05	-3.48±0.01	0.36
in FaSSIF (pH6.5)	Bzt	-4.83±0.01	-4.62±0.04	0.21
	Iso	-4.07±0.04	-4.02±0.01	0.05
	Pir	-3.51±0.09	-3.21±0.06	0.30

$logS_{(aq)}$ aqueous solubility. $logS_{(BDM)}$ solubility in the respective biorelevant dissolution media.

When FaSSIF is used the pH changes to 6.5 and no micelles are expected. Iso shows nearly no variation in $\log S$ at difference from FeSSIF. The 100% ionised species of Iso do not interact with the FaSSIF constituents. In case of Bzt, where it remains around 50% neutral, the increment in its solubility is not as high as in FeSSIF. However, some hydrophobic interactions with the free components from FaSSIF must be present to produce this solubility enhancement. Interestingly, despite of the high deprotonated state of Pir (> 90%) at pH 6.5, the effect of FaSSIF on the increment of its solubility is practically the same as in FeSSIF, probably due to interactions between the ionic species of Pir with the constituents from FaSSIF.

Figure 47 shows the $\log S_{aq}$ obtained for Bzt, Iso and Pir in aqueous media at pH 5.8 (left panels) and 6.5 (right panels), together with the effect of the studied

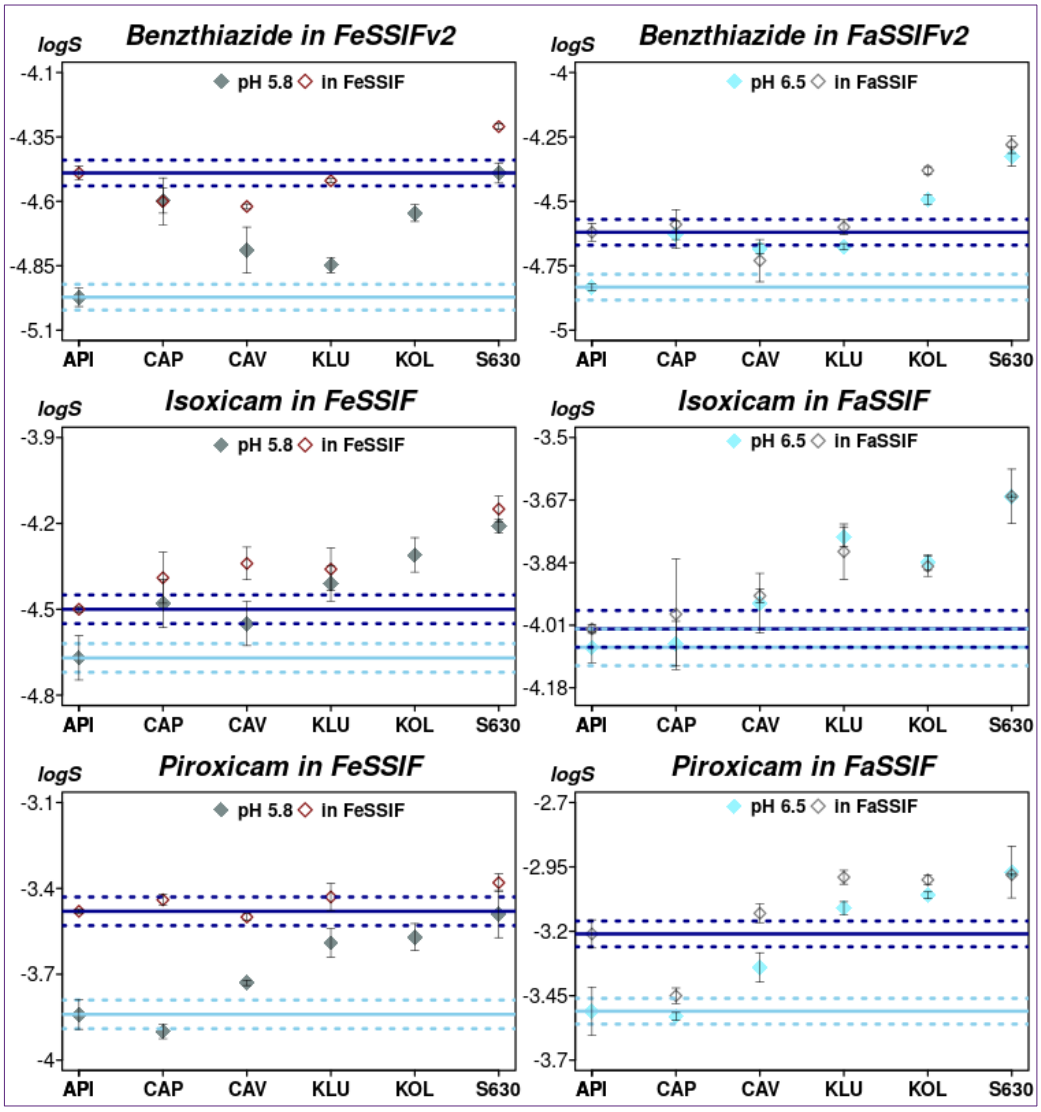

Fig 47: Experimental logS in aqueous (filled diamond) and BDM (empty diamond) for the three studied compounds alone and in presence of excipients. (pH 5.8) and (pH 6.5) corresponding to aqueous media solubilities. (In FeSSIF) and (in FaSSIF) for solubilities in the respective BDM.

excipients in the solubility (as in Figure 45 for pH 5.8 and 6.5). Additionally, for the sake of comparison, in same Figure are also included the solubilities in BDM $(\log S_{BDM})$ obtained in FeSSIF (left side) and FaSSIF (right side) for

APIs alone, and solubilities in the presence of excipients ($\log S_{BDM}^{exc}$). Initially, the solubilities of Bzt and Pir alone are increased by BDM, whereas solubility of Iso alone suffers a minor effect by FeSSIF and none with FaSSIF.

When the excipients are introduced, the solubilities in BDM change in different ways and also depending on the API tested (see Figure 47). For example, when CAP is used the $\log S_{BDM}^{exc}$ of Bzt seems to be lower respect to its value of $\log S_{BDM}$ obtained in FeSSIF. Nevertheless, when its $\log S_{BDM}^{exc}$ is compared to the respective $\log S_{aq}$ value, they are virtually the same. Hence, the effect of FeSSIF is lost, meaning that Bzt has total affinity for CAP instead of the micelles. When CAV is used in FeSSIF, the solubility of Bzt diminishes but it is still better than the aqueous value. In this case, most of the Bzt is interacting with CAV and some with FeSSIF, the effect of the latter is still present but in a lesser degree than FeSSIF without CAV. Could be possible that a mixed micelle formed by FeSSIF constituents and excipient can interact with the API, but in a lesser degree than FeSSIF alone and in a higher degree than excipient alone.

On the contrary, the solubility of Iso in FeSSIF with presence of CDs seems to be enhanced, due to a synergistic or additive effect between the excipient and the BDM. In case of Pir, its solubility is not enhanced in presence of excipients and FeSSIF, though, it is not lower than the solubility produced only by FeSSIF. The presence of excipients do not alter the action mechanism of FeSSIF, in this case, the effect of the excipients is practically null (see Figure 47).

The hydroxypropylcellulose (KLU) and PVP (S630) excipients seem to work better than CDs in presence of FeSSIF (pH 5.8). For Bzt, the presence of KLU is not relevant since the solubility is the same as in FeSSIF without excipient, but at least the solubility is not reduced. Nonetheless, S630 exerts an additive

action to the enhancer effect of FeSSIF, yielding a higher solubility. A similar behaviour is observed when Pir is tested. On the contrary, the solubility of Iso with KLU or S630 in presence of FeSSIF is statistically the same as the solubility generated by these excipients in aqueous media alone, as can be appreciated in Figure 47, where the error bars are overlapped. Unfortunately, it was not possible to test KOL in FeSSIF.

In FaSSIF medium the obtained results do not reveal either a clear trend: in some cases the effect of the BDM is nullified, in other cases the effect of the excipient is almost null or at least very low, and in a few other cases there is a synergic action between the enhancers and the FaSSIF (see Figure 47). Besides, polymeric excipients seems to work better than CDs, while FeSSIF do the same respect to FaSSIF. In FeSSIF, S630 yields the highest increase in solubility, particularly in the case of Iso. However, since S630 yields the highest $\log S_{aq}^{exc}$ values of in aqueous medium, and the results are quite similar to those in BDM, it means that the APIs are more likely to interact with this excipient than with FeSSIF or FaSSIF constituents. Thus, these BDM do not alter or change the action mechanisms of this excipient, having also no synergic effect. However, this synergic effect is observed with CAV and KLU, at time that KOL in FaSSIF shows an intermediate behaviour between KLU and S630 (see Figure 47).

4.4 Dissolution rate: effect of pH, enhancers and media

Previously, the property of solubility of benzthiazide, isoxicam and piroxicam was determined under some conditions that could be applied to extend a parallel study of the Dissolution Rate (DR) of the same compounds. As was described in the introduction chapter, since solubility is affected by pH and DR is directly related to the solubility of the compounds, pH also affects the DR. Then, the determination of DR of the mentioned compounds was conducted under one pH sector model, i.e. pH 2.0, 5.8 or 6.5, which are values of physiological interest, for 120 minutes per pH value. Simultaneously, DR assays with two pH sectors model were also performed to simulate the pass of the drug from stomach to duodenum. For the two sector model the experiment started at pH 2.0, keeping this value for 30 minutes (stomach lifetime), then the pH was immediately changed to 5.8 (small intestine fed state) or to 6.5 (small intestine fasted state) and kept during 120 minutes, accounting approximately for the small intestine lifetime of the ingested food or drug[6]. The aqueous media used for these assays were prepared using an Ac/P buffer, and the pH value was adjusted by the instrument, using HCl or KOH 0.5M. The used buffer is suitable due to their low spectral interference with the samples and low absorbance in UV spectral range.

As some excipients were previously studied in order to figure out if they improve the solubility of the APIs, the same excipients were used to stablish its effect on the DR, applying them at three levels of concentration, 1:3, 1:1 and 3:1 ratios of Excipient:API (w/w) respectively, in the arrange of one pH sector. After this study, the 1:1 Excipient:API ratio was selected to be applied for the two pH sectors array. The DR assays were also extended using Biorelevant Dissolution Media, i.e. FeSSIFv2 and FaSSIFv2.

Whereas the solubility refers to how much a compound can be dissolved in a certain volume of medium, the DR represents how fast the compound reaches that solubility in that medium, under specific pH, stirring conditions and other controlled parameters. Since DR is related with the solubility, if the excipients generate an improvement on this solubility, it could be also expected a positive effect on DR.

As was described in the experimental section, the solid mixtures of Excipient:API were introduced as tablets, to keep constant the surface contact area between the solution and the solid.

4.4.1 Dissolution Rate of benzthiazide, isoxicam and piroxicam in aqueous media

4.4.1.1 The pH effect

The effect of pH on the DR was first measured under the one pH sector model, where each sample remained at least 120 minutes at the respective pH value to ensure the solubilisation of enough amount of sample, expecting the appearance of a plateau. As described in the experimental section, the determination of the sample concentrations were performed using a miniaturized spectrophotometric method[32]. At each time point the concentration is calculated and plotted in front of time, allowing it to obtain the dissolution rate profiles and the determination, among other parameters, of the DR by usage of Equation 29 (see Introduction, section 1.3).

The dissolution rate profiles determined for the pure APIs studied at one pH stage model are presented in Figure 48, where each profile corresponds to the average of several determinations. The DR and the concentration at the end of the assay for the three studied pH values are shown in Table 17.

As can be appreciated in Figure 48, Bzt shows very similar profiles at pH 2.0 and 5.8, with similar DR values and final concentrations $[C]_f$ (see Table 17) that are not statistically different. This is due to the low ionisation degree of this compound (unionised at pH 2.0 and <15% ionised at pH 5.8). The pH value of 6.5 is close to the pK_a value of Bzt, and thus the ionisation degree of this acidic API increases up to 50%. Ionisation enhances the DR of Bzt and its concentration in solution rises. As can be seen in Table 17, the DR at pH 6.5 is more than twice the DR at pH 2 or 5.8, and the $[C]_f$ at pH 6.5 is about 1.7 times higher than that of the lower pH values.

Table 17: Dissolution rate (DR) and concentration at the end of the assay ($[C]_f$) for the studied compounds at one pH sector model.

API	*pH*	*Extrapolated DR (µg/min)*	$[C]_f$ $(\mu g/mL)$	$\frac{DR(pH_i)}{DR(pH_2)}$	$\frac{DR(pH_{6.5})}{DR(pH_{5.8})}$	$S_{(SF)}$ $(\mu g/mL)$
Bzt	1.93±0.09	0.35±0.19	1.09±0.29	--	--	4.31±0.01
	5.72±0.03	0.33±0.17	1.20±0.20	0.9	--	4.61±0.77
	6.45±0.13	0.79±0.11	1.80±0.37	2.3	2.4	6.35±0.38
Iso	1.86±0.02	0.18±0.05	0.17±0.03	--	--	0.70±0.04
	5.66±0.10	0.35±0.08	1.58±0.53	1.9	--	7.13±1.28
	6.45±0.06	0.61±0.03	3.44±0.28	3.3	1.8	28.86±2.78
Pir	1.91±0.01	2.89±0.06	12.97±1.31	--	--	14.59±1.89
	5.65±0.02	4.38±0.19	20.15±0.59	1.5	--	48.05±11.58
	6.37±0.05	9.21±1.52	44.13±4.40	3.1	2.1	101.36±44.33

$S_{(SF)}$ concentration from solubility obtained by SF assays at the respective pH value.

Nevertheless, in the three studied pH values the concentrations of Bzt are lower than the corresponding solubilities measured by SF. This is because during the assay time the dissolution profiles do not achieve a plateau, which indicates that the saturation of the system has not yet been reached at the end of the assay. The comparison of $[C]_f$ with the solubility values allows to determine how close is the system from its saturation.

As expected from its acid-base properties, the dissolution profiles of Iso (Figure 48) change significantly with the pH. At pH 2.0 Iso is in its neutral form and, due to the low solubility of the sample, the amount of substance delivered in the medium is also very low. In fact, the concentration in solution is close to the limit of quantification, and even close to the limit of detection in some instances at the beginning of the experiment. At pH 5.8 Iso is nearly 100% ionised, and at pH 6.5 it is fully deprotonated. Therefore, the DR and concentration are considerably changed from pH 2.0 to 5.8, and also increased at pH 6.5. The DR raises almost two times from pH 2.0 to pH 5.8, and 3.3 times to pH 6.5. Moreover, at pH 5.8 Iso reaches a $[C]_f$ almost ten times higher than that at pH 2.0, and when pH is 6.5 its concentration is more than twice at previous pH value. When the final concentration for Iso at each single pH value is compared to the respective solubility found by SF at those pH values, the concentration reached is nearly 7 times lower, confirming that the given solution is not saturated (see Table 17).

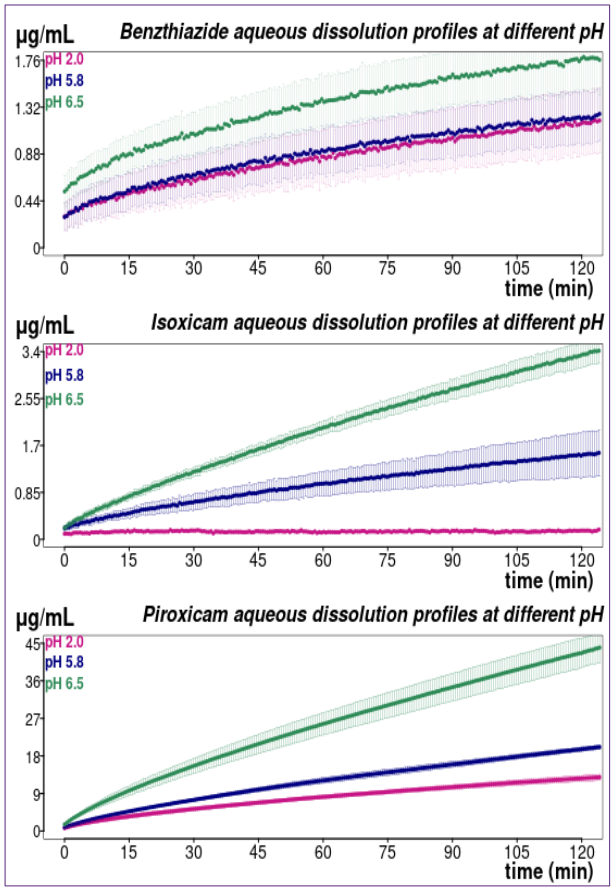

Fig 48: Dissolution profiles for Bzt, Iso and Pir in aqueous medium at pH 2.0 (magenta), pH 5.8 (blue), pH 6.5 (green).

The conditions for Pir at pH 2.0 correspond to around 40% protonated, at pH 5.8 it is almost 80% negatively charged and at pH 6.5 it is more than 90% deprotonated. Thus, considering the three pH values, the DR and $[C]_f$ for Pir are increased while pH increases. Due to Pir is the most soluble of the studied compounds, its DR at each pH value and its $[C]_f$ are also the highest of the three studied APIs. However, its changes in DR are in same magnitudes than the others. At pH 5.8, it is only around 1.5 times higher than its DR at pH 2.0, and 3.1 times faster at pH 6.5 respect to the first pH value. The more significant increase on DR takes place between pH 5.8 and 6.5, when DR is improved by a factor of 2.1 (see Table 17). Moreover, the increment of its concentration at each pH stage is only around twice of that found at previous pH stage, whereas Iso yielded 10 or 20 times more concentration with the respective pH change. This could be attributed to the ionisation degree, where Iso suffers a more substantial change in its charged state when pH changes from 2.0 to 5.8 or to 6.5. As Bz and Iso, the concentrations of Pir at the end of the assay ($[C]_f$) at each pH are lower than the solubility values determined by SF method (see Table 17), indicating that the systems have not reached saturation either.

4.4.1.2 Dissolution profiles at two pH sectors model

The pass of drugs through the GIT implicates a direct transition from pH 2.0 (stomach pH), to pH 5.8 or 6.5 (small intestine pH depending of the feeding state as early explained). To simulate these physiological conditions the dissolution profiles were obtained with the two pH sectors model. First, the pH was kept constant at pH 2.0 for 30 min (expected time for the drug to remain in the stomach) and then changed either to 5.8 or 6.5 (according to the simulating conditions required), keeping this second pH value for 120 minutes (time needed for the drug to pass the small intestine).

Figure 49 and Table 18 show that no significant differences are observed for Bz when the profiles at two pH sectors are compared to the profiles at one pH sector (Figure 48). Although no difference should be observed in DR value at pH 2, the ones obtained in the first of the two stages seem to be higher. Notice, however, that the standard deviation of DR in Table 17 is high and some individual replicates at pH 2.0 are similar to those obtained in the experiments performed with two pH sectors model. This slightly increase should be due to subtle differences in the elaboration of the pill (such as the own nature of the powder obtained for each API), or to the delay time at the beginning of the assay due to experimental configuration of the instrument used.

As expected, when the pH changes from 2.0 to 5.8 or 6.5, the DR at the second pH sector is lower because of the presence of already dissolved API coming from the first sector. Although the DRs at pH 5.8 and 6.5 in the two sectors model are lower than those in single pH stages, the $[C]_f$ in both models are not significantly different. When pH changes from 2.0 to 5.8 the dissolution profile of Bzt follows a continuous trend and no variation is observed in the

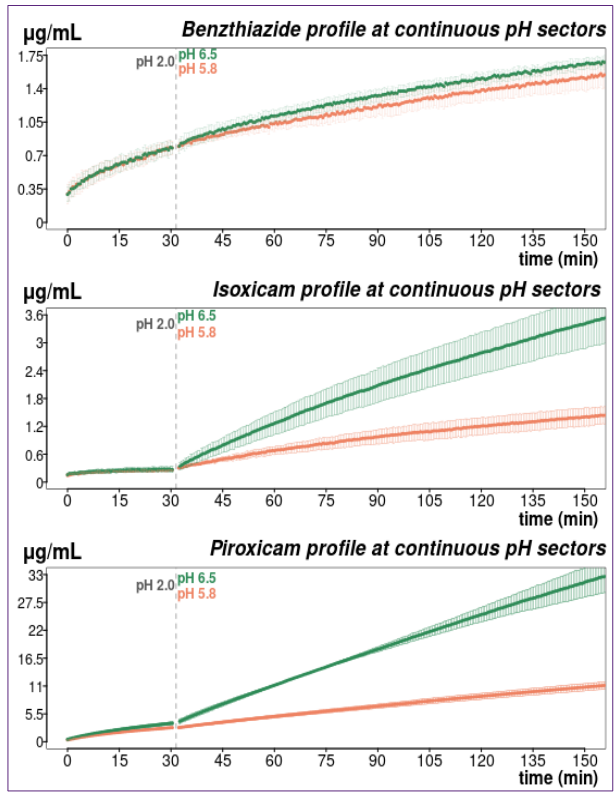

Fig 49: Aqueous dissolution profiles for the studied APIs at two pH stages model. (orange) pH 2 – 5.8 (green) pH 2 – 6.5

transition between both pH values. This is because the ionisation degree of Bz remains low. However, the increase in the ionisation at pH 6.5 leads to a slight enhancement in the dissolution rate and in the dissolution profile (see Figure 49).

Table 18: Dissolution Rate (DR) and Final Concentration ($[C]_f$) obtained for the studied compounds at two pH sectors model.

API	pH	Extrapolated DR (µg/min)	$[C]_f$ $(\mu g/mL)$	$\frac{DR(pH_i)}{DR(pH_2)}$	$\frac{DR(pH_y)}{DR(pH_x)}$	$S_{(SF)}$ $(\mu g/mL)$
Bzt	1.89±0.01	0.63±0.10	0.77±0.11	--	--	4.31±0.01
	5.68±0.06	0.20±0.07	1.54±0.17	0.3	--	4.61±0.77
	6.36±0.03	0.29±0.02	1.68±0.06	0.4	1.4	6.35±0.38
Iso	1.92±0.06	0.49±0.29	0.26±0.08	--	--	0.70±0.04
	5.73±0.04	0.29±0.09	1.45±0.26	0.6	--	7.13±1.28
	6.42±0.04	0.64±0.18	3.56±0.67	1.3	2.2	28.86±2.78
Pir	1.92±0.05	2.68±0.46	3.22±0.48	--	--	14.59±1.89
	5.75±0.04	1.70±0.13	11.18±1.05	0.6	--	48.05±11.58
	6.44±0.01	4.81±0.22	32.94±4.71	1.8	2.8	101.36±44.33

$S_{(SF)}$ concentration from solubility obtained by Shake Flask assays at the respective pH value.

Related to Iso, no significant differences are observed in either the DR and $[C]_f$ at pH 5.8 or 6.5 between single stage and two stages models. This is because of the extensive ionisation suffered by Iso when pH changes and the consequent great increase in its solubility. Therefore, the small amount of Iso solubilised at pH 2.0 stage does not affect in the DR of the next stage.

Values of DR obtained for Pir at two pH sectors are statistically similar to those at one pH sector at pH 2.0. However, at pH 5.8 and 6.5 the DR in the two sectors model are unexpectedly lower compared to those obtained in the one pH sector model. This could be due to, as already pointed before in the case of Bzt, the DR of the second sector is influenced by the amount of Pir in solution at the end of the first sector. As a consequence of these inferior dissolution rates in the

second sectors, the $[C]_f$ of the drug at the end of the assay is also lower with respect to that in one pH sector. At the beginning of the assays performed at a single pH value there is no previously dissolved API, and therefore DRs and $[C]_f$ are higher for Pir.

In case of Iso, the observed disintegration of the tablet surface is different from that in the other two molecules, which causes a higher variability – especially at the beginning of the second sector, as can be seen in Figure 49 – when pH changes. Additionally, this variability is increased for the three drugs when the elapsed time is higher, due to the tablets are suffering more disintegration but not enough disaggregation (see introduction, Figures 8 and 9). Then the variability of the concentration is given by this heterogeneous disintegration of the tablets in different replicates, probably because of a certain heterogeneity in the wettability of the samples.

4.4.2 The effect of excipients on the DR

Two excipients were selected to test their effect on the DR of the studied APIs, CAV as cyclodextrin representative and KOL as polyvinylpyrrolidone type, variating their concentration in mixtures at ratios 1:3, 1:1 and 3:1 of Excipient:API (w/w) respectively, and tested under same conditions as the APIs alone, this is, by one pH sectors (pH 2.0, 5.8 and 6.5) and by two pH sectors (2.0 – 5.8 and 2.0 – 6.5) models. The dissolution profiles and DR obtained in one pH sector model, using both excipients, are shown in Figures 50 – 51 and Tables 19 – 20, respectively. The effect of CAV and KOL in dissolution profiles and DR depends on the drugs, the concentration of the excipients and the pH.

In relation to Bzt (Figure 50-1A,2A,3A), the addition of 25% of CAV at the three studied pH values produces dissolution profiles with similar shapes, but

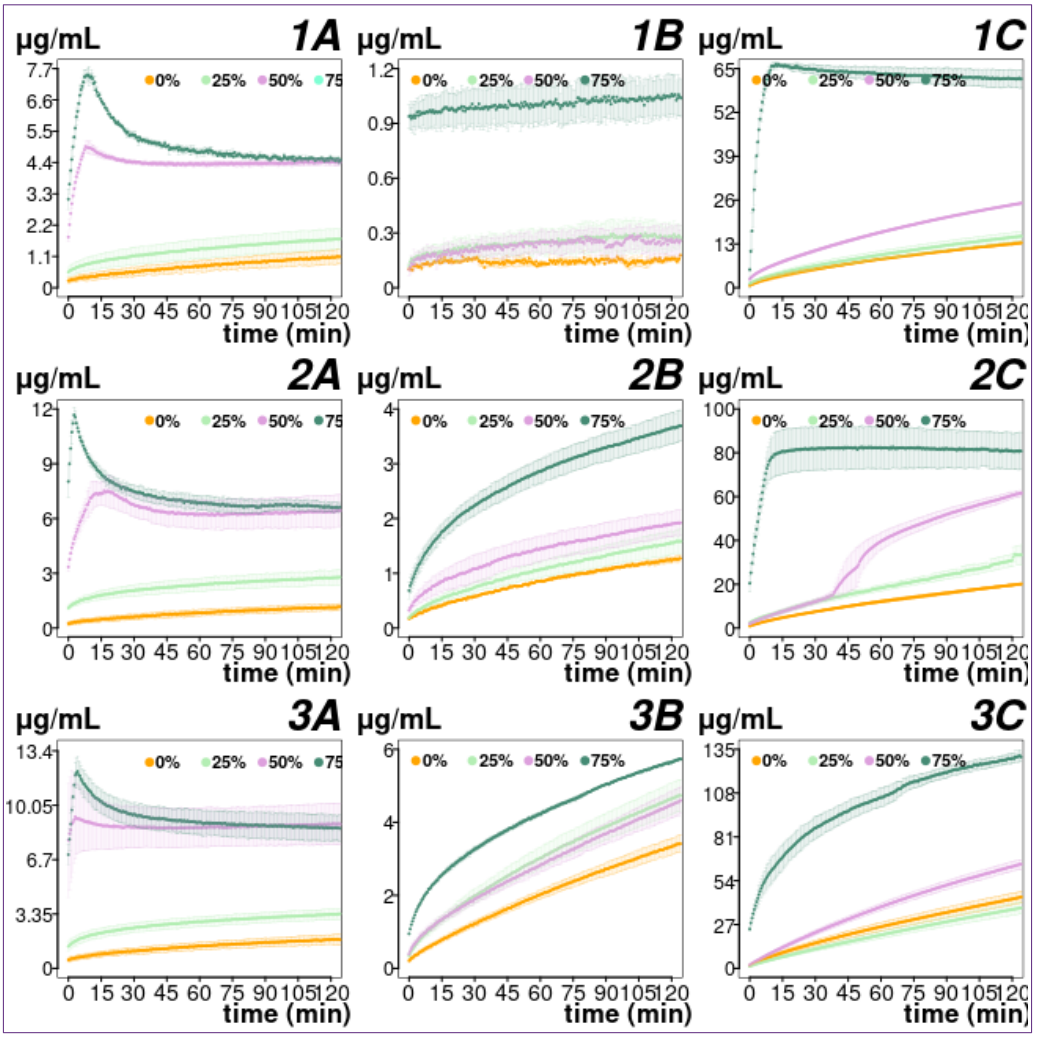

Fig 50: Dissolution profiles for the studied compounds in presence of CAV from 0 to 75%w/w, where: (A) Bzt, (B) Iso, (C) Pir, (1) pH 2.0, (2) pH 5.8, (3) pH 6.5.

reasonably increased DR and final concentration $[C]_f$ in comparison with the profile of API alone. When 50% or 75% of CAV is added, the dissolution profiles at the three pH stages show peaks that indicate supersaturation of the system, taking them around 5 to 10 minutes to reach the maximum value, followed by a drop of concentration. The higher the amount of CAV the higher the supersaturation extension. Moreover, although the duration of the supersaturation at pH 2.0 is similar to the others in the following pH stages, its

extension is lower (see Figure 50). In reference to the $[C]_f$ at any pH stage for Bzt, the saturation of the systems it is not reached when 25% of CAV is used. Nevertheless, once the systems reach the supersaturation at 50% and 75% of CAV, the samples start to precipitate until the achievement of saturated solutions. Surprisingly, while at pH 5.8 and 6.5 the systems with 50% of CAV reach concentrations close to the value given by SF at same conditions, at pH 2.0 the $[C]_f$ is lower than the solubility given by SF for Bzt at this %CAV, but this $[C]_f$ is close to the solubility given by SF for Bzt alone (see Table 19). This behaviour of Bzt could be attributed to a low dissolution of the tablet at pH 2.0, which does not generate enough amount of Excipient and/or API in the aqueous boundary layer that let to form the complex CAV:Bzt. Then, the API precipitates until reaching a concentration close to or lower than the corresponding by SF assay.

On the other hand, at pH 5.8 the DR is increased with the concentration of CAV up to about 271 times (see Table 19). However, not great differences are observed in DR values when %CAV is increased from 25% to 50%, at pH 2.0 and 5.8. Nonetheless, a considerably high change of DR is observed when 75% of the excipient is added. Additionally, when pH changes from 5.8 to 6.5 at 50% of CAV the observed DR is much higher. These results suggest that the low ionisation degree of Bzt (<15% at pH 5.8) has nearly none influence in the DR, but ionisation has possibly an additive dissolution effect to that given by CAV at pH 6.5 (ionisation degree is >40% deprotonated).

In order to corroborate this hypothesis, in Table 19 the values given in the fifth column $\left(\left[DR(\%CAV_i)/DR(API)\right]_{[pH]}\right)$ indicate how higher is the DR obtained with each %CAV with respect to the API alone at the same pH value. The following column accounts for the effect of the concentration of CAV at a certain pH

Table 19: Dissolution Rate (DR), Final concentration ($[C]_f$) and relative DR for Bzt, Iso and Pir in the presence of different proportions of CAV at each single pH stage studied.

%CAV	pH	Extrapolated DR (μg/min)	$[C]_f$ ($\mu g/mL$)	$\left[\frac{DR(\%CAV_i)}{DR(API)}\right]_{[pH]}$	$\left[\frac{DR(\%CAV_j)}{DR(\%CAV_i)}\right]_{[pH]}$	$\left[\frac{DR(pH_i)}{DR(pH_2)}\right]_{[\%]}$	$\left[\frac{DR(pH_{6.5})}{DR(pH_{5.8})}\right]_{[\%]}$	$S_{(SF)}$ $\mu g/mL$
Bzt								
0	1.93±0.09	0.35±0.19	1.09±0.29	--	--	--	--	4.31±0.01
25	1.89±0.02	1.01±0.38	1.72±0.43	2.9	--	--	--	
50	1.90±0.02	18.62±2.30	4.43±0.14	53.2	18.3	--	--	7.12±0.46
75	1.90±0.01	28.81±1.60	4.54±0.03	82.3	1.5	--	--	
0	5.72±0.03	0.33±0.17	1.20±0.20	--	--	0.9	--	4.61±0.38
25	5.73±0.04	2.44±0.54	2.76±0.44	7.4	--	2.4	--	
50	5.81±0.06	13.88±1.90	6.43±1.05	42.1	5.7	0.7	--	7.03±1.45
75	5.77±0.07	89.57±8.76	6.61±0.34	271.4	6.5	3.1	--	
0	6.45±0.13	0.79±0.11	1.80±0.37	--	--	2.2	2.4	6.35±0.19
25	6.40±0.03	3.27±0.68	3.36±0.41	4.2	--	3.2	1.3	
50	6.42±0.01	58.34±6.28	8.93±1.55	74.2	17.9	3.1	4.2	8.94±0.41
75	6.37±0.01	71.14±4.19	8.62±0.97	90.5	1.2	2.5	0.8	
Iso								
0	1.86±0.02	0.18±0.05	0.17±0.03	--	--	--	--	0.70±0.04
25	1.92±0.01	0.25±0.17	0.28±0.09	1.4	--	--	--	
50	1.87±0.00	0.29±0.13	0.27±0.09	1.6	1.1	--	--	4.02±2.25
75	1.94±0.01	0.16±0.04	0.62±0.46	0.9	0.5	--	--	
0	5.66±0.10	0.35±0.08	1.58±0.53			1.6	--	7.13±1.28
25	5.75±0.03	0.52±0.15	1.59±0.28	1.7		2.1	--	
50	5.67±0.04	0.91±0.39	1.92±0.29	3.0	1.7	3.1	--	9.45±1.69
75	5.95±0.04	1.95±0.35	3.70±0.35	6.5	2.2	12.4	--	

%CAV	pH	Extrapolated DR (μg/min)	$[C]_f$ $(\mu g/mL)$	$\left[\frac{DR(\%CAV_i)}{DR(API)}\right]_{[pH]}$	$\left[\frac{DR(\%CAV_j)}{DR(\%CAV_i)}\right]_{[pH]}$	$\left[\frac{DR(pH_i)}{DR(pH_2)}\right]_{[\%]}$	$\left[\frac{DR(pH_{6.5})}{DR(pH_{5.8})}\right]_{[\%]}$	$S_{(SF)}$ μg/mL
0	6.45±.06	0.61±0.03	3.44±0.28	--	--	3.3	2.0	28.86±2.78
25	6.38±0.02	1.19±0.10	4.75±0.54	2.0	--	4.7	2.3	
50	6.41±.01	1.41±0.14	4.56±0.38	2.3	1.2	4.8	1.6	37.95±7.15
75	6.53±0.01	3.42±0.08	5.74±0.02	5.6	2.4	21.7	1.7	
				Pir				
0	1.91±0.01	3.33±0.76	12.97±1.31	--	--	--	--	14.59±0.95
25	1.96±0.01	4.98±1.09	15.35±1.71	1.5	--	--	--	
50	1.92±0.02	3.22±0.25	7.98±0.51	1.0	0.6	--	--	18.87±1.37
75	1.91±0.02	250.13±15.77	61.95±3.07	75.1	77.7	--	--	
0	5.65±0.02	4.38±0.19	20.15±0.59	--	--	1.5	--	48.05±5.79
25	5.73±0.05	6.97±.28	36.13±8.54	1.6	--	1.4	--	
50	5.75±0.03	6.36±0.75	53.62±14.56	1.5	0.9	0.9	--	61.52±1.31
75	5.70±0.06	232.55±.90	89.26±12.69	53.1	36.6	0.9	--	
0	6.37±0.05	9.21±1.52	44.13±.40	--	--	3.2	2.1	101.36±22.17
25	6.35±0.02	6.62±1.37	37.35±4.49	0.7	--	1.3	0.9	
50	6.34±0.00	11.91±1.66	64.39±3.49	1.3	1.8	1.8	1.9	152.75±20.28
75	6.30±0.01	160.00±7.21	151.06±23.50	17.4	13.4	0.6	0.7	

$S_{(SF)}$ concentration from the solubility found by Shake Flask at the respective % of CAV and pH.

value $\left(\left[DR(\%CAV_j)/DR(\%CAV_i)\right]_{[pH]}\right)$. The seventh column $\left(\left[DR(pH_i)/DR(pH_2)\right]_{[\%]}\right)$ establishes the increasing factors of DR given by the pH change at same %CAV. Finally, the next column $\left(\left[DR(pH_{6.5})/DR(pH_{5.8})\right]_{[\%]}\right)$ is a measure of the improvement on DR at pH 6.5 in relation to 5.8 at same %CAV. Since the values in columns 7 and 8 are lower than those in columns 5 and 6 for Bzt, it could be concluded that the effect of the pH on dissolution is lower than the effect of the excipient. Besides, DR ratios lower than 1 show that the DR at the respective condition is lower than the reference value. On the contrary, ratios equal or higher than one, means that the effect of that condition is the same or better than the reference.

At pH 2.0 Iso is completely neutral and it has the lowest solubility. The addition of 25% or 50% of CAV causes a faintly increased DR and $[C]_f$ compared to the API alone, added to the fact that the amount obtained is close or lower to the quantification limits of the sample, creating similar dissolution profiles. The addition of 75% of CAV increases the concentration obtained for Iso at a level close to the solubility of the API alone, but far from the concentration of Iso given also by SF with 50% of CAV. This can be attributable to the low solubility of the compound, which could be precipitating nearby the surface of the tablet when it is released, without enough time to make any interaction with the solubilized excipient. However, the DR calculated at 75% of CAV is similar to the DR at the other percentages, due to the instrumental delay or lack time (see Figure 50).

At pH 5.8 and 6.5, a better increment of DR and $[C]_f$ of Iso is observed. The addition of 25% or 50% of CAV generates more concentration in comparison with the API alone, but similar concentrations between them, whereas at 75% of

CAV the increment in concentration and DR are considerably higher. However, none of the percentages causes a saturation of the systems. The produced enhancement is due to the presence of the excipient, but this is synergic to the effect of the ionisation degree of the API. As can be seen in Table 19, the relative DR respect to the %CAV (column 5) is lower than the relative DR respect to pH (column 7), suggesting that the effect of the pH is predominant in front of the effect of the excipient.

In case of Pir, the addition of 25% of CAV almost does not show an enhancement in DR and $[C]_f$ at any of the pH values. Better dissolution profiles are observed when 50% of CAV is used, however, at pH 5.8 a jump or suddenly increased concentration is observed in the profile, due to a breakage of the tablet. Besides, saturation is achieved when 75% of CAV is used at pH 2.0 and 5.8, where Pir is <40% protonated and about 75% deprotonated, respectively. Additionally, at pH 2.0 a supersaturated solution is also formed in no more than 10 minutes with same %CAV. Nevertheless, when the pH is 6.5 and the sample is around 90% deprotonated, the system does not reach saturation even with 75% of CAV. As can be appreciated in Table 19, with the exception of 75% of CAV, the relationships of DR given by %CAV (column 5) are in similar order to those given by DR respect to pH (column 7). This suggests that the effect of the excipient and the effect of the ionisation degree are influencing in a similar magnitude on the DR and dissolution of the API.

As reviewed in SF chapter, CAV interacts with the three APIs in different degree (Figure 46), and this is also happening in terms of Dissolution Profiles. Although the neutral form of Iso (pH 2.0) is showing the highest interaction with CAV (Table 15), these mixtures cannot supersaturate the solutions in DR experiments. Meanwhile, with Bzt a supersaturation is observed in its

dissolution profiles at 50% and 75% of CAV in all the pH stages. In case of Pir, a supersaturation is observed only with 75% of CAV at pH 2.0 and 5.8. Since the DR is affected by the dissolution of the drugs, Iso has the lowest solubility and also the lowest DR, whereas Pir has the highest solubility and DR.

Moreover, the lower DR values for Iso with respect to the others could be attributed to the possibly low wettability of its tablets, because of the nature of the powder formed by CAV:Iso mixture, which could develop different physical properties when it is compressed into a tablet form in comparison with the other mixture powders studied. Each solid mixture API:Excipient shows visual differences, and tablets prepared with Iso behave particularly distinct at the moment of compression, which could form tablets of high hardness, hindering its surface to get moisturised by the dissolution media. On the contrary, the tablets from mixtures with Bzt or Pir could have better wettability, which causes the big jumps at the start of the assays – during the delay time – and/or the breakage of the surface of the tablets, depending on the case.

Although DRs for Pir present the fastest values, their relative variation with the addition of excipients (column 5 in Table 19) do not show the highest figures. In the case of Bzt the enhancement effect given by CAV is predominant in front of the effect of the pH, for Iso it is the contrary and in Pir the effect produced by the enhancer in front of the pH is not as predominant as in Bzt. It also seems that the effect of the pH exerted in Iso is higher than its effect produced in Pir, this could be attributed to the more drastic ionisation suffered by Iso respect to Pir when pH changes from 2.0 to 5.8 or 6.5, due to their pK_a values. Besides, due to the presence of the additive effect of the ionisation degree, it is not clear how much the effect of the excipient is pH-dependent.

The presence of KOL induces a better dissolution of Bzt, increasing the $[C]_f$ of this compound in all the pH stages with respect to CAV (see Figure 51 and Table 20). Whereas in CAV a considerable gap between the dissolution profiles

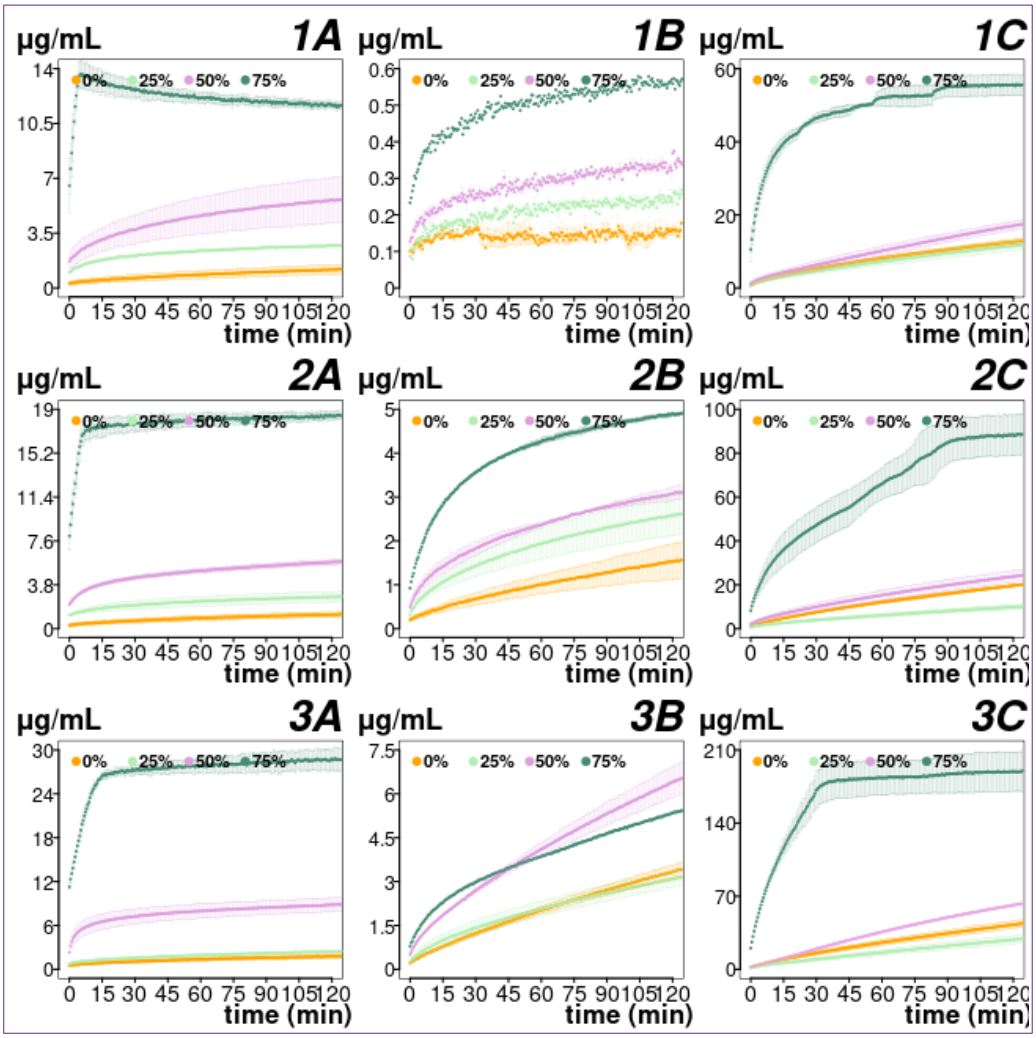

Fig 51: Dissolution profiles for studied compounds in presence of KOL from 0 to 75%w/w, where: (A) Bzt, (B) Iso, (C) Pir, (1) pH 2.0, (2) pH 5.8, (3) pH 6.5.

is observed from 25% to 50% of CAV, when KOL is added this gap happens between 50% to 75% of this excipient. In fact, a supersaturation is only present with 75% of KOL at pH 2.0. At this %KOL the DRs slightly decrease with pH

increment (Table 20), and no supersaturation is observed at pH 5.8 and 6.5, whereas the profiles seem to be stabilised in a concentration higher than the solubility given by SF with 50% of KOL.

The presence of KOL induces a progressive augmentation of the concentration of Iso at each pH stage studied, but without the presence of saturation in any level of excipient or pH stages. In general, the use of KOL produces a slightly better enhancement on the dissolution and DR of Iso respect to CAV, at the studied conditions. Besides, the dissolution profile with 25% of KOL at pH 5.8 is more related to the behaviour with 50% than Iso alone, whereas at pH 6.5 the profile with 25% of KOL is similar to the API alone (see Figure 51).

Related to Pir, the presence of KOL causes dissolution profiles, DRs and $[C]_f$ similar in shapes and magnitudes to those obtained with CAV at same levels of excipient percentages. The exception is found at pH 5.8 with 50% of KOL, where in contrast to CAV, the heterogeneous disintegration of the tablet is not observed. Although at 75% of KOL a stable concentration seems to be achieved at the end of the experiments for the three studied pH values, at pH 2.0 and 5.8 this possible saturation could be arrived due to a heterogeneous disintegration of the tablets. On the contrary, at pH 6.5 the systems with CAV and KOL behave in similar way but with the last one saturates faster (see Figures 50 and 51).

The principal difference observed in DR and $[C]_f$ of APIs can be attributed not only to the type and percentage of excipients used, but also to the ionisation degree of the drugs. For Bzt, which suffer less ionisation, the influence of the excipient is higher than the influence of the pH. On the contrary, for Iso it is the pH that causes a more significant effect than the excipient, because Iso can be

Table 20: Dissolution Rate (DR), Final concentration ($[C]_f$) and relative DR for Bzt, Iso and Pir in presence of different proportions of KOL at each separated pH stage studied.

% KOL	pH	Extrapolated DR (µg/min)	$[C]_f$ $(\mu g/mL)$	$\left[\frac{DR(\%KOL_i)}{DR(API)}\right]_{[pH}$	$\left[\frac{DR(\%KOL_j)}{DR(\%KOL_i)}\right]_{[pH}$	$\left[\frac{DR(pH_i)}{DR(pH_2)}\right]_{[\%}$	$\left[\frac{DR(pH_{6.5})}{DR(pH_{5.8})}\right]_{[\%]}$	$S_{(SF)}$ $\mu g/mL$
Bzt								
0	1.97±0.13	0.41±0.19	1.19±0.34	--	--	--	--	4.31±0.01
25	1.92±0.00	2.38±0.00	2.73±0.00	5.8	--	--	--	
50	1.87±0.00	2.54±0.32	4.62±0.06	6.2	1.1	--	--	7.12±0.46
75	1.95±0.04	71.73±2.50	11.66±0.23	175.7	28.3	--	--	
0	5.62±0.15	0.33±0.17	1.22±0.28	--	--	0.8	--	4.61±0.38
25	5.80±0.10	1.79±0.63	2.77±0.56	5.4	--	0.8	--	
50	5.74±0.04	5.78±0.81	5.81±0.29	17.4	3.2	2.3	--	7.03±1.45
75	5.69±0.03	63.14±2.64	18.43±0.47	190.0	10.9	0.9	--	
0	6.45±0.13	0.79±0.11	1.80±0.37	--	--	1.9	2.4	6.35±0.19
25	6.44±0.01	1.15±0.26	2.45±0.02	1.5	--	0.5	0.6	
50	6.39±0.02	19.76±7.27	8.90±1.43	25.1	17.1	7.8	3.4	8.94±0.41
75	6.38±0.02	49.11±7.71	28.92±1.55	62.5	2.5	0.7	0.8	
Iso								
0	1.86±0.02	0.18±0.05	0.17±0.03	--	--	--	--	0.70±0.04
25	1.92±0.00	0.22±0.07	0.26±0.01	1.2	--	--	--	
50	1.96±0.01	0.34±0.06	0.36±0.02	1.9	1.6	--	--	4.02±2.25
75	1.97±0.05	0.85±0.02	0.59±0.02	4.6	2.5	--	--	
0	5.73±0.14	0.35±0.08	1.58±0.53	--	--	1.9	--	7.13±1.28
25	5.89±0.02	1.30±0.28	2.62±0.57	3.7	--	5.9	--	
50	5.79±0.13	1.92±0.47	3.11±0.24	5.6	1.5	5.6	--	9.45±1.69
75	5.70±0.04	3.98±0.50	4.92±0.04	11.5	2.1	4.7	--	

% KOL	pH	Extrapolated DR (µg/min)	$[C]_f$ $(\mu g/mL)$	$\left[\frac{DR(\%KOL_i)}{DR(API)}\right]_{[pH}$	$\left[\frac{DR(\%KOL_j)}{DR(\%KOL_i)}\right]_{[pH}$	$\left[\frac{DR(pH_i)}{DR(pH_2)}\right]_{[\%}$	$\left[\frac{DR(pH_{6.5})}{DR(pH_{5.8})}\right]_{[\%]}$	$S_{(SF)}$ µg/mL
0	6.45±0.06	0.61±0.03	3.44±0.28	--	--	3.3	1.8	28.86±2.78
25	6.52±0.01	1.10±0.29	3.15±0.35	1.8	--	5.1	0.9	
50	6.44±0.04	1.83±0.12	6.55±0.80	3.0	1.7	5.3	0.9	37.95±7.15
75	6.90±0.69	2.85±0.02	18.87±18.99	4.7	1.6	3.4	0.7	
				Pir				
0	1.91±0.01	4.20±0.76	12.93±0.93	--	--	--	--	14.59±0.95
25	1.91±0.01	3.36±0.89	11.76±1.62	0.8	--	--	--	
50	1.96±0.07	3.60±0.58	17.52±1.46	0.9	0.1	--	--	34.559±1.14
75	1.90±0.01	90.92±14.94	55.45±3.38	21.6	2.5	--	--	
0	5.65±0.02	4.38±0.19	20.15±0.59	--	--	1.0	--	48.05±5.79
25	5.70±0.03	2.50±0.55	10.11±1.33	0.6	--	0.7	--	
50	5.70±0.04	6.32±1.70	24.37±3.30	1.4	0.2	1.8	--	88.76±9.70
75	5.68±0.07	58.78±15.78	88.46±11.61	13.4	1.4	0.6	--	
0	6.37±0.05	9.21±1.52	44.13±4.40	--	--	2.2	2.1	101.36±22.17
25	6.40±0.04	4.97±1.33	29.27±4.92	0.5	--	1.5	2.0	
50	6.40±0.02	10.43±0.31	63.17±0.92	1.1	0.2	2.9	1.7	289.19±8.34
75	6.29±0.03	164.57±17.06	189.15±22.01	17.9	3.7	1.8	2.8	

$S_{(SF)}$ solubility found by Shake Flask expressed in µg/mL.

$[C]_f$ final concentration found at the end of these assays.

fully ionised at pH 5.8 and above. For Pir, which is highly ionised, both the excipient and pH contribute synergically. In general, the presence of KOL allows to obtain higher $[C]_f$ than with CAV. This behaviour is also observed in the SF assays (see Table 15, Figure 46), where the variation of *logS* is higher for KOL with respect to CAV. However, KOL does not always produce better DR than CAV. This is suggesting that the action mechanism of KOL (for example HB) in dissolution processes is more effective than the mechanism produced by CAV (complexation and/or HB) under these conditions, even if its releasing process from the tablet is slower. Additionally, the wettability and hardness of the tablets are not the same due to the existing differences between the used excipients, despite that the tablets are compressed under same pressure.

4.4.3 The effect of the excipients at two pH sector model

Figures 52 and 53 show the dissolution profiles for Bzt, Iso and Pir using CAV or KOL respectively, when the assays are conducted in the two pH sector model (pH 2.0 – 5.8 or pH 2.0 – 6.5). In Tables 21 and 22 are summarized the DR, $[C]_f$ and other parameters.

When pH changes from 2.0 to 5.8 the dissolution profile of Bzt in absence of excipient and mixed with 25% of CAV is not altered, obtaining a continuous plot in both systems. When 50% and 75% of CAV are used the solutions get immediately supersaturated at the beginning of the second sector, during the transition time from pH 2.0 to 5.8, gaining the same level of extension of this supersaturation. Then precipitation takes place producing a sudden drop in the concentration. Due to this fast supersaturation, it is impossible to calculate a DR for the second sector at 50% or 75% of CAV. Additionally, similarly to the single pH sector, the pH exerts a lower effect on the increment of the final concentration than the effect of the excipient.

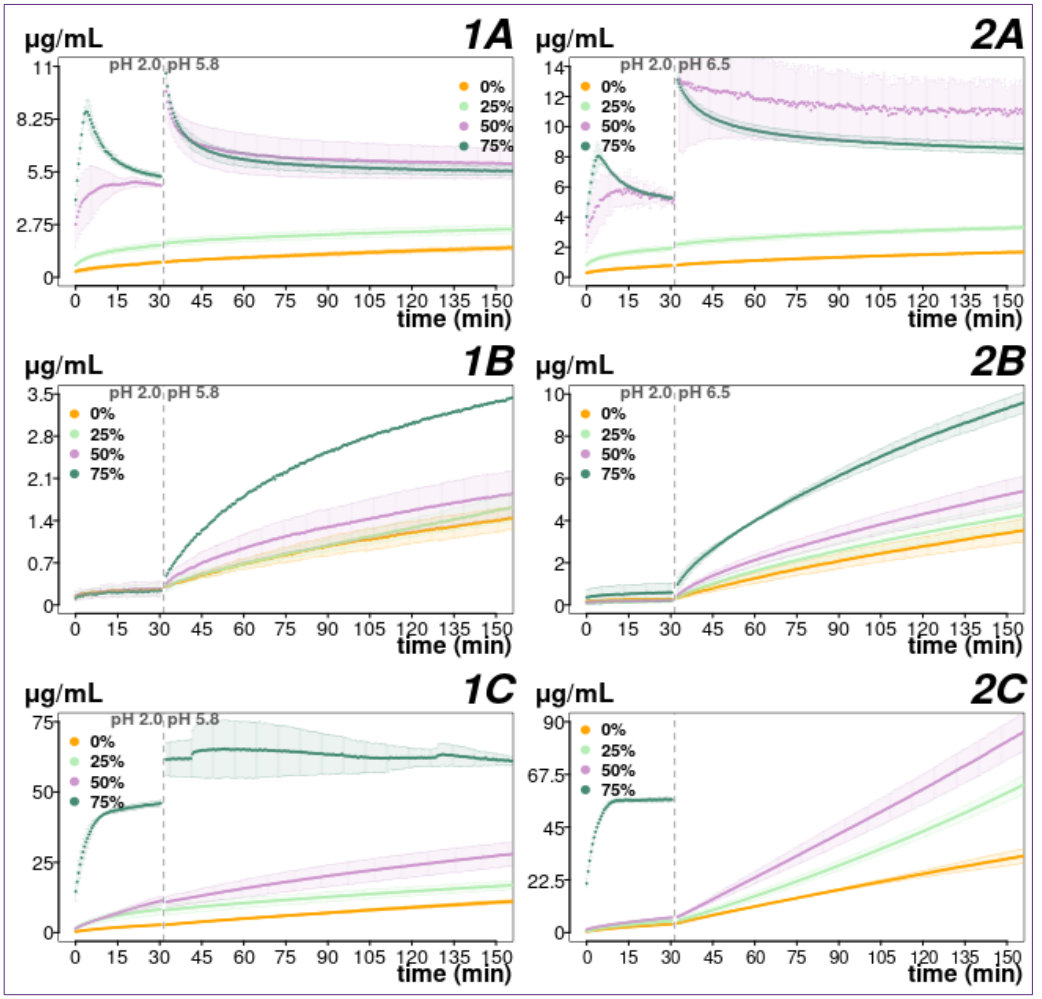

Fig 52: Dissolution profiles for Bzt (A), Iso (B) and Pir (C) in presence of 0 - 75% of CAV, at continued pH 2-5.8 (1) and pH 2-6.5 (2).

When the pH changes from 2.0 to 6.5, the profiles for Bzt alone and with CAV are similar to those observed in pH 2.0 – 5.8 stages. Maintaining the continuity at 0% and 25% of CAV and yielding the supersaturation at 50% and 75% of CAV. The $[C]_f$ at the end of the second sector (pH 6.5) are slightly better than at pH 5.8, as expected from the higher ionisation degree. The DR at the second sectors are close or lower to the DR at pH 2.0, this is due to the initial amount of sample dissolved in the 30 minutes of the first sector (see Table 21).

Moreover, the $[C]_f$ at the end of the second sector are also better than in the one pH sector model, because these latter are 30 minutes shorter.

The dissolution profiles for Iso follow the same tendency as in the one pH sector model, increasing the concentration of the API with the respective increase of DR, when the excipient is also augmented. When 25% of CAV is applied the profile obtained is similar to the profile of API alone in pH 2.0 – 5.8, whereas when the pH changes from 2.0 – 6.5, the profile is intermediate between 50% of CAV and Iso alone (Figure 52-1B,2B). Another accomplished condition is that the pH effect (ionisation degree) is exerting a major effect than the excipient, as can be observed in Table 21 (columns 5 – 8). The difference for Iso between models of one and two pH sectors is that in the last one the $[C]_f$ values are higher due to the longer assay time, but the DR are similar or lower.

The behaviour given by Pir in the two pH sectors model (Figure 52-1C,2C) adding CAV as excipient is in concordance with the single model (Figure 50), obtaining similar profile shapes, observing a sustained dissolution with no saturation of the systems, reaching similar or higher $[C]_f$ than those at the other pH arrangement, as expected due to the longer duration of the two pH sector model. When 75% of CAV is added there is slight supersaturation of the solution with a short extension in the second sector. However, the high variability observed (Figure 52-1C) is given by the heterogeneous way in which the surface of the pellets is disintegrating, but always reaching the same level of $[C]_f$ and same shape in the profile. Moreover, at pH 2.0 – 6.5 the $[C]_f$ are also in higher level than in pH 2.0 – 5.8, due to the increased ionisation of the sample. Unfortunately, it was not possible to work at 75% of CAV at this second array.

Table 21: Extrapolated and calculated parameters for dissolution of the three APIs with different concentrations of CAV and at different pH using the continued model.

%CAV	pH	Extrapolated DR ($\mu g/min$)	$[C]_f$ ($\mu g/mL$)	$\left[\frac{DR(\%CAV_i)}{DR(API)}\right]_{[pH]}$	$\left[\frac{DR(\%CAV_j)}{DR(\%CAV_i)}\right]_{[pH]}$	$\left[\frac{DR(pH_i)}{DR(pH_2)}\right]_{[\%]}$	$\left[\frac{DR(pH_{6.5})}{DR(pH_{5.8})}\right]_{[\%]}$	$S_{(SF)}$ ($\mu g/mL$)
Bzt								
	1.88±0.02	0.68±0.16	0.78±0.07	--	--	--	--	4.31±0.01
0	5.68±0.06	0.20±0.07	1.54±0.17	--	--	0.3	--	4.61±0.38
	6.36±0.03	0.29±0.02	1.68±0.06	--	--	0.4	1.4	6.35±0.19
	1.89±0.02	2.95±0.50	1.74±0.23	4.3	--	--	--	--
25	5.68±0.04	0.44±0.06	2.51±.29	2.2	--	0.1	--	--
	6.37±0.04	0.77±0.23	3.31±0.19	2.7	--	0.3	1.8	--
	1.88±0.02	6.94±1.77	4.05±1.17	10.2	2.4	--	--	7.12±0.46
50	5.65±0.04	--	5.47±0.97	--	--	--	--	7.03±1.45
	6.39±.01	--	5.86±1.55	--	--	--	--	8.94±0.41
	1.89±0.03	59.26±5.39	5.28±0.13	87.3	8.5	--	--	--
75	5.73±0.07	--	5.54±0.29	--	--	--	--	--
	6.38±0.02	--	8.55±0.42	--	--	--	--	--
Iso								
	1.91±0.05	0.41±0.10	0.26±0.06	--	--	--	--	0.70±0.04
0	5.73±0.04	0.29±0.09	1.45±0.26	--	--	0.7	--	7.13±1.28
	6.42±0.04	0.64±0.18	3.56±0.67	--	--	1.6	2.2	28.86±2.78
	1.91±0.01	0.38±0.15	0.22±0.10	0.93	--	--	--	--
25	5.82±0.06	0.32±0.11	1.63±0.28	1.11	--	0.84	--	--
	6.48±0.06	0.94±0.19	4.31±0.69	1.47	--	2.48	2.96	--
	1.91±0.01	0.39±0.11	0.25±0.10	0.94	1.02	--	--	4.02±2.25
50	5.71±0.05	0.63±0.33	1.85±0.47	2.22	1.99	1.64	--	9.45±1.69
	6.38±0.01	1.29±0.16	5.44±0.87	2.00	1.37	3.32	2.03	48.88±7.15

%CAV	pH	Extrapolated DR ($\mu g/min$)	$[C]_f$ ($\mu g/mL$)	$\left[\frac{DR(\%CAV_i)}{DR(API)}\right]_{[pH]}$	$\left[\frac{DR(\%CAV_j)}{DR(\%CAV_i)}\right]_{[pH]}$	$\left[\frac{DR(pH_i)}{DR(pH_2)}\right]_{[\%]}$	$\left[\frac{DR(pH_{6.5})}{DR(pH_{5.8})}\right]_{[\%]}$	$S_{(SF)}$ ($\mu g/mL$)
	1.95±0.01	0.78±0.66	0.47±0.50	1.90	2.01	--	--	--
75	5.81	1.28	3.44	4.47	2.01	1.64	--	--
	6.50±0.03	2.60±0.21	9.64±0.69	4.06	2.03	3.34	2.04	--
				Pir				
	1.92±0.03	2.68±0.46	3.22±0.57	--	--	--	--	14.59±0.95
0	5.75±0.04	1.70±0.13	11.18±1.05	--	--	0.6	--	48.05±5.79
	6.44±0.01	4.81±0.22	32.94±4.71	--	--	1.8	2.8	101.36±22.17
	1.91±0.02	6.43±2.30	5.95±1.26	2.4	--	--	--	--
25	5.68±0.03	2.84±0.71	16.91±1.87	1.7	--	0.4	--	--
	6.63±0.09	7.49±revisar	64.07±5.07	1.6	--	1.2	2.6	--
	1.90±0.01	7.12±1.44	9.25±2.98	2.7	1.1	--	--	18.87±1.37
50	5.67±0.05	3.86±1.45	28.82±4.41	2.3	1.4	0.5	--	61.52±1.31
	6.52±0.02	--	86.48±10.10	--	--	--	--	152.75±20.28
75				----				--

$[C]_f$ final concentration found at the end of these assays. Dissolution Rate $DR[pH]_{(x,y)}$ at one pH compared to base $DR[pH]_{(a)}$ at same amount of excipient (%w/w). Dissolution Rate $DR[\%]_{(j,k)}$ from different amount of excipient applied compared to $DR[\%]_i$ at 25% of excipient at same pH. $S_{(SF)}$ solubility found by Shake Flask for the substances at the respective pH and % of excipient, expressed in µg/mL. Values with SD are average from at least three replicates.

Addition of KOL to the APIs in the two pH sectors model generates the profiles given in Figure 53. The situation observed with Bzt is similar to that in the one pH sector model, with slightly better $[C]_f$ due to the longer time needed for this type of assay, as previously pointed. The profiles using 75% of KOL show a possible saturation at the end of the experiment, and with 25% the profiles are slightly better than the profiles of the lonely drug at pH 2.0 – 5.8 and pH 2.0 – 6.5.

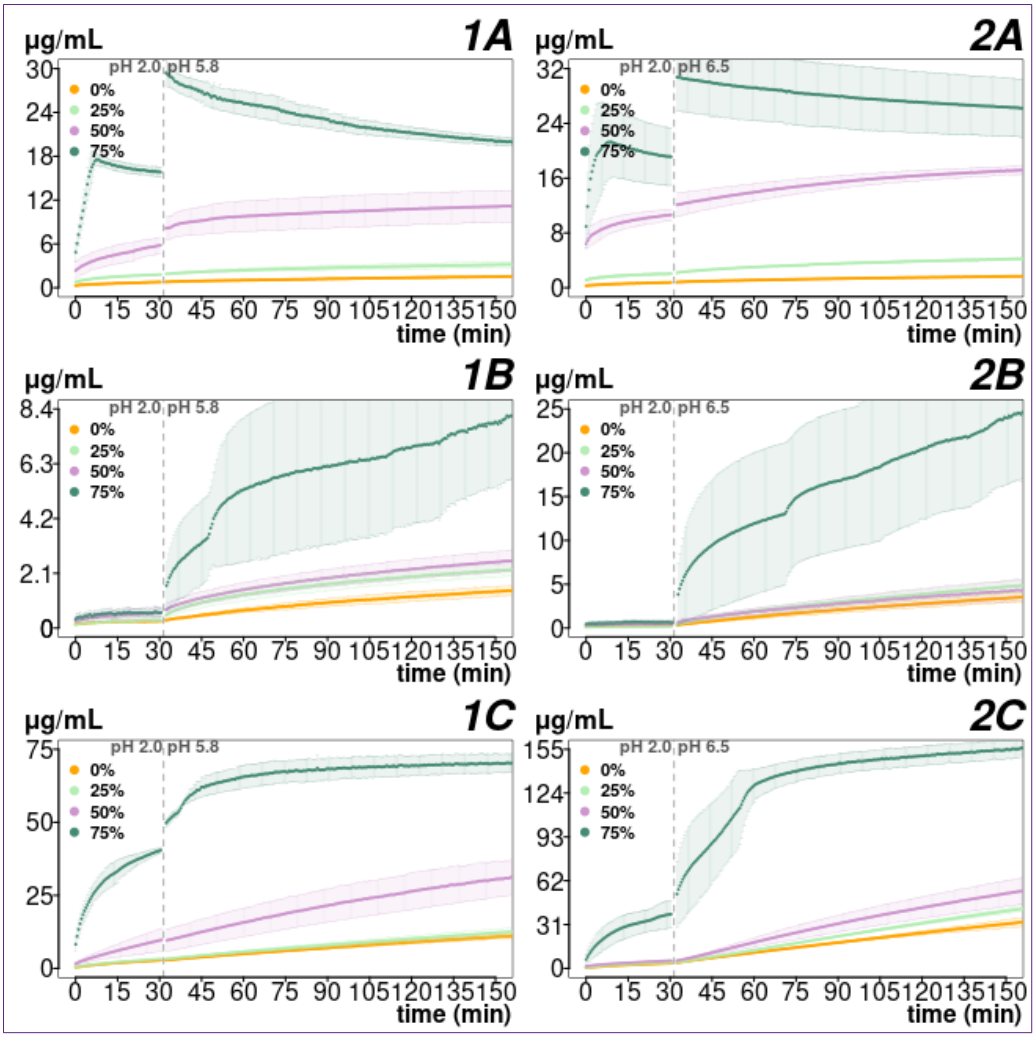

Fig 53: Dissolution Rate for Bzt (1), Iso (2) and Pir (3) in presence of 0 - 75% of KOL, at continued pH 2-5.8 (left side) and 2-6.5 (right side).

Table 22: Extrapolated and calculated parameters for dissolution of the three APIs with different concentrations of KOL and at different pH using the two sectors model.

% KOL	pH	Extrapolated DR ($\mu g/min$)	$[C]_f$ ($\mu g/mL$)	$\left[\frac{DR(\%KOL_i)}{DR(API)}\right]_{[pH]}$	$\left[\frac{DR(\%KOL_j)}{DR(\%KOL_i)}\right]_{[pH]}$	$\left[\frac{DR(pH_i)}{DR(pH_2)}\right]_{[\%]}$	$\left[\frac{DR(pH_{6.5})}{DR(pH_{5.8})}\right]_{[\%]}$	$S_{(SF)}$ ($\mu g/mL$)
Bzt								
	1.88±0.02	0.68±0.16	0.78±0.07	--	--	--	--	4.31±0.01
0	5.68±0.06	0.20±0.07	1.54±0.17	--	--	0.29	--	4.61±0.38
	6.36±0.03	0.29±0.02	1.68±0.06	--	--	0.42	1.45	6.35±0.19
	1.93±0.01	2.47±0.27	1.92±0.20	3.63	--	--	--	--
25	5.70±0.03	0.67±0.24	3.19±0.57	3.42	--	0.27	--	--
	6.44±0.08	1.38±0.18	4.22±0.25	4.83	--	0.56	2.04	--
	1.89±0.01	5.04±0.67	5.62±1.06	7.43	2.04	--	--	7.48±0.31
50	5.72±0.02	5.81±4.84	17.00±4.81	29.45	8.61	1.15	--	9.77±0.75
	6.35±0.01	3.78±0.31	17.19±0.77	13.24	2.74	0.75	0.65	13.89±0.60
	1.93±0.01	44.87±13.73	15.82±0.89	66.07	8.90	--	--	--
75	5.71±0.06	--	19.90±0.67	--	--	--	--	--
	6.37±0.02	--	26.20±5.14	--	--	--	--	--
Iso								
	1.92±0.06	0.49±0.29	0.27±0.08	--	--	--	--	0.70±0.04
0	5.73±0.04	0.29±0.09	1.94±0.27	--	--	0.58	--	7.13±1.28
	6.42±0.04	0.64±0.18	6.29±1.92	--	--	1.30	2.25	28.86±2.78
	1.92±0.07	0.35±0.23	0.21±0.09	0.71	--	--	--	--
25	5.76±0.13	1.10±0.45	1.76±0.44	3.87	--	3.15	--	--
	6.47±0.08	1.40±0.19	3.42±0.40	2.18	--	4.00	1.27	--
	1.86±0.06	0.86±0.49	0.47±0.31	1.74	2.44	--	--	1.69±1.84
50	5.67±0.04	1.05±0.10	1.99±0.53	3.69	0.95	1.23	--	16.56±2.31
	6.36±0.01	1.25±0.27	3.03±0.97	1.94	0.89	1.46	1.18	48.20±2.30

% KOL	pH	Extrapolated DR (μg/min)	$[C]_f$ (μg/mL)	$\left[\frac{DR(\%KOL_i)}{DR(API)}\right]_{[pH]}$	$\left[\frac{DR(\%KOL_j)}{DR(\%KOL_i)}\right]_{[pH]}$	$\left[\frac{DR(pH_i)}{DR(pH_2)}\right]_{[\%]}$	$\left[\frac{DR(pH_{6.5})}{DR(pH_{5.8})}\right]_{[\%]}$	$S_{(SF)}$ (μg/mL)
	1.92±0.09	1.11±0.96	0.79±0.52	2.25	1.30	--	--	--
75	5.74±0.10	5.26±3.93	4.90±2.00	18.43	5.00	4.75	--	--
	6.41±0.03	18.46±20.58	16.28±7.73	28.78	14.82	16.66	3.51	--
Pir								
	1.92±0.05	2.68±0.65	4.02±0.37	--	--	--	--	14.59±0.95
0	5.75±0.04	1.70±0.13	16.00±1.51	--	--	0.63	--	48.05±5.79
	6.44±0.01	4.81±0.22	86.99±59.69	--	--	1.79	2.84	101.36±22.17
	1.90±0.03	3.89±1.15	3.26±0.41	1.45	--	--	--	--
25	5.73±0.05	1.72±0.29	28.10±9.21	1.02	--	0.44	--	--
	6.44±0.01	5.77±0.22	321.17±247.03	1.20	--	1.48	3.35	--
	1.89±0.01	9.44±7.19	9.22±8.31	3.52	2.43	--	--	34.59±1.14
50	5.93±0.47	4.85±1.64	63.35±14.78	2.86	2.82	0.51	--	88.76±9.70
	6.39±0.01	9.00±3.02	131.63±11.01	1.87	1.56	0.95	1.85	289.19±8.34
	1.94±0.02	66.76±25.24	35.27±4.98	24.88	7.07	--	--	--
75	5.72±0.01	112.30±0.14	68.49±10.71	66.20	23.14	1.68	--	--
	6.32±0.00	53.14±20.00	268.25±27.65	11.04	5.90	0.80	0.47	--

$[C]_f$ final concentration found at the end of these assays. Dissolution Rate $DR[pH]_{(x,y)}$ at one pH compared to base $DR[pH]_{(a)}$ at same amount of excipient (%w/w). Dissolution Rate $DR[\%]_{(j,k)}$ from different amount of excipient applied compared to $DR[\%]_i$ at 25% of excipient at same pH. $S_{(SF)}$ solubility found by Shake Flask for the substances at the respective pH and % of excipient, expressed in μg/mL.

Moreover, the DR at the second sectors are a bit lower than those at first sector, and DR in general are similar to the DR given in the single pH sector model (see Table 22).

In the case of Iso, the addition of KOL in the two pH sectors model causes progressive augmentation of the concentration of Iso with the increment of %KOL. It also produces profiles very similar to those obtained with CAV with the exception of 75% of excipient. At this percentage there is evidence of high disintegration of the surface of the tablets, generating small jumps in the profile which increases the variability of the concentration of Iso especially at the second sector, but without saturation of the systems. The arrangement of pH 2.0 – 6.5 yielded slightly higher $[C]_f$ than the previous array (Figure 53-1B,2B and Table 22).

The dissolution profiles for Pir using KOL are in same line as with CAV, this is, a 25% of KOL yields profiles more similar to Pir alone than to 50% of KOL. In the latter case the augmentation of concentration is remarkable and, with 75% of KOL there is high heterogeneous disintegration of the surfaces of the tablets, generating a much higher $[C]_f$ with high variability, but no supersaturation as showed in Figure 53-1C,2C (see Tables 21 and 22). Nevertheless, it seems that these last systems could be saturated because the profiles show the shape of a plateau formation.

Interestingly, in general the $[C]_f$ achieved with KOL are slightly better than those with CAV, however the DRs are close or slower than those with CAV. Moreover, while CAV can supersaturate a few systems under certain conditions in the two sectors model, with KOL that supersaturation is not reached.

Although the results obtained with CAV and KOL working at the two pH

sectors model are in agreement with the results found with the one sector model, the assays performed in the two pH sectors model (2.0 – 5.8 or 2.0 – 6.5) are more interesting because they mimic the physiological conditions in the gastrointestinal tract, allowing us to observe changes in the dissolution behaviour in the transition between pH values.

4.4.4 The effect of the nature of the excipients

In section 4.3.2 it was discussed the effectiveness of the excipients in the enhancement of the solubility of the APIs from SF assays. Then it was expected that the use of the same excipients could also increase the dissolution rate of the APIs. In this section the study of dissolution profiles was extended beyond CAV and KOL to the other excipients previously used, these are Captisol (CAP), Klucel (KLU) and Plasdone S630 (S630).

The comparative study is conducted only in the two pH sectors model because of its physiological relevance. As was observed in this model with CAV and KOL, the usage of 25% of these excipients hardly increases the DR or the concentration of the APIs, obtaining dissolution profiles very similar to those from the API alone. On the contrary, when 75% of the enhancer was applied, most of the times the tablets tended to suffer rapid and aggressive breakage, or at least the releasing of the API was very heterogeneous causing very high variability. Thus, ratio 1:1 is selected for this part of the study. Figure 54 shows the dissolution profiles obtained for the drugs alone and with excipients at the mentioned ratio. In general, all the excipients increase the concentration and Dissolution Rate of the samples, although in different levels.

The dissolution profiles obtained for Bzt (Figure 54-1A,2A) show that the usage of CAV develops a supersaturated system at pH 2.0 and in the transition to pH 5.8, where at the beginning of this latter sector there is an immediate drop

of the concentration. This supersaturation is not present with the other cyclodextrin. On the contrary, profile with CAP does not create jumps and it has a continued shape like the profile from Bzt alone. The other excipients are all of them causing jumps of their profiles in the region of pH transition. Additionally, KLU and S630 show similar profiles with very similar $[C]_f$ (see Table 23), although lower than KOL, which is showing higher variability due to heterogeneous disintegration of the tablets. These behaviours are also

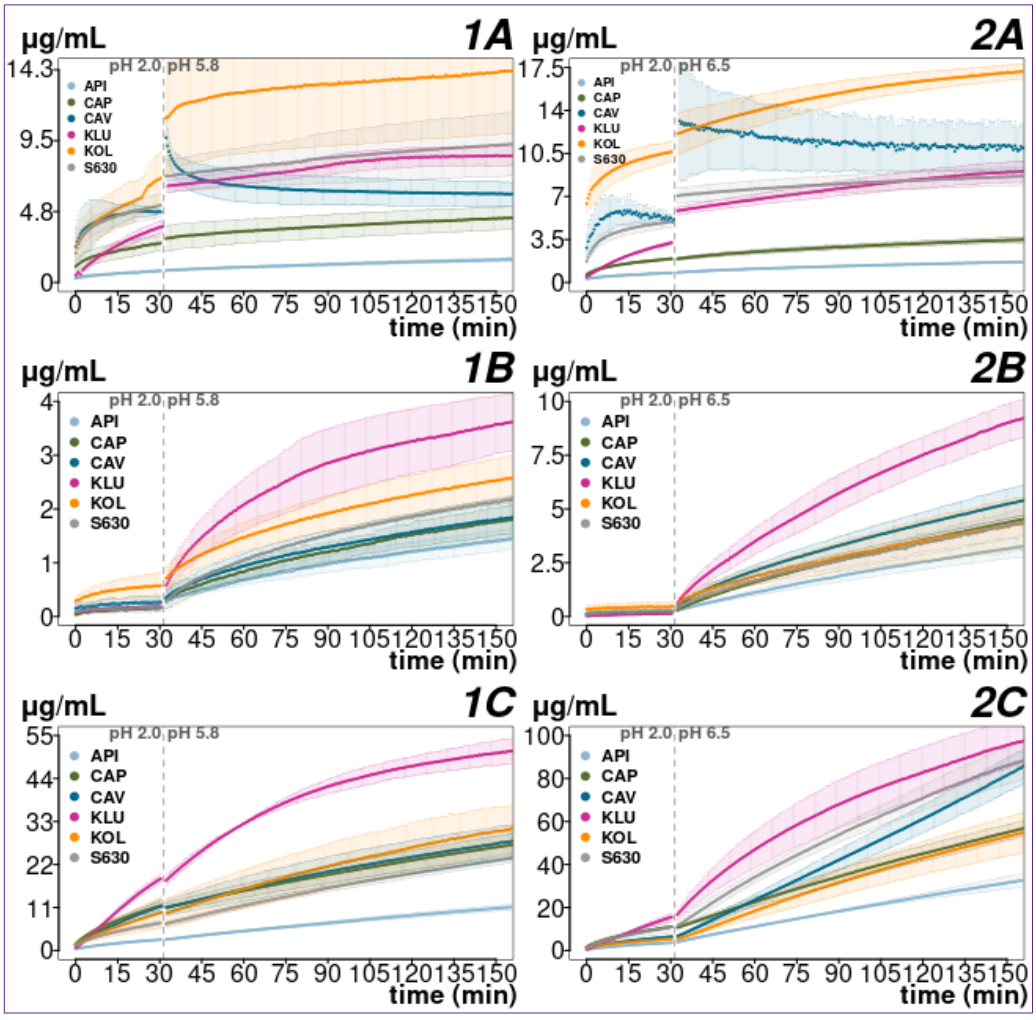

Fig 54: Dissolution profiles of APIs with different excipients. (A) benzthiazide, (B) isoxicam, (C) piroxicam, (1) pH 2.0 – 5.8, (2) pH 2.0 – 6.5.

happening in the pH 2.0 – 6.5 array, but with the difference that now the profile with CAV is lower than KOL, but higher than KLU and S630. Since Bzt is more ionised at pH 6.5, the $[C]_f$ obtained in the profiles at pH 2.0 – 6.5 are slightly higher than those obtained at pH 2.0 – 5.8 (Table 23). The DRs are generally lower in the second sector for all of the excipients with respect to the first sector. However, within these second sectors their DRs are not too different (Table 23). Moreover, the relative DRs in column 7 are higher than the values in column 5, suggesting that the effect of the excipient is higher than the effect of the pH for Bzt, as previously pointed.

The treatment of Iso with KLU yielded the highest concentration of the API. At pH 2.0 all the excipients produce relatively similar levels of concentration of API, but scarcely higher than the profile for Iso alone. This could be due to the poor solubility of Iso and the short run time (30 min) of this pH stage. When pH changes to the next step, at pH 5.8 each excipient increases the profile in different levels (see Figure 54-1B), where the cyclodextrins are very similar between them and lower than the polymeric excipients. These results are in concordance with those obtained in SF experiments (see Figure 46), excepting for S630 which in SF assays is causing the highest variation of log*S* (like in Bzt), but in dissolution profiles at pH 2.0 – 5.8 it is in lower level respect to the other polymeric excipients. When pH changes from 2.0 to 6.5 all the excipients increase the concentration of Iso, but it is KLU which highlights among the others. At this pH it seems that the ionisation degree of Iso exerts even more effect than the excipients, although none of these effects are limiting each other (see Table 23, columns 5 – 7). At difference from Bzt, CAV cannot produce supersaturation of systems with Iso.

Table 23: Dissolution Rates, Relative DR and Final Concentrations for the APIs obtained in presence of different enhancers.

Excipient	pH	*Extrapolated DR* $(\mu g/min)$	$[C]_f$ $(\mu g/mL)$	$\left[\frac{DR(pH_i)}{DR(pH_2)}\right]_{[excip]}$	$\left[\frac{DR(pH_{6.5})}{DR(pH_{5.8})}\right]_{[excip]}$	$\left[\frac{DR(Excip_i)}{DR(API)}\right]_{[pH]}$	$S_{(SF)}$ $(\mu g/mL)$
Bzt							
	1.88±0.02	0.68±0.16	0.78±0.07	--	--	--	4.31
API	5.68±0.06	0.20±0.07	1.54±0.17	0.29		--	4.61
	6.36±0.03	0.29±0.02	1.68±0.06	0.42	1.45	--	6.35
	1.91±0.01	2.72±0.06	2.03±0.25	--	--	4.01	12.44
CAP	5.63±0.01	1.10±0.19	4.34±0.96	0.40	--	5.56	10.93
	6.34±0.01	1.08±0.38	3.50±0.28	0.40	0.99	3.79	10.14
	1.88±0.02	6.94±1.77	4.05±1.17	--	--	10.22	7.12
CAV	5.65±0.04	--	5.94±0.78	--	--	--	7.03
	6.39±0.01	--	11.11±1.91	--	--	--	8.94
	1.91±0.02	3.03±0.67	3.50±0.44	--	--	4.46	5.38
KLU	5.65±0.05	1.94±0.45	8.47±0.77	0.64	--	9.85	6.12
	6.36±0.02	1.20±0.41	9.05±1.05	0.39	0.62	4.19	9.11
	1.89±0.01	5.04±0.67	5.62±1.06	--	--	7.43	7.48
KOL	5.72±0.02	5.81±4.84	17.00±4.81	1.15	--	29.45	9.77
	6.35±0.01	3.78±0.31	17.19±0.77	0.75	0.65	13.24	13.89
	1.94±0.09	13.94±3.09	5.06±0.72	--	--	20.53	9.08
S630	5.68±0.02	1.07±0.51	9.28±2.59	0.08	--	5.43	13.97
	6.36±0.01	1.39±0.13	8.65±0.88	0.10	1.30	4.86	20.43
Iso							
	1.92±0.06	0.49±0.29	0.27±0.08	--	--	--	0.70
API	5.73±0.04	0.29±0.09	1.45±0.26	0.58	--	--	7.13
	6.42±0.04	0.64±0.18	3.56±0.67	1.30	2.25	--	28.86

Excipient	pH	*Extrapolated DR* ($\mu g/min$)	$[C]_f$ ($\mu g/mL$)	$\left[\frac{DR(pH_i)}{DR(pH_2)}\right]_{[excip]}$	$\left[\frac{DR(pH_{6.5})}{DR(pH_{5.8})}\right]_{[excip]}$	$\left[\frac{DR(Excip_i)}{DR(API)}\right]_{[pH]}$	$S_{(SF)}$ ($\mu g/mL$)
	1.90±0.01	0.28±0.23	0.17±0.08	--	--	0.57	1.84
CAP	5.64±0.00	0.59±0.08	1.81±0.32	2.11	--	2.07	11.03
	6.35±0.00	0.99±0.08	4.56±0.24	3.51	1.67	1.54	29.24
	1.91±0.01	0.39±0.11	0.25±0.10	--	--	0.79	4.02
CAV	5.71±0.05	0.63±0.33	1.85±0.47	1.64	--	2.22	9.45
	6.38±0.01	1.29±0.16	5.44±0.87	3.32	2.03	2.00	37.95
	1.89±0.02	0.17±0.17	0.16±0.02	--	--	0.35	7.43
KLU	5.66±0.01	1.80±0.54	3.62±0.66	10.46	--	6.30	13.16
	6.35±0.02	2.31±0.89	9.24±1.06	13.42	1.28	3.60	56.77
	1.86±0.06	0.86±0.49	0.47±0.31	--	--	1.74	1.69
KOL	5.67±0.04	1.05±0.10	2.59±0.48	1.23	--	3.69	16.56
	6.36±0.01	1.25±0.27	4.39±1.37	1.46	1.18	1.94	48.20
	1.97±0.01	0.29±0.15	0.18±0.02	--	--	0.58	6.75
S630	5.64±0.02	0.79±0.07	3.33±1.31	2.76	--	2.78	20.71
	6.36±0.02	1.00±0.31	6.04±2.00	3.49	1.26	1.56	73.31
Pir							
	1.92±0.05	2.68±0.65	4.02±0.37	--	--	--	14.59
API	5.75±0.04	1.70±0.13	11.18±1.05	0.63	--	--	48.05
	6.44±0.01	4.81±0.22	32.94±4.71	1.79	2.84	--	101.36
	1.79±0.01	10.78±1.30	11.27±1.03	--	--	4.02	47.09
CAP	5.49±0.02	3.25±0.72	27.13±3.45	0.30	--	1.91	41.38
	6.23±0.01	8.01±2.03	57.08±4.26	0.74	2.47	1.66	97.80
	1.90±0.01	7.12±1.44	9.25±2.98	--	--	2.65	18.87
CAV	5.67±0.05	3.86±1.45	28.82±4.41	0.54	--	2.27	61.52
	6.52±0.02	--	86.48±10.10	--	--	--	152.75

Excipient	pH	*Extrapolated DR* $(\mu g/min)$	$[C]_f$ $(\mu g/mL)$	$\left[\frac{DR(pH_i)}{DR(pH_2)}\right]_{[excip]}$	$\left[\frac{DR(pH_{6.5})}{DR(pH_{5.8})}\right]_{[excip]}$	$\left[\frac{DR(Excip_i)}{DR(API)}\right]_{[pH]}$	$S_{(SF)}$ $(\mu g/mL)$
KLU	1.78±0.01	16.96±2.21	9.70±1.42	--	--	6.32	46.30
	5.54±0.03	16.25±2.17	51.05±3.92	0.96	--	9.58	85.79
	6.23±0.03	27.30±9.00	97.71±13.25	1.61	1.68	5.67	255.60
KOL	1.89±0.01	9.44±7.19	9.22±8.31	--	--	3.52	34.59
	5.93±0.47	4.85±1.64	31.58±6.99	0.51	--	2.86	88.76
	6.39±0.01	9.00±3.02	55.22±11.43	0.95	1.85	1.87	289.19
S630	1.86±0.05	8.36±1.48	8.07±1.81	--	--	3.11	43.89
	5.54±0.02	3.31±0.29	23.70±1.35	0.40	--	1.95	107.73
	6.32±0.01	15.95±0.49	89.02±10.90	1.91	4.82	3.31	359.05

$S_{(SF)}$ concentration obtained from the solubility determined in SF experiments.

In the case of Pir (Figure 54-1C,2C), which is structurally similar to Iso, it is also KLU the one that produces the highest elevation in the dissolution profile, particularly in pH 2.0 – 5.8 assay. In turn, when pH changes from 2.0 to 6.5, CAV and S630 tends to reach similar levels of concentration of Pir compared to the higher value of KLU at the end of the assay. The profile from CAV:Pir has a more linear shape indicating a sustained release of the API at difference from the other profiles, whose shapes are more typical to a first order kinetic process (Figure 54-2C). This difference could be due to the fact that the tablets with CAV might be suffering a different – and more homogeneous – disintegration and deaggregation at this pH value. Since Pir is also ionised in high degree at pH 6.5, the combination of these phenomena could cause the sustained release of the drug, which was also observed in Figure 52.

In general, the relative DR (Table 23, columns 5 – 7) are different for each API which in turn suggests that, as pointed before, the effect of pH on the dissolution processes is different and it may become more important than the effect given by the excipient. Nonetheless, the effect of the excipient seems to be better when the molecule is in its neutral form. Since the excipients are hydrophilic they can be wetted and rapidly dissolved in the aqueous boundary layer, making them available for interactions. On the other hand, the increasingly ionisation degree of the samples elevates their solubility, allowing them to be carried by the solubilized excipient from the ABL to the bulk. In case of S630 better Dissolution Rates and higher dissolution profiles could be expected according to the results obtained in SF experiments (Figure 46). However, the results show lower dissolution profiles that could be related to a slower releasing mechanism of API, which could be different from the other excipients, due to the possibly higher hardness of the tablets that could difficult

their surface wettability and the release of the drug. These differences in those physical properties of the tablets could be given by the nature of the powder obtained after the mixing of the different excipients with the respective APIs. Thus, in order to determine possible interactions given in the solid-solid mixtures, DSC analyses were programmed.

4.4.5 Solid mixture analysis by Differential Scanning Calorimetry.

Performing Differential Scanning Calorimetry analysis (DSC) allows to obtain the thermograms from the drugs, excipients and their solid-solid mixture powders. The studied interval of temperature is from 35 ºC to 285 ºC, in order to determine principally the temperature when the samples undergo melting and/or degradation processes. All the samples show thermal events above 120 ºC. Comparing the thermograms of the mixtures taking as reference each one of the thermograms from the APIs and excipients by separate, allows us to determine differences between the mixtures and their isolated components. Those differences could be due to interactions between excipient and the respective API.

Figure 55A shows the individual normalized thermograms for the excipients, 55B to F, show the thermograms for mixtures with Bzt and the respective excipient compared to the API alone. Evidences of interaction between Bzt with each excipient are found excepting for the mixture Bzt:CAV (Figure 55C). In Figure 55B, whereas Bzt shows two exothermic peaks (238 ºC and 242 ºC) corresponding to the melting point of its two different crystalline forms, the thermogram for CAP shows a softening and melting point interval between ~175 °C – 200 ºC, followed by its degradation. However, the thermogram line for Bzt:CAP blend is showing evidence of interaction with possibly formation of an eutectic, which can be observed by the thermal event that includes an

exothermic peak, in the interval ~150 – 168 ºC, process which is not present in the isolated components and whose temperature range is lower than the events encountered on each separated components.

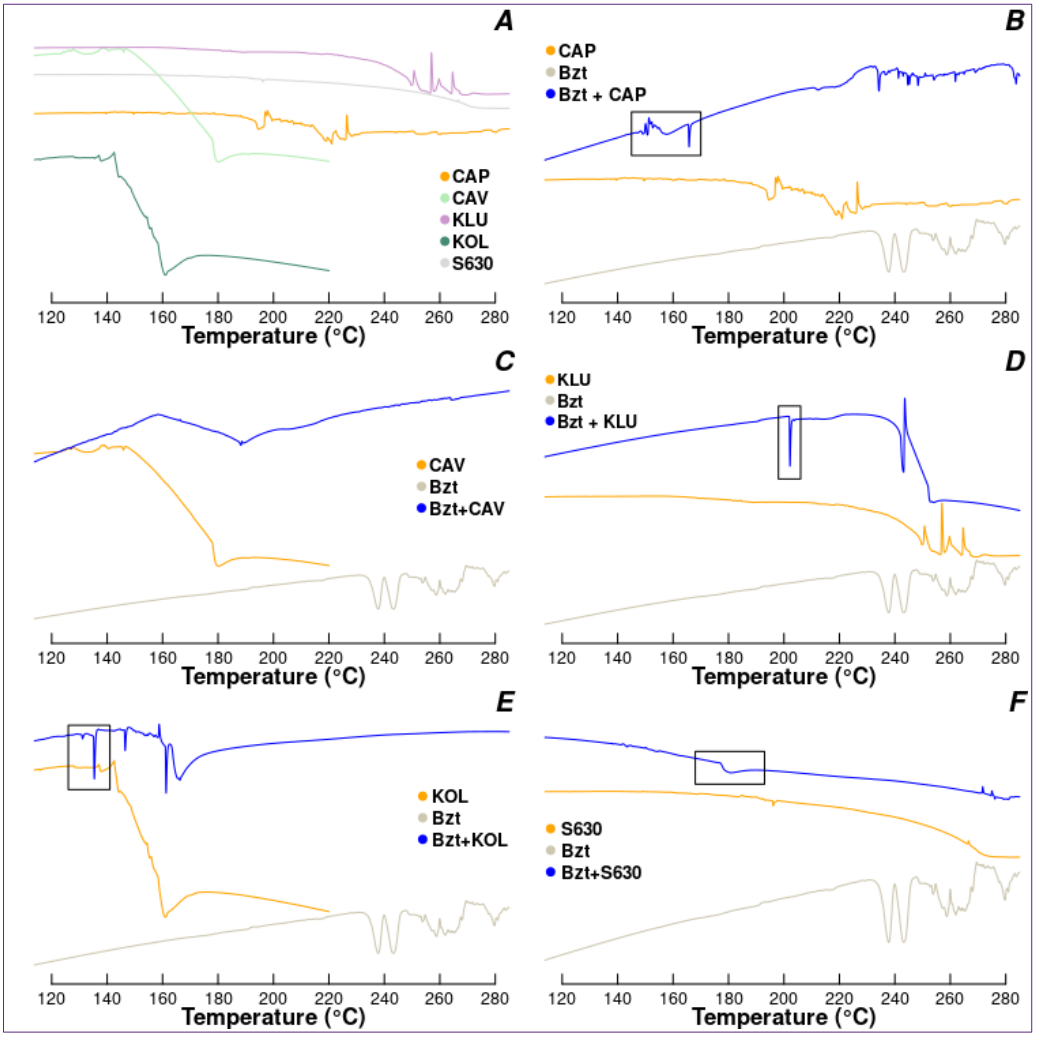

Fig 55: Thermograms for excipients, Bzt and their respective solid mixtures.

When mixtures of Bzt with the remaining excipients are analysed, interactions similar to Bzt:CAP are found (see Figure 55D,E,F). However, in none of the cases with positive evidence of interactions it is possible to elucidate if only one or both of the crystalline forms of Bzt are interacting with the respective

excipient, neither it is possible to say if one of the crystalline form of Bzt is reconverting into the other one and then interacting with the excipient.

As previously introduced, the analysis of mixture Bzt:CAV shows no evidence of interaction between these solids. Despite that in the thermogram of this mixture there are no peaks corresponding to the crystalline phase of Bzt, these could be overlapped by the exothermic process of degradation of CAV (see Figure 55C).

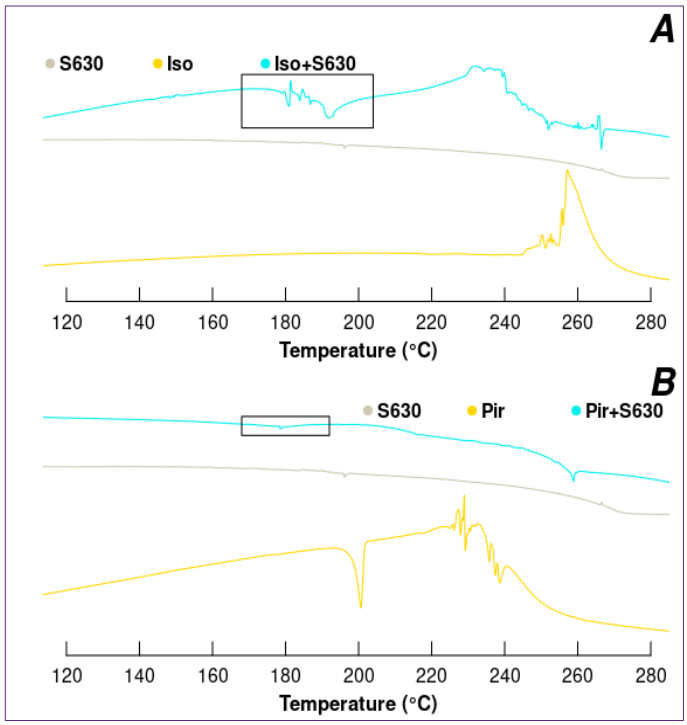

Fig 56: Thermograms for (A) Iso, and (B) Pir, compared with Plasdone S630 and with their respective mixtures.

In case of Iso, there is evidence of interaction with S630 (Figure 56A) due to the presence of an exothermic event (~180 – 210 ºC), which is at lower interval than the given for the melting of S630 (~205 – 210 ºC, exothermic) or Iso (~245 – 270 ºC, endothermic). Similar situation is observed with the Pir:S630 mixture (Figure 56B), showing an exothermic event below 190 ºC, while the exothermic melting of Pir is at ~198 – 205 ºC.

The observed interactions could be due to either an inclusion of the API in the crystalline lattice of the excipient, or a reorganization of both API and

excipients into a new crystalline lattice. Due to the solid blends were prepared using manual grinding, it is not expected that these applied forces could be strong enough to change the crystal phases of neither APIs nor excipients.

The presence of these solid-solid interactions observed in DSC could explain why some of these mixtures are not behaving in DR assays in the same way as expected by the results obtained by SF. These interactions observed could have almost no relevance in SF assays for the reason that the solubility determination by this technique is a long-term experiment that allows to stablish equilibria between the solid and aqueous phases. On the other hand, the Dissolution Profiles are determined in a relatively short time (around 150 min) and, the respective Dissolution Rate is calculated by the data obtained within the few first minutes of the start of the assay, just after the instrumental delay time. This could cause a simultaneous release of both API and excipient, in a process limited by the disintegration of the surface of the tablet containing this complex, which could explain the apparent “flat” or “straight” shapes of the dissolution profiles of some of the samples. On the contrary, where there are no interactions in the solids, the hydrophilic excipient in the surface of the tablets could be causing a rapid disintegration of the tablet because of a better wettability, obtaining profiles with a typical shape of first order kinetic. This process, as pointed before, could provide enough amount of excipient to be available in the aqueous boundary layer between the surface of the tablet and the solution, to carry the solubilized API to the bulk. Interestingly, in the observed “straight” profiles that show different kinetic release processes, these could have properties of a controlled release systems with a constant DR.

4.4.6 The effect of the BDM on the DR

Since in the previous section it was demonstrated that the tablets made with KLU and KOL as excipients yielded the highest dissolution profiles and $[C]_f$ for their respective API in aqueous media, same mixtures were selected to be tested in this section with Biorelevant Dissolution Media (BDM) for the determination of the DR and Dissolution Profiles. Figure 57 shows the obtained profiles for

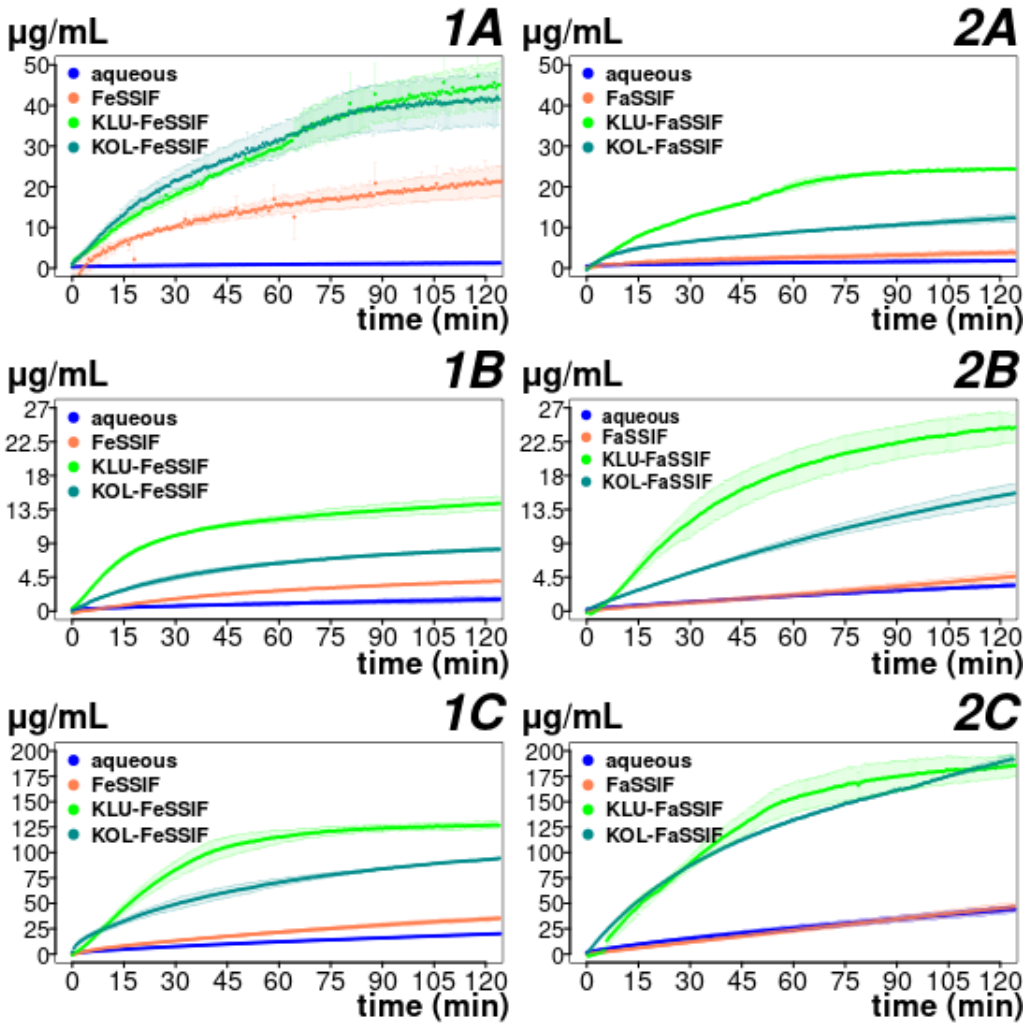

Fig 57: Dissolution profiles for (A) Bzt, (B) Iso and (C) Pir, with presence of KLU (green) and KOL (cyan), in FeSSIF (1) and FaSSIF (2) media.

Bzt, Iso and Pir in FeSSIFv2 for pH 5.8 and FaSSIFv2 for pH 6.5, their mixtures with KLU and KOL, and for the sake of comparison the profiles of APIs alone in aqueous media. Table 24 contains the calculated DR and $[C]_f$ for all the assays under the described conditions.

Table 24: Dissolution Rate and Final Concentration ($[C]_f$) calculated for the studied APIs in aqueous and BDM media with KLU or KOL as excipients

BDM	*pH*	*Extrapolated DR* $(\mu g/min)$	$[C]_f$ $(\mu g/mL)$	$S_{(SF)}$ $(\mu g/mL)$
		Bzt		
API	5.62±0.15	0.33±0.17	1.26±0.25	4.61±0.38
FeSSIF	5.8	27.33±18.63	21.24±5.16	13.90±0.82
FeSSIF-KLU	5.8	10.70±3.25	45.05±5.82	13.10±0.24
FeSSIF-KOL	5.8	15.70±1.60	41.46±6.23	--
API	6.45±0.13	0.79±0.11	1.73±0.33	6.35±0.19
FaSSIF	6.5	1.53±1.16	3.79±0.78	10.45±0.83
FaSSIF-KLU	6.5	9.74±0.65	24.33±0.11	10.96±0.71
FaSSIF-KOL	6.5	8.24±2.48	12.29±0.95	17.83±0.59
		Iso		
API	5.66±0.10	0.35±0.08	1.57±0.42	7.13±1.28
FeSSIF	5.8	0.90±0.03	3.97±0.02	10.67±0.25
FeSSIF-KLU	5.8	7.62±0.73	14.31±0.91	14.57±2.45
FeSSIF-KOL	5.8	2.83±0.49	8.23±0.26	--
API	6.45±0.06	0.61±0.03	3.42±0.23	28.86±2.78
FaSSIF	6.5	0.55±0.13	4.61±0.61	31.89±0.91
FaSSIF-KLU	6.5	6.41±1.19	24.39±2.05	51.83±8.97
FaSSIF-KOL	6.5	2.13±0.12	15.66±1.31	47.77±2.97
		Pir		
API	5.65±0.02	4.38±0.19	20.11±0.49	48.05±5.79
FeSSIF	6.5	8.20±0.52	35.20±2.31	109.05±1.88
FeSSIF-KLU	6.5	46.37±8.33	126.68±3.82	122.06±13.28
FeSSIF-KOL	6.5	42.17±11.28	94.29±1.00	--
API	6.37±0.05	9.21±1.52	43.96±3.55	101.36±22.17
FaSSIF	6.5	4.57±0.46	46.73±4.25	205.96±26.07
FaSSIF-KLU	6.5	56.67±9.52	185.62±10.90	341.66±21.30
FaSSIF-KOL	6.5	44.87±1.47	191.45±4.08	334.23±14.84

FaS and FeS are for FaSSIF and FeSSIF biorelevant media respectively

In Figure 57 the respective profiles show that the usage of FaSSIF slightly increases the dissolution of Bzt and Iso respect to their aqueous profiles, whereas for Pir there is no a significant improvement. On the contrary, FeSSIF enhances the dissolution of the APIs. This can be attributed to the different

interactions that could be present on each BDM, particularly the micelles formation in FeSSIF. These micelles could allow hydrophobic and HB interactions that, as expected, are higher when the sample is in its neutral form like in Bzt, where the profile is more differentiated from the aqueous one (see Figure 57-1A).

Figure 57 also shows that the use of KLU or KOL, at proportion 1:1 (w/w) in mixture with the APIs in presence of BDM, develops an enormously increased dissolution profiles. In the case of Bzt both excipients reach similar $[C]_f$ and similar profiles in FeSSIF medium (Figure 57-1A), suggesting that the interactions given between this medium and drug are predominant against the interactions given between Bzt and these excipients. On the contrary, in FaSSIF the profiles are lower because of the absence of the micelles, obtaining also dissolution profiles with well differentiated shapes. Despite the fact that the DR of Bzt with KLU is not much higher than that with KOL, the $[C]_f$ yielded with KLU is twice that of KOL (Figure 57-2A, Table 24). This is suggesting that in general the releasing mechanism of the API is different depending on the excipient used. The mixture Bzt:KOL in FaSSIF shows a more sustained release of Bzt compared to its profile in aqueous medium (Figure 51), that can be attributable to its preferred interactions with FaSSIF components than with KOL, even with a possible competition for Bzt between KOL and medium components. In turn, the augmented profile observed for Bzt:KLU could be possibly explained by synergic mechanism between this excipient together to medium components.

The Dissolution profiles for Iso and Pir in FaSSIF with presence of KLU and KOL (Figure 57) have similar behaviour than those in aqueous medium (Figure 54), but with an increased $[C]_f$. Then, at difference from Bzt, the excipients and

FaSSIF seem to interact with a synergic mechanism for the increment of the release of both APIs, mechanism that apparently is higher for KLU. When FeSSIF is used these profiles are showing a tendency to stabilise the concentration. In this BDM KLU seems to work better than KOL yielding higher profiles, since KOL seems to have some competitive interactions with FeSSIF components for the respective API. These profiles also show lower $[C]_f$ than in FaSSIF. This could be attributed to the high ionisation degree of the drugs that could give preference to the electrostatic interactions respect to the hydrophobic ones. The difference between Iso and Pir is that for the first one its profiles in FaSSIF with KLU and KOL are more differentiated than with Pir, and for the latter there is only a minimal gap in the middle sector but at the end of the assay their $[C]_f$ have a difference statistically non-significant (Figure 57-2B,2C, Table 24).

In the same Table can be appreciated that in FeSSIF medium KLU is capable of increase the $[C]_f$ of Iso and Pir up to same levels of those given by SF under same conditions. This increment is even higher for Bzt and the respective profile does not show signs of plateau formation, evidencing that this system has a quite big extension of supersaturation. This behaviour of Bzt is repeated in FaSSIF with same excipient. On the contrary, Iso and Pir reaches about half the $[C]_f$ respect to the values given by SF in this conditions. The usage of KOL in mixture with all the APIs does not allow to get saturation levels of any of them in presence of FaSSIF with respect to the solubility given by SF under these conditions. However, these concentrations are better than those in aqueous media, or without excipient, confirming that the combination of both excipient and BDM has a positive effect in the dissolution of the analytes.

The concomitant use of excipients and BDM increases considerably the DR of all the APIs respect to their velocity in aqueous media or in BDM without excipient. However, this velocity is not the same for each API using the same excipient in different BDM or *vice versa*, confirming that each excipient and media make their own process. Moreover, based on the differences observed in the profiles depending on the experimental conditions, it can be concluded that the releasing process from the surface of the tablet is different in each case, with the exceptions given in FeSSIF with Bzt (Figure 57-1A) and in FaSSIF for Pir (Figure 57-2C). In general, FeSSIF alone tends to produce higher DR with respect to aqueous medium particularly for low ionised compounds, whereas FaSSIF tends to maintain the same or slightly lower DR compared to the aqueous values for each API (see Table 24).

As observed in Figure 57 and Table 24, the combination of excipients and FeSSIF, in general, raises the DR in a better degree than the excipients and FaSSIF, and KLU produces better enhancement of the DR in these type of BDM. It is difficult to explain how the disintegration and disaggregation are occurring, because it could be that the API and excipient are releasing each one by separate, or could be releasing together at the same time in the ABL. Then, it could be that the BDM (whether they are forming micelles or not) could help on the release of APIs and excipients from tablets, or in carrying the APIs and/or the excipients, and/or its complexes from the ABL to the bulk. It is also very important the ionisation degree of the samples, because this could favour hydrophobic and/or HB interactions. All of these factors generate very complicated matrices, where each case have its own specificities.

The behaviour of the drugs in DR assays with excipients and BDM is sometimes different compared to the SF assays under the same conditions. In

some instances the long time needed for SF assays could allow to break some interactions that could be present in the relatively short time for Dissolution Profiles and Rates assays or on the contrary, some interactions could be completed during the long-term assays of SF and those could be absent in the short DR assays. Moreover, in SF the samples are introduced as loose powder whereas in DR those powders are first compressed in tablets, making the contact between samples and media very different.

5 CONCLUSIONS

The present work has been focused in the study of the variation of two physicochemical properties, Solubility and Dissolution Rate, directly related to the adsorption of the API through the gastrointestinal tract, when several conditions of the medium are changed. Although they are both fundamental measurements of the dissolution capacity of a compound of pharmaceutical interests, each property shows its own particularities and challenges. In this section are presented the general conclusions about the comparison of the two main methods for solubility measurements, and the effect of pH, enhancers and biorelevant media in both the solubility and the dissolution rates of some selected acidic APIs. Finally, this work is concluded with general remarks about the necessity of specific dissolution studies for a particular drug, and with the observed differences between solubility and dissolution rate assays.

5.1 Methods for solubility determinations

- The solubility behaviour of glimepiride, pioglitazone and sibutramine, compounds with different acid-base properties (acid, ampholyte and base, respectively) have been studied in detail using the Shake-Flask (SF) and CheqSol methods, which let to establish a comparison between both approaches to point out their advantages and complementarity.

  On the one hand, SF is a time-consuming method, but allows to measure the solubility of a compound at any pH value. Thus it can be applied to determine not only the solubility of the neutral free species, but also that of their corresponding conjugated ionised forms and even their salts. Moreover, SF allows the detection and quantification of aggregation and complexation reactions concurrent with solubility equilibria, and the solid precipitated can be easily collected to be identified or characterised by X-

ray diffraction or DSC. On the other hand, although the automated CheqSol is limited to the measurement of the solubility of neutral species, it provides additional information on kinetic solubility and supersaturation behaviour of the compound. Therefore, SF and CheqSol are complementary methods, and their combined information provides an accurate picture of the solubility behaviour of the studied drugs.

- When only acid-base equilibria are present in solution, both SF and CheqSol approaches allow an accurate determination of the intrinsic solubility. Thus, in the absence of concurrent aggregation or complexation equilibria, and provided that pK_a values are precisely determined, the same solubility-pH profiles are obtained with both methods. When complex equilibria are present, both approaches can conduct to the obtention of apparent intrinsic solubilities and/or mismatched solubility-pH profiles. This is because CheqSol approach do not consider the influence of additional aggregation equilibria and thus it always assumes a Henderson-Hasselbalch behaviour. The intrinsic solubility and aggregation number and constants can be obtained when an appropriated model is fitting the experimental SF solubility-pH data.

- Regarding to the compounds studied, on the one hand CheqSol shows that glimepiride and pioglitazone behave as a chaser compound, this is, they are prone to supersaturation, as expected from their relatively high polar surface area and hydrogen-bonding capabilities, being the glimepiride the one with the best supersaturation. On the contrary, sibutramine does not supersaturate and initially it behaves as a non-chaser compound, but in the course of the titration it changes to a chaser behaviour. On the other hand, SF method suggests the formation of neutral aggregates of glimepiride and

pioglitazone, and permits the study of the effect of buffering species on the formation of sibutramine salts, showing that TFA, a constituent of the recommended MS-MUB buffer, induces the salt precipitation with a K_{sp} lower than the hydrochloride salt.

5.2 Effect of pH, enhancers and biorelevant dissolution media on the solubility

- The solubility of the selected acidic compounds, benzthiazide, isoxicam and piroxicam, is pH dependent and it is not affected by the components of the studied buffers (acetate, phosphate and maleate). Provided that the pK_a values of the drugs are accurately determined, the solubility data obtained at three different pH values of physiological interest (2.0, 5.8 and 6.5) allows the detection of neutral aggregates for isoxicam, with an apparent intrinsic solubility about one unit higher than that of the free monomer. No effect of pH is observed over the studied excipients.

- The addition of excipients tends to increase the solubility of the APIs, but in different degrees depending on the API, excipient, and pH conditions. Thus, among the tested excipients, CAP (cyclodextrin) is the one that mostly enhance the solubility of Bz, particularly when the drug is in its neutral (unionised) form. Better solubility results are obtained for Iso and Pir using polymeric excipients, especially with Iso and plasdone S630 (polyvinylpyrrolidone). The solubility of Pir is similarly enhanced by plasdone and KLU (hydroxypropylcellulose).

- The principal interactions between excipient and API driven by cyclodextrins are of hydrophobic nature. Then, the more ionised is the API, the weakest interaction with the cyclodextrin. Moreover, the inclusion of

the drug into the cyclodextrin cavity depends on the size of its entrance, which is affected by the functional groups modifying the cyclodextrin. The sulfonic substituents in CAP enlarge the entrance of the cavity due to electrostatic repulsion between them, whereas the hydroxyl groups in CAV are closer each other, reducing the cavity entrance. The external substituents can also interact with the API by electrostatic interactions. Then, the neutral form of Iso interacts with CAV by formation of hydrogen bonds (HB), whereas the protonated species of Pir interacts with the negatively charge sulfonic group of CAP by ion pairing.

- The polymeric excipients interact with APIs by HB interactions. Substances with high ability to donate and/or accept HB will increase its solubility in the presence of the excipient. Polyvinylpyrrolidones (PVPs) show HB acceptor capability, and this feature is increased in S630 due to the presence of vinylacetate groups. Then, HB donor substances, as Bz, Iso and Pir, can interact with PVPs. The most significant increase on solubility is observed between S630 and the neutral form of Iso, which exhibits the greatest HB donor capacity. KLU is a hydroxypropylcellulose characterised for being a HB donor and substances with HB acceptor capability can interact with this excipient. This type of interaction can explain the solubility enhancement observed for neutral form of Iso and Pir, and the poor activity of KLU on the neutral species of Bzt due to the low HB acceptor ability of the drug.

- The use of Biorelevant Dissolution Media (BDM) as FeSSIF or FaSSIF allows the solubility determination of APIs in conditions closer to the physiological ones. In these cases, solubility enhancement is only observed when interactions between some components of the medium and the API take place. The solubility of neutral APIs is normally increased in the

presence of FeSSIF due to the partition of the uncharged form of the compound into the micelles of the BDM.

- The addition of excipients to FeSSIF or FaSSIF media can improve or decrease the solubility of APIs. A synergically effect of FeSSIF is observed for Pir in the presence of cyclodextrins, but the contrary outcome occurs for Bzt in the same BDM with the excipient CAV. This antagonistic effect is also observed for Bz when CAV and S630 excipients are added to FaSSIF medium; in fact, the solubility is almost the same than the observed in absence of this BDM, which means that FaSSIF does not alter the interaction mechanisms of these excipients.

5.3 Effect of pH, enhancers and biorelevant dissolution media on the Dissolution Rate

- The dissolution profiles of the selected compounds, benzthiazide, isoxicam and piroxicam, are pH dependent. The more ionised the API is, the higher its dissolution rate and the concentration at the end of the assay. Although the dissolution rate is related to the solubility of the compound, a direct relation between these two dissolution properties cannot be established, since the dissolution rate depends also on other parameters such tablet hardness or wettability.

- Dissolution profiles conducted at the two pH sectors model mimic the physiological conditions in the gastrointestinal tract and allow the study of the effect of the abrupt pH change on the dissolution behaviour of the drugs.

- The addition of the studied excipients in the tablet formulation improves the

dissolution of the API. Nevertheless, under the same medium and/or API conditions, the improvement observed depends on the excipient used and does not follow the same trend observed in solubility measurements. For instance, the studied cyclodextrins yield lower dissolution profiles with respect to polymeric excipients, despite SF assays show better solubilities when cyclodextrins are used in comparison with KLU and KOL. The presence of solid-solid interactions observed in DSC could explain these different behaviours. Since solid-solid interactions are expected to be weak in the physical mixtures used in this work, they should be irrelevant in the long-term solubility equilibrium corresponding to the SF assays, particularly when excipient:API mixtures are introduced as uncompressed powder. As a counterpoint, dissolution profiles are obtained in relatively short-time assays and solid samples consist of compressed tablets.

- The effect of the addition of excipients in the tablet formulation depends on the medium used (aqueous pH or BDM). The ionisation seems to play a more relevant role on the dissolution of the API than the addition of excipient. The FaSSIF medium does not significantly alter the dissolution behaviour of the studied APIs, whereas the use of FeSSIF increases the dissolution rate of the drugs. This increase is more significant for Bz, which at the pH of FeSSIF is practically in its neutral form and can interact with the hydrophobic part of the micelles. The addition of KOL and particularly KLU clearly improve the dissolution of the studied APIs in both BDM. However, the factors that contributed to this improvement are unclear and their elucidation require a further study, especially in FeSSIF medium where complicated matrices can be generated.

5.4 General Remarks

- The solubility and dissolution rate of a potential drug candidate are key properties affecting its success as an active pharmaceutical ingredient, since the bioavailability of a drug greatly depends on its capacity to be dissolved in the most convenient body fluid at the corresponding therapeutic dosage. Some compounds of pharmaceutical interest are poorly soluble and, particularly in the case of oral administration, are formulated with excipients to enhance its solubility and/or dissolution rate. However, the study of the dissolution properties of a compound in the presence of different excipients and media, either aqueous buffers or simulated intestinal fluids, is really challenging due to the complex interactions taking place between drug, excipient and medium.

- The establishment of accurate relationships between a family of excipients and its capacity to improve the dissolution profile of a particular drug candidate is at the present time unreliable. Each system API:Excipient, even among excipients presenting relatively similar features, represents an individual case requiring an extensive study in order to find the most convenient excipient to improve its solubility and/or dissolution rate.

- The ionisation degree of the drug and the use of simulated gastrointestinal fluids as dissolution media are general factors improving the solubility, but the addition of an excipient is not always favourable. In fact, in a few cases the combination of a certain excipient with a specific BDM results in a diminished activity of one of them, or even the cancellation of the solubility enhancement observed for any of them alone when they are assayed separately with the drug.

- Although dissolution rate depends on solubility, the excipients and media improving the latter not necessarily enhance the former. Some excipients allow to achieve drug final concentrations in DR assays in the range of their corresponding solubilities, but they might not be releasing the API from the tablet at the same velocity or rate. These differences between solubility and dissolution rate behaviour are due to additional factors influencing the drug release, mainly related to the aqueous boundary layer between the tablet and the bulk solution. ABL is practically a micro-environment where many phenomena or subprocesses occur. The solid sample dissolves and then diffuses, leading to a relatively high concentration of the sample in the ABL with respect to the bulk solution, and this in turn might generate an specific pH in this micro-environment, which could alter the conditions of releasing, ionising and solubilising of the drug. Differences between solubility and dissolution rate might also be devoted to the initial solid form employed and the duration of the assays. Whereas solubility is determined after a long period of equilibration and from loose powder, DR is measured within the few first minutes of the assay and with compressed tablets as starting solid, where solid-solid interactions might occur, conditioning the disintegrating and deaggregating processes.

6 BILBIOGRAPHY AND REFERENCES

BIBLIOGRAPHY AND REFERENCES

[1]. TEKADE, Rakesh K. *DOSAGE FORM DESIGN CONSIDERATIONS*. London : Academic Press, 2018. ISBN 9780128144237.

[2]. NIAZI, Sarfaraz K. *Handbook of Preformulation. Chemical, Biological and Botanical Drugs*. First. New York : informa Healthcare, 2007. ISBN 9780849371936.

[3]. GIBSON, Mark. *Pharmaceutical Preformulation and Formulation: A Practical Guide from Candidate Drug Selection to Commercial Dosage Form.* Second edi. New York : informa Healthcare, 2009. ISBN 9781420073171.

[4]. AVDEEF, Alex. *Absorption and Drug Development: Solubility, Permeability and Charge State*. Hoboken : John Wiley & Sons, Inc., 2003. ISBN 0-471-42365-3.

[5]. GOLAN, David E., ARMSTRONG, Ehrin J., ARMSTRONG, April W. and TASHJIAN, Armen H. *Principles of pharmacology: The pathophysiologic basis of drug therapy*. Third edit. Wolters Kluwer | Lippincott Williams & Wilkins, 2012. ISBN 9781608312792.

[6]. GUYTON, Arthur C. and HALL, John E. *Textbook of Medical Physiology*. eleventh e. Philadelphia : Elsevier Saunders, 2006. ISBN 0721602401.

[7]. HALL, John E. (John Edward). *Guyton y Hall. Tratado de fisiología médica.* thirteenth. Barcelona : Elsevier Health Sciences Spain - T, 2016. ISBN 9788491130246.

[8]. BICKMORE, Barry R. and WANDER, Matthew C. F. Activity and Activity Coefficients. In : WHITE, William M (ed.), *Encyclopedia of Geochemistry: A Comprehensive Reference Source on the Chemistry of the Earth*. Cham : Springer International Publishing, 2018. p. 1–89. ISBN 978-3-319-39312-4.

[9]. BLACK, Jay R. Debye-Hückel Equation. In : WHITE, William M (ed.), *Encyclopedia of Geochemistry: A Comprehensive Reference Source on the Chemistry of the Earth* [online]. Cham : Springer International Publishing, 2018. p. 345–347. ISBN 978-3-319-39312-4. Available from: https://doi.org/10.1007/978-3-319-39312-4_61

[10]. AVDEEF, A., VOLOBOY, D. and FOREMAN, A. Dissolution and Solubility. In : *Comprehensive Medicinal Chemistry II*. Elsevier, 2007. p. 399–423. ISBN 9780080450445.

[11]. AVDEEF, Alex. pKa Determination. In : *Absorption and Drug Development*. 2012. p. 31–173. Wiley Online Books. ISBN 9781118286067.

[12]. AVDEEF, Alex. Solubility of sparingly-soluble ionizable drugs. *Advanced Drug Delivery Reviews*. 2007. Vol. 59, no. 7, p. 568–590. DOI 10.1016/j.addr.2007.05.008.

[13]. POBUDKOWSKA, Aneta, RÀFOLS, Clara, SUBIRATS, Xavier, BOSCH, Elisabeth and AVDEEF, Alex. Phenothiazines solution complexity – Determination of pKa and solubility-pH profiles exhibiting sub-micellar aggregation at 25 and 37°C. *European Journal of Pharmaceutical Sciences*. 2016. Vol. 93, p. 163–176. DOI https://doi.org/10.1016/j.ejps.2016.07.013.

[14]. SKOOG, DOUGLAS A.; WEST, DONALD M.; HOLLER, F. JAMES; CROUCH, Stanley R. *Fundamentals of Analytical Chemistry*. Ninth edit. Belmont : Cengage Learning, 2013. ISBN 9780495558286.

[15]. AVDEEF, Alex. pH-metric solubility. 1. Solubility-pH profiles from Bjerrum plots. Gibbs buffer and pK(a) in the solid state. *Pharmacy and Pharmacology Communications*. 1998. Vol. 4, no. 3, p. 165–178. DOI 10.1111/j.2042-7158.1998.tb00328.x.

[16]. STRENG, William H. The Gibbs constant and pH solubility profiles. *International Journal of Pharmaceutics*. 1999. Vol. 186, no. 2, p. 137–140. DOI 10.1016/S0378-5173(99)00155-6.

[17]. SINGH, Saumya, PARIKH, Tapan, SANDHU, Harpreet K., SHAH, Navnit H., MALICK, A. Waseem, SINGHAL, Dharmendra and SERAJUDDIN, Abu T.M. Supersolubilization and amorphization of a model basic drug, haloperidol, by interaction with weak acids. *Pharmaceutical Research*. 2013. Vol. 30, no. 6, p. 1561–1573. DOI 10.1007/s11095-013-0994-7.

[18]. SERAJUDDIN, Abu T.M. M. Salt formation to improve drug solubility. *Advanced Drug Delivery Reviews*. 2007. Vol. 59, no. 7, p. 603–616. DOI https://doi.org/10.1016/j.addr.2007.05.010. From Duplicate 1 (Salt formation to improve drug solubility - Serajuddin, Abu T M)Drug Solubility: How to Measure it, How to Improve it

[19]. COMER, J. E.A. A. Ionization constants and ionization profiles. In : TAYLOR, John B and TRIGGLE, David J (eds.), *Comprehensive Medicinal Chemistry II*. Oxford : Elsevier, 2006. p. 357–397. ISBN 9780080450445.

[20]. LONG, Michelle and CHEN, Yisheng. Dissolution Testing of Solid Products. In : *Developing Solid Oral Dosage Forms*. 2009. p. 319–340. ISBN 9780444532428.

[21]. FELTON, Linda. *Remington Essentials of Pharmaceutics*. First edit. London : Pharmaceuticals Press, 2013. ISBN 9780857111050.

[22]. HAYES, Sheila. Remington: The Science and Practice of Pharmacy, volume I and volume II. In : *Journal of the Medical Library Association : JMLA*. 22nd editi. Hartford : University of Pittsburgh, University Library System, 2014. Accession Number: 103977927. Language: English. Entry Date: 20140722. Revision Date: 20150710. Publication Type: Journal Article; book review. Journal Subset: Computer/Information Science; Double Blind Peer Reviewed; Editorial Board Reviewed; Expert Peer Reviewed; Peer Reviewed; USA. NLM UID: 101132728.

[23]. HIGUCHI, Takeru. Rate of release of medicaments from ointment bases containing drugs in suspension. *Journal of Pharmaceutical Sciences*. 1961. Vol. 50, no. 10, p. 874–875. DOI 10.1002/jps.2600501018.

[24]. CHEN, Yisheng and FLANAGAN, Douglas. Theory of Diffusion and Pharmaceutical Applications. In : YIHONG QIU, YISHENG CHEN, GEOFF G.Z. ZHANG, LIRONG LIU, William Porter (ed.), *Developing Solid Oral Dosage Forms*. First edit. London : Academic Press, 2009. p. 147–162. ISBN 9780444532428.

[25]. NOYES, Arthur A. and WHITNEY, Willis R. The rate of solution of solid substances in their own solutions. *Journal of the American Chemical Society*. 1897. Vol. 19, no. 12, p. 930–934. DOI 10.1021/ja02086a003.

[26]. BRÜNNER, Erich., NERNST, W, BRÜNNER, Erich. and NERNST, W. Theorie der Reaktionsgeschwindigkeit in heterogenen Systemen. *Zeitschrift für Physikalische Chemie*. 1904. Vol. 47U, no. 1, p. 52–55. DOI 10.1515/zpch-1904-4705.

[27]. HISASHI NOGAMI, Tsuneji Nagari and Akira Suzuki and NOGAMI, Tsuneji Nagari and Akira Suzuki Hisashi. Studies on Powered preparations. Dissolition

Rate of Sulfonamides by Rotating Disk Method. *Chem. Pharm. Bull.* 1966. Vol. 14, p. 329–338.

[28]. WANG, Jianzhuo and FLANAGAN, Douglas R. Fundamentals of Dissolution. In : *Developing Solid Oral Dosage Forms*. First edit. London : Academic Press, 2009. p. 309–318. ISBN 9780444532428.

[29]. SEAGER, R. J., ACEVEDO, Andrew J., SPILL, Fabian and ZAMAN, Muhammad H. Solid dissolution in a fluid solvent is characterized by the interplay of surface area-dependent diffusion and physical fragmentation. *Scientific Reports*. 2018. Vol. 8, no. 1, p. 1–17. DOI 10.1038/s41598-018-25821-x.

[30]. SMITH, Blaine Templar. Solubility and Dissolution. In : *Remington Education: Physical Pharmacy*. Hoboken : Pharmaceutical Press, 2017. p. 31–50. ISBN 9780857112521.

[31]. GRAVESTOCK, Tom, BOX, Karl, COMER, John, FRAKE, Elizabeth, JUDGE, Sam and RUIZ, Rebeca. The “gI dissolution” method: A low volume, in vitro apparatus for assessing the dissolution/precipitation behaviour of an active pharmaceutical ingredient under biorelevant conditions. *Analytical Methods*. 2011. Vol. 3, no. 3, p. 560–567. DOI 10.1039/c0ay00434k.

[32]. AVDEEF, Alex and TSINMAN, Oksana. Miniaturized rotating disk intrinsic dissolution rate measurement: Effects of buffer capacity in comparisons to traditional Wood’s apparatus. *Pharmaceutical Research*. 2008. Vol. 25, no. 11, p. 2613–2627. DOI 10.1007/s11095-008-9679-z.

[33]. SAARINEN-SAVOLAINEN, Paula, JÄRVINEN, Tomi, TAIPALE, Hannu and URTTI, Arto. Method for evaluating drug release from liposomes in sink conditions. *International Journal of Pharmaceutics*. 1997. Vol. 159, no. 1, p. 27–33. DOI 10.1016/S0378-5173(97)00264-0.

[34]. WILLIAMS, Adrian C., TIMMINS, Peter, LU, Mingchu and FORBES, Robert T. Disorder and dissolution enhancement: Deposition of ibuprofen on to insoluble polymers. *European Journal of Pharmaceutical Sciences*. 2005. Vol. 26, no. 3–4, p. 288–294. DOI 10.1016/j.ejps.2005.06.006.

[35]. FAGERBERG, Jonas H., TSINMAN, Oksana, SUN, Na, TSINMAN, Konstantin, AVDEEF, Alex and BERGSTRÖM, Christel A.S. Dissolution rate and apparent solubility of poorly soluble drugs in biorelevant dissolution media.

Molecular Pharmaceutics. 2010. Vol. 7, no. 5, p. 1419–1430. DOI 10.1021/mp100049m.

[36]. TINKE, A. P., VANHOUTTE, K., DE MAESSCHALCK, R., VERHEYEN, S. and DE WINTER, H. A new approach in the prediction of the dissolution behavior of suspended particles by means of their particle size distribution. *Journal of Pharmaceutical and Biomedical Analysis*. 2005. Vol. 39, no. 5, p. 900–907. DOI 10.1016/j.jpba.2005.05.014.

[37]. KANSY, Manfred, AVDEEF, Alex and FISCHER, Holger. Advances in screening for membrane permeability: High-resolution PAMPA for medicinal chemists. *Drug Discovery Today: Technologies*. 2004. Vol. 1, no. 4, p. 349–355. DOI 10.1016/j.ddtec.2004.11.013.

[38]. CARON, Giulia, ERMONDI, Giuseppe, DAMIANO, Alessandro, NOVAROLI, Laura, TSINMAN, Oksana, RUELL, Jeffrey A. and AVDEEF, Alex. Ionization, lipophilicity, and molecular modeling to investigate permeability and other biological properties of amlodipine. *Bioorganic and Medicinal Chemistry*. 2004. Vol. 12, no. 23, p. 6107–6118. DOI 10.1016/j.bmc.2004.09.004.

[39]. DI, Li and KERNS, Edward H. Chapter 19 – Pharmacokinetics. *Drug-Like Properties*. 2016. No. Iv, p. 267–281. DOI 10.1016/B978-0-12-801076-1.00019-8.

[40]. QIU, Yihong. In Vitro-In Vivo Correlations: Fundamentals, Development Considerations, and Applications. *Developing Solid Oral Dosage Forms*. 2009. P. 379–406. DOI 10.1016/B978-0-444-53242-8.00017-5.

[41]. FOOD AND DRUG ADMINISTRATION, U.S. Department of Health and Human. Guidance for Industry: Statistical Approaches to Establishing Bioequivalence. In : *FDA Guidance for Industry* [online]. 2001. p. 48. Available from: http://www.lexjansen.com/pharmasug/2008/sp/sp04.pdf

[42]. HE, Xiaorong. Integration of Physical, Chemical, Mechanical, and Biopharmaceutical Properties in Solid Oral Dosage Form Development. In : *Developing Solid Oral Dosage Forms*. London : Academic Press, 2009. ISBN 9780444532428.

[43]. NIAZI, Sarfaraz K. *Handbook of Preformulation. Chemical, Biological and Botanical Drugs*. Second ed. Boca Raton : CRC Press, 2019. ISBN 9781138297555.

[44]. AMIDON, GORDON L.; LENNERNAS, H.; SHAH, VINOD P.; CRISON, J. R. A theoretical basis for a biopharmaceutic drug classification: The correlation of in vitro drug product dissolution and in vivo bioavailability. *AAPS Journal*. 25 September 2014. Vol. 16, no. 5, p. 894–898. DOI 10.1208/s12248-014-9620-9.

[45]. BOU-CHACRA, Nadia, MELO, Katherine Jasmine Curo, MORALES, Ivan Andrés Cordova, STIPPLER, Erika S., KESISOGLOU, Filippos, YAZDANIAN, Mehran and LÖBENBERG, Raimar. Evolution of Choice of Solubility and Dissolution Media After Two Decades of Biopharmaceutical Classification System. *AAPS Journal*. 2017. Vol. 19, no. 4, p. 989–1001. DOI 10.1208/s12248-017-0085-5.

[46]. BERGSTRÖM, Christel A.S., ANDERSSON, Sara B.E., FAGERBERG, Jonas H., RAGNARSSON, Gert and LINDAHL, Anders. Is the full potential of the biopharmaceutics classification system reached? *European Journal of Pharmaceutical Sciences*. 2014. Vol. 57, no. 1, p. 224–231. DOI 10.1016/j.ejps.2013.09.010.

[47]. BUTLER, James M and DRESSMAN, Jennifer B. The developability classification system: Application of biopharmaceutics concepts to formulation development. *Journal of Pharmaceutical Sciences*. 2010. Vol. 99, no. 12, p. 4940–4954. DOI 10.1002/jps.22217.

[48]. BERGSTRÖM, Christel A.S., BOX, Karl, HOLM, René, MATTHEWS, Wayne, MCALLISTER, Mark, MÜLLERTZ, Anette, RADES, Thomas, SCHÄFER, Kerstin J. and TELEKI, Alexandra. Biorelevant intrinsic dissolution profiling in early drug development: Fundamental, methodological, and industrial aspects. *European Journal of Pharmaceutics and Biopharmaceutics*. 2019. Vol. 139, no. October 2018, p. 101–114. DOI 10.1016/j.ejpb.2019.03.011.

[49]. BONILLA VALLADARES, Pablo. *Formación y caracterización de nanosistemas terapéuticos con alginato. (Tesis doctoral)* [online]. University of Barcelona, 2015. Available from: http://hdl.handle.net/2445/106878

[50]. AULTON, M E and TAYLOR, K M G. *Aulton's Pharmaceutics E-Book: The Design and Manufacture of Medicines* [online]. Elsevier Health Sciences, 2017. ISBN 9780702070013. Available from: https://books.google.es/books?id=HXfODgAAQBAJ

[51]. DI, Li, KERNS, Edward H., DI, Li and KERNS, Edward H. Chapter 41 – Formulation. In : *Drug-Like Properties*. 2016. p. 497–510. ISBN 9780128010761.

[52]. KARPINSKI, P. H. Polymorphism of Active Pharmaceutical Ingredients. *Chemical Engineering & Technology*. February 2006. Vol. 29, no. 2, p. 233–237. DOI 10.1002/ceat.200500397.

[53]. MATSUNAGA, YASUSHI; BANDO, NOBUYUKI; YUASA, HIROSHI; KANAYA, Yoshio. Effects of Grinding and Tableting on Physicochemical Stability of an Anticancer Drug, TAT-59. *Chemical Pharmaceutical Bulletin*. 1996. Vol. 10, no. 44, p. 1931–1934.

[54]. LEFEBVRE, C, GUYOT-HERMANN, A M, DRAGUET-BRUGHMANS, M, BOUCHÉ, R and GUYOT, J C. Polymorphic Transitions of Carbamazepine During Grinding and Compression. *Drug Development and Industrial Pharmacy*. 1 January 1986. Vol. 12, no. 11–13, p. 1913–1927. DOI 10.3109/03639048609042617.

[55]. NARANG, Ajit S., RAO, Venkatramana M. and RAGHAVAN, Krishnaswamy S. Excipient Compatibility. In : *Developing Solid Oral Dosage Forms*. London : Academic Press, 2009. p. 125–145. ISBN 9780444532428.

[56]. SUN, Changquan Calvin. A classification system for tableting behaviors of binary powder mixtures. *Asian Journal of Pharmaceutical Sciences*. 2016. Vol. 11, no. 4, p. 486–491. DOI https://doi.org/10.1016/j.ajps.2015.11.122.

[57]. *USP-NF online* [online]. 2020. Rockville : USPC,. [Accessed 15 May 2020]. Available from: https://www.usp.org

[58]. EDQM COUNCIL OF EUROPE. *European Pharmacopoeia 10.2* [online]. 2020. Strasbourg. Available from: https://pheur.edqm.eu/

[59]. KARTHIK VARMA V. Excipients used in the Formulation of Tablets. *RR J. Chem*. 2016. Vol. 5, no. 2, p. 143–154.

[60]. GOSWAMI, Sathi, MAJUMDAR, Anupa and SARKAR, Munna. Painkiller Isoxicam and Its Copper Complex Can Form Inclusion Complexes with Different Cyclodextrins: A Fluorescence, Fourier Transform Infrared Spectroscopy, and Nuclear Magnetic Resonance Study. *Journal of Physical*

Chemistry B. 2017. Vol. 121, no. 36, p. 8454–8466. DOI 10.1021/acs.jpcb.7b05649.

[61]. LOFTSSON, T, HREINSDÓTTIR, D, OF, M Másson - International journal and 2005, Undefined. Evaluation of cyclodextrin solubilization of drugs. *International Journal of Pharm*. 2005. Vol. 302, p. 18–28. DOI 10.1016/j.ijpharm.2005.05.042.

[62]. JANSOOK, Phatsawee, OGAWA, Noriko and LOFTSSON, Thorsteinn. Cyclodextrins: structure, physicochemical properties and pharmaceutical applications. *International Journal of Pharmaceutics*. 2018. Vol. 535, no. 1–2, p. 272–284. DOI 10.1016/j.ijpharm.2017.11.018.

[63]. JAMBHEKAR, Sunil S and BREEN, Philip. Cyclodextrins in pharmaceutical formulations I : structure and physicochemical properties , formation of complexes , and types of complex. . 2016. Vol. 21, no. 2, p. 356–362. DOI http://dx.doi.org/10.1016/j.drudis.2015.11.017.

[64]. JAMBHEKAR, Sunil S. and BREEN, Philip. Cyclodextrins in pharmaceutical formulations II: Solubilization, binding constant, and complexation efficiency. *Drug Discovery Today*. 2016. Vol. 21, no. 2, p. 363–368. DOI 10.1016/j.drudis.2015.11.016.

[65]. AVDEEF, Alex. Composition of ternary (metal-ligand-hydrogen) complexes experimentally determined from titrations using only a pH electrode. *Inorganic Chemistry*. 1 October 1980. Vol. 19, no. 10, p. 3081–3086. DOI 10.1021/ic50212a051.

[66]. SUBIRATS, X., FUGUET, E., ROSÉS, M., BOSCH, E. and RÀFOLS, C. Methods for pKa Determination (I): Potentiometry, Spectrophotometry, and Capillary Electrophoresis. In : *Reference Module in Chemistry, Molecular Sciences and Chemical Engineering*. Waltham : Elsevier Inc., 2015. p. 1–10. ISBN 9780124095472.

[67]. SALGADO, L. E. Vidal and VARGAS-HERNÁNDEZ, C. Spectrophotometric Determination of the pKa, Isosbestic Point and Equation of Absorbance vs. pH for a Universal pH Indicator. *American Journal of Analytical Chemistry*. 4 December 2014. Vol. 05, no. 17, p. 1290–1301. DOI 10.4236/ajac.2014.517135.

[68]. TAM, Kin Y. and TAKÁCS-NOVÁK, Krisztina. Multi-wavelength spectrophotometric determination of acid dissociation constants: A validation

study. *Analytica Chimica Acta*. 2001. Vol. 434, no. 1, p. 157–167. DOI 10.1016/S0003-2670(01)00810-8.

[69]. STUART, Martin and BOX, Karl. Chasing Equilibrium: Measuring the Intrinsic Solubility of Weak Acids and Bases. *Analytical Chemistry*. 2005. Vol. 77, no. 4, p. 983–990. DOI https://10.1021/ac048767n. From Duplicate 1 (Chasing Equilibrium: Measuring the Intrinsic Solubility of Weak Acids and Bases - Stuart, Martin; Box, Karl)

[70]. AVDEEF, Alex., COMER, John E A and THOMSON, Simon J. pH-Metric log P. 3. Glass electrode calibration in methanol-water, applied to pKa determination of water-insoluble substances. *Analytical Chemistry*. 1 January 1993. Vol. 65, no. 1, p. 42–49. DOI 10.1021/ac00049a010.

[71]. AVDEEF, A, BOX, K J, COMER, J E A, GILGES, M, HADLEY, M, HIBBERT, C, PATTERSON, W and TAM, K Y. PH-metric logP 11. pKa determination of water-insoluble drugs in organic solvent–water mixtures. *Journal of Pharmaceutical and Biomedical Analysis*. 1999. Vol. 20, no. 4, p. 631–641. DOI https://doi.org/10.1016/S0731-7085(98)00235-0.

[72]. BOX, Karl J, VÖLGYI, Gergely, BAKA, Edit, STUART, Martin, TAKÁCS-NOVÁK, Krisztina and COMER, John E A. Equilibrium versus kinetic measurements of aqueous solubility, and the ability of compounds to supersaturate in solution—a validation study. *Journal of Pharmaceutical Sciences*. 2006. Vol. 95, no. 6, p. 1298–1307. DOI 10.1002/jps.20613.

[73]. AVDEEF, Alex, FUGUET, Elisabet, LLINÀS, Antonio, RÀFOLS, Clara, BOSCH, Elisabeth, VÖLGYI, Gergely, VERBIC, Tatjana, BOLDYREVA, Elena and TAKÁCS-NOVÁK, Krisztina. Equilibrium solubility measurement of ionizable drugs - consensus recommendations for improving data quality. *ADMET and DMPK*. 2016. Vol. 4, no. 2, p. 117–178. DOI 10.5599/admet.4.2.292.

[74]. SKOOG, DOUGLAS A.; HOLLER, F. JAMES; CROUCH, Stanley R. *Principles of Instrumental Analysis*. Seventh ed. Boston : Cengage Learning, 2018. ISBN 978-1-305-57721-3.

[75]. *Advanced Chemistry Development ACD/Labs Software, Ontario, 2020* [online]. Ontario - Canada : Advanced Chemistry Development Inc. 11.02. Available from: https://www.acdlabs.com

[76]. YASUDA, Motoo. Dissociation Constants of Some Carboxylic Acids in Mixed Aqueous Solvents. *Bulletin of the Chemical Society of Japan*. 1959. Vol. 32, no. 5, p. 429–432. DOI 10.1246/bcsj.32.429.

[77]. BOX, Karl, COMER, John E., GRAVESTOCK, Tom and STUART, Martin. New ideas about the solubility of drugs. *Chemistry and Biodiversity*. 2009. Vol. 6, no. 11, p. 1767–1788. DOI 10.1002/cbdv.200900164.

[78]. *Martindale : guía completa de consulta farmacoterapéutica / dirigida por Sean C. Sweetman*. Barcelona : Pharma, 2008. ISBN 9788495993505.

[79]. MCLAMORE, W. M.; LAUBACH, G.D. Benzthiazide Synthesis. U.S. Patent 3,11,517. 1993. US.

[80]. ACDLABS. *ACD/ChemSketch (Freeware) 2019.1.3 - Advanced Chemistry Development* [online]. 2019. Advanced Chemistry Development Inc. 2019.1.3. Available from: https://www.acdlabs.com

[81]. NATIONAL CENTER FOR BIOTECHNOLOGY INFORMATION. National Center for Biotechnology Information. PubChem Database. Sibutramine, CID=5210, https://pubchem.ncbi.nlm.nih.gov/compound/Sibutramine (accessed on Apr. 10, 2020). .

[82]. BUDAVARI, S. (ed.). *The Merck Index - An Encyclopedia of Chemicals, Drugs, and Biologicals.* Whitehouse Station, NJ : Merck and Co., Inc., 1996.

[83]. HOU, T. J., ZHANG, W., XIA, K., QIAO, X. B. and XU, X. J. ADME evaluation in drug discovery. 5. Correlation of caco-2 permeation with simple molecular properties. *Journal of Chemical Information and Computer Sciences*. 2004. Vol. 44, no. 5, p. 1585–1600. DOI 10.1021/ci049884m.

[84]. VAN DE WATERBEEMD, H. In silico models to predict oral absorption. *Comprehensive Medicinal Chemistry II*. 2006. Vol. 5, p. 669–697. DOI 10.1016/b0-08-045044-x/00145-0.

[85]. TANDON, Hiteshi, RANJAN, Prabhat, CHAKRABORTY, Tanmoy and SUHAG, Vandana. Polarizability: a promising descriptor to study chemical–biological interactions. *Molecular Diversity*. 2020. No. 2. DOI 10.1007/s11030-020-10062-w.

[86]. JAIN, Neera and YALKOWSKY, Samuel H. Estimation of the aqueous solubility I: Application to organic nonelectrolytes. *Journal of Pharmaceutical*

Sciences. 2001. Vol. 90, no. 2, p. 234–252. DOI https://doi.org/10.1002/1520-6017(200102)90:2<234::AID-JPS14>3.0.CO;2-V.

[87]. ADVANCED CHEMISTRY DEVELOPMENT. *ACD/Percepta User Manual*. 2020.

[88]. RÀFOLS, Clara, SUBIRATS, Xavier, RUBIO, Javier, ROSÉS, Martí and BOSCH, Elisabeth. Lipophilicity of amphoteric and zwitterionic compounds: A comparative study of determination methods. *Talanta*. 2017. Vol. 162, no. October 2016, p. 293–299. DOI 10.1016/j.talanta.2016.10.038.

[89]. GRBIC, Sandra, PAROJCIC, Jelena, MALENOVIC, Andjelija, DJURIC, Zorica and MAKSIMOVIC, Milica. A contribution to the glimepiride dissociation constant determination. *Journal of Chemical and Engineering Data*. 11 March 2010. Vol. 55, no. 3, p. 1368–1371. DOI 10.1021/je900546z.

[90]. SEEDHER, Neelam and KANOJIA, Mamta. Co-solvent solubilization of some poorly-soluble antidiabetic drugs Solubilization antidiabetic drugs. *Pharmaceutical Development and Technology*. 2009. Vol. 14, no. 2, p. 185–192. DOI 10.1080/10837450802498894.

[91]. LAKSHMI NARASIMHAM, Y S; and VASANT, D Barhate. Kinetic and intrinsic solubility determination of some β-blockers and antidiabetics by potentiometry. *Journal of Pharmacy Research*. 2011. Vol. 4, no. 2, p. 532–536.

[92]. DEMIRALAY, Ebru Çubuk and YILMAZ, Hülya. Potentiometric pKa Determination of Piroxicam and Tenoxicam in Acetonitrile-Water Binary Mixtures. *SDU Journal of Science*. 2012. Vol. 7, no. 1, p. 34–44.

[93]. FORNELLS, Elisenda, FUGUET, Elisabet, MAÑÉ, Meritxell, RUIZ, Rebeca, BOX, Karl, BOSCH, Elisabeth and RÀFOLS, Clara. Effect of vinylpyrrolidone polymers on the solubility and supersaturation of drugs; a study using the Cheqsol method. *European Journal of Pharmaceutical Sciences*. 2018. Vol. 117, no. February, p. 227–235. DOI 10.1016/j.ejps.2018.02.025.

[94]. MAREN, T. H. Direct measurements of the rate constants of sulfonamides with carbonic anhydrase. *Molecular Pharmacology*. 1992. Vol. 41, no. 2, p. 419–426.

[95]. ISHIHAMA, Yasushi, NAKAMURA, Masahiro, MIWA, Toshinobu, KAJIMA, Takashi and ASAKAWA, Naoki. A rapid method for pKa determination of

drugs using pressure-assisted capillary electrophoresis with photodiode array detection in drug discovery. *Journal of Pharmaceutical Sciences*. 2002. Vol. 91, no. 4, p. 933–942. DOI 10.1002/jps.10087.

[96]. RODRÍGUEZ-BARRIENTOS, Damaris, ROJAS-HERNÁNDEZ, Alberto, GUTIÉRREZ, Atilano, MOYA-HERNÁNDEZ, Rosario, GÓMEZ-BALDERAS, Rodolfo and RAMÍREZ-SILVA, María Teresa. Determination of pKa values of tenoxicam from 1H NMR chemical shifts and of oxicams from electrophoretic mobilities (CZE) with the aid of programs SQUAD and HYPNMR. *Talanta*. 2009. Vol. 80, no. 2, p. 754–762. DOI 10.1016/j.talanta.2009.07.058.

[97]. TANAKA, Yusuke, SUGIHARA, Masahisa, KAWAKAMI, Ayaka, IMAI, So, ITOU, Takafumi, MURASE, Hirokazu, SAIKI, Kazunori, KASAOKA, Satoshi and YOSHIKAWA, Hiroshi. In vivo analysis of supersaturation/precipitation/absorption behavior after oral administration of pioglitazone hydrochloride salt; determinant site of oral absorption. *European Journal of Pharmaceutical Sciences*. 2017. Vol. 106, no. April, p. 431–438. DOI 10.1016/j.ejps.2017.06.011.

[98]. HENNIG, U G G, CHATTEN, L G, MOSKALYK, R E and EDISS, C. Benzothiadiazine Dissociation Constants Parts I and II. *Analyst*. 1981. Vol. 106, p. 557–573.

[99]. RIVED, Fernando, ROSÉS, Martí and BOSCH, Elisabeth. Dissociation constants of neutral and charged acids in methyl alcohol. The acid strength resolution. *Analytica Chimica Acta*. 1998. Vol. 374, no. 2–3, p. 309–324. DOI 10.1016/S0003-2670(98)00418-8.

[100]. ALBERT, Adrien and SERJEANT, E P. Determination of ionization constants by spectrophotometry. In : *The Determination of Ionization Constants: A Laboratory Manual*. Dordrecht : Springer Netherlands, 1984. p. 70–101. ISBN 978-94-009-5548-6.

[101]. IN-ADME RESEARCH. *pDisol-X (TM)* [online]. 2012. in-ADME Research. 3.0 (2012-Q4). Available from: http://www.in-adme.com/pdisol_x.html

[102]. IWATA, Mariko, NAGASE, Hiromasa, ENDO, Tomohiro and UEDA, Haruhisa. Glimepiride. *Acta Crystallographica Section C: Crystal Structure*

Communications. 1997. Vol. 53, no. 3, p. 329–331. DOI 10.1107/S0108270196002363.

[103]. BONFILIO, Rudy, PIRES, Sumaia A, FERREIRA, Leonardo M B, DE ALMEIDA, Adélia E, DORIGUETTO, Antônio C, DE ARAÚJO, Magali B and SALGADO, Hérida R N. A Discriminating Dissolution Method for Glimepiride Polymorphs. *Journal of Pharmaceutical Sciences*. 2012. Vol. 101, no. 2, p. 794–804. DOI https://doi.org/10.1002/jps.22799.

[104]. ENDO, T, IWATA, M, NAGASE, H, SHIRO, M and UEDA, H. Polymorphism of glimepiride: crystallographic study, thermal transitions behavior and dissolution study. *STP PHARMA SCIENCES*. 2003. Vol. 13, no. 4, p. 281–286.

[105]. TIAN, F.; ZIMMERMAN, A. Method for preparing glimepiride α crystal form. CN106866486A. 2017. China : Faming Zhuanli Shenqing.

[106]. TIAN, F.; ZIMMERMAN, A. β Crystal form of glimepiride and preparation method thereof. CN106883161A. 2017. Faming Zhuanli Shenqing.

[107]. TIAN, F.; ZIMMERMAN, A. Method for preparing glimepiride δ crystal form. CN106866485A. 2017. China : Faming Zhuanli Shenqing.

[108]. TIAN, F.; ZIMMERMAN, A. Preparation of glimepiride crystal form ε. CN106866487A. 2017. Faming Zhuanli Shenqing.

[109]. TIAN, F.; ZIMMERMAN, A. Glimepiride γ crystal form and preparation method thereof. CN106699631A. 2017. Faming Zhuanli Shenqing.

[110]. GRYL, Marlena, KRAWCZUK-PANTULA, Anna and STADNICKA, Katarzyna. Charge-density analysis in polymorphs of urea-barbituric acid co-crystals. *Acta Crystallographica Section B: Structural Science*. 2011. Vol. 67, no. 2, p. 144–154. DOI 10.1107/S0108768111002412.

[111]. BERGSTRÖM, Christel A.S., WASSVIK, Carola M., JOHANSSON, Kajsa and HUBATSCH, Ina. Poorly soluble marketed drugs display solvation limited solubility. *Journal of Medicinal Chemistry*. 2007. Vol. 50, no. 23, p. 5858–5862. DOI 10.1021/jm0706416.

[112]. AVDEEF, Alex. Solubility temperature dependence predicted from 2D structure. *ADMET and DMPK*. 2015. Vol. 3, no. 4, p. 298–344. DOI 10.5599/admet.3.4.259.

[113]. TAUPITZ, Thomas, DRESSMAN, Jennifer B. and KLEIN, Sandra. New formulation approaches to improve solubility and drug release from fixed dose combinations: Case examples pioglitazone/glimepiride and ezetimibe/simvastatin. *European Journal of Pharmaceutics and Biopharmaceutics*. 2013. Vol. 84, no. 1, p. 208–218. DOI 10.1016/j.ejpb.2012.11.027.

[114]. GEBAUER, Denis, KELLERMEIER, Matthias, GALE, Julian D., BERGSTRÖM, Lennart and CÖLFEN, Helmut. Pre-nucleation clusters as solute precursors in crystallisation. *Chemical Society Reviews*. 2014. Vol. 43, no. 7, p. 2348–2371. DOI 10.1039/c3cs60451a.

[115]. IRWIN, John J., DUAN, Da, TOROSYAN, Hayarpi, DOAK, Allison K., ZIEBART, Kristin T., STERLING, Teague, TUMANIAN, Gurgen and SHOICHET, Brian K. An Aggregation Advisor for Ligand Discovery. *Journal of Medicinal Chemistry*. 2015. Vol. 58, no. 17, p. 7076–7087. DOI 10.1021/acs.jmedchem.5b01105.

[116]. SUGITA, Masaru, KATAOKA, Makoto, SUGIHARA, Masahisa, TAKEUCHI, Susumu and YAMASHITA, Shinji. Effect of excipients on the particle size of precipitated pioglitazone in the gastrointestinal tract: Impact on bioequivalence. *AAPS Journal*. 2014. Vol. 16, no. 5, p. 1119–1127. DOI 10.1208/s12248-014-9646-z.

[117]. SCHÖNHERR, D., WOLLATZ, U., HAZNAR-GARBACZ, D., HANKE, U., BOX, K. J., TAYLOR, R., RUIZ, R., BEATO, S., BECKER, D. and WEITSCHIES, W. Characterisation of selected active agents regarding pKa values, solubility concentrations and pH profiles by SiriusT3. *European Journal of Pharmaceutics and Biopharmaceutics*. 2015. Vol. 92, p. 155–170. DOI 10.1016/j.ejpb.2015.02.028.

[118]. LAI, F., PINI, E., ANGIONI, G., MANCA, M. L., PERRICCI, J., SINICO, C. and FADDA, A. M. Nanocrystals as tool to improve piroxicam dissolution rate in novel orally disintegrating tablets. *European Journal of Pharmaceutics and Biopharmaceutics*. 2011. Vol. 79, no. 3, p. 552–558. DOI 10.1016/j.ejpb.2011.07.005.

[119]. BOX, K. and COMER, J. Using Measured pKa, LogP and Solubility to Investigate Supersaturation and Predict BCS Class. *Current Drug Metabolism*. 2008. Vol. 9, no. 9, p. 869–878. DOI 10.2174/138920008786485155.

[120]. AVDEEF, Alex. Prediction of aqueous intrinsic solubility of druglike molecules using Random Forest regression trained with Wiki-pS0 database. *ADMET and DMPK*. 2020. Vol. 8, no. 1, p. 29–77. DOI 10.5599/admet.766.

[121]. IGO, David H., BRENNAN, Timothy D. and PULLEN, Eric E. Development of an automated in-line microfiltration system coupled to an HPLC for the determination of solubility. *Journal of Pharmaceutical and Biomedical Analysis*. 2001. Vol. 26, no. 3, p. 495–500. DOI 10.1016/S0731-7085(01)00434-4.

[122]. LLINÀS, Antonio, GLEN, Robert C. and GOODMAN, Jonathan M. Solubility challenge: Can you predict solubilities of 32 molecules using a database of 100 reliable measurements? *Journal of Chemical Information and Modeling*. 2008. Vol. 48, no. 7, p. 1289–1303. DOI 10.1021/ci800058v.

[123]. BAKA, Edit, COMER, John E.A. and TAKÁCS-NOVÁK, Krisztina. Study of equilibrium solubility measurement by saturation shake-flask method using hydrochlorothiazide as model compound. *Journal of Pharmaceutical and Biomedical Analysis*. 2008. Vol. 46, no. 2, p. 335–341. DOI 10.1016/j.jpba.2007.10.030.

[124]. AVDEEF, Alex. Multi-lab intrinsic solubility measurement reproducibility in CheqSol and shake-flask methods. *ADMET and DMPK*. 2019. Vol. 7, no. 3, p. 210–219. DOI 10.5599/admet.698.

[125]. PAAVER, Urve, LUST, Andres, MIRZA, Sabiruddin, RANTANEN, Jukka, VESKI, Peep, HEINÄMÄKI, Jyrki and KOGERMANN, Karin. Insight into the solubility and dissolution behavior of piroxicam anhydrate and monohydrate forms. *International Journal of Pharmaceutics*. 2012. Vol. 431, no. 1–2, p. 111–119. DOI 10.1016/j.ijpharm.2012.04.042.

APPENDIX

A1. *PXRD peak lists (position, 2θ(º)) of glimepiride crystal forms reported in published patents (α, β, γ, δ, ε), simulated peak lists from crystal structures (forms I and II) and the new sodium salt phase characterised in this work.*

Glimepiride polymorphs reported							***New phase sodium salt***
α[1]	**β**[2]	**γ**[3]	**δ**[4]	**ε**[5]	**I**[6]	**II**[7]	
6.916					6.480	7.950	3.259
7.200					10.970	10.527	9.785
8.748		9.729		9.478	12.484	12.057	11.153
10.378	10.895	10.033		10.110	13.140	12.503	12.767
11.166	11.515	10.667	11.521	10.869	13.495	13.874	13.084
14.017	12.316	12.995	14.231	11.447	13.863	14.389	14.399
15.654	14.534	13.408	15.061	12.390	14.707	15.437	14.962
17.107	14.923	17.854	16.529	13.044	16.756	15.934	15.216
17.330	15.287	19.537	18.775	14.414	17.222	16.119	15.553
18.349	16.277		20.536	15.694	18.206	16.967	15.828
19.152	16.549		22.156	18.650	19.239	18.280	16.287
21.103	17.645		30.579	18.984	20.713	18.621	17.998
23.222	19.019		31.025	19.334	21.101	19.545	18.573
23.662	21.952		31.708	21.828	21.348	19.823	19.052
24.038	22.295			22.291	21.530	20.304	20.112
24.332	23.539			22.805	22.030	21.234	20.354
26.197	25.103			23.637	22.320	21.437	21.132
27.055	26.261			24.693	22.994	21.535	21.900
27.888	31.841			25.725	23.189	22.063	22.183
28.178	33.044			27.188	23.332	22.849	22.780
28.634	33.955			31.680	23.739	23.246	24.677
29.085				34.046	25.295	23.781	25.156
30.534					25.847	23.921	25.531
33.804					26.426	24.014	26.581
34.546					26.717	24.283	27.109
35.048					28.945	24.384	31.071
					29.510	25.158	31.397
					30.322	27.946	31.510
					31.939	29.454	34.087

A.2. PXRD peak list of the sibutramine salts phases characterised in this work.

Sibutramine TFA salt		***Sibutramine phosphate salt***	
Position 2θ (º)	***Relative intensity (%)***	***Position 2θ (º)***	***Relative intensity (%)***
8.479	8.4	5.593	20.5
9.917	14.1	5.855	100.0
10.353	18.1	8.202	78.6
11.588	21.8	11.471	17.3
11.993	3.9	11.727	30.3
13.386	16.0	12.789	37.6
15.859	100.0	13.957	20.9
16.977	63.8	14.431	64.7
17.759	44.6	14.550	61.2
18.048	17.6	16.453	52.7
20.631	56.0	17.639	48.2
20.806	22.5	18.014	46.9
22.284	8.4	18.413	20.9
22.500	28.1	18.887	22.9
23.127	5.2	20.103	57.2
23.391	55.6	20.318	40.6
24.918	15.6	22.160	23.5
26.928	9.8	22.734	40.2
27.050	11.9	23.634	26.1
28.890	8.6	24.510	21.8
32.018	6.1	25.014	50.6
35.989	8.3	25.745	19.5
--	--	28.775	28.0
--	--	29.540	18.3

The powder diffractogram was indexed and the lattice parameters were refined by means of the LeBail method, program Dicvol04[8], and the space group was determined from the systematic absences. The cell volume is compatible with 1 molecule of sibutramine and 1 molecule of trifluoroacetic acid in the asymmetric unit, Z=4, (assuming a density value of 1.3).

A.3: *experimental logS values for benzthiazide, isoxicam and piroxicam at different pH in aqueous media (Ac/P and MM) without excipients.*

Buffer	***pH***	***mg/L***	***log S (mol/L)***	***pH***	***mg/L***	***log S (mol/L)***	***pH***	***mg/L***	***log S (mol/L)***
		Bzt			***Iso***			***Pir***	
Ac/P	2.096	4.310	-5.001	2.088	5.488	-4.786	2.072	15.570	-4.328
	2.114	4.304	-5.002	2.085	0.669	-5.700	2.191	15.269	-4.336
	2.136	4.319	-5.000	2.069	0.727	-5.664	2.062	13.932	-4.376
	5.894	4.583	-4.974	5.882	7.174	-4.670	5.838	44.387	-3.873
	5.883	4.173	-5.015	5.894	9.351	-4.555	5.933	40.005	-3.918
	5.913	4.671	-4.966	5.872	7.047	-4.678	5.893	51.134	-3.812
	6.578	6.387	-4.830	6.579	33.573	-4.000	6.602	198.351	-3.223
	6.588	6.360	-4.832	6.585	28.856	-4.065	6.593	140.315	-3.373
	6.596	6.697	-4.810	6.571	30.111	-4.047	6.608	112.233	-3.470
MM	5.759	5.343	-4.908	5.768	6.063	-4.743	5.747	49.608	-3.825
	5.754	4.567	-4.976	5.765	7.963	-4.624	5.754	56.716	-3.767
	5.766	4.387	-4.993	5.761	5.752	-4.766	5.750	48.198	-3.837
	6.493	6.273	-4.838	6.553	29.237	-4.060	6.426	95.672	-3.540
	6.493	6.241	-4.840	6.509	25.809	-4.114	6.449	85.774	-3.587
	6.489	6.129	-4.848	6.478	26.257	-4.106	6.444	82.788	-3.602
Ac/P	--	--	--	--	--	--	3.643	7.091	-4.670
	--	--	--	--	--	--	3.573	7.344	-4.654
	--	--	--	--	--	--	3.526	6.477	-4.709

***A4**: average logS of benzthiazide, isoxicam and piroxicam at different pH in aqueous media including excipients.*

	Bzt		Iso		Pir	
	pH	**log S (M)**	**pH**	**log S (M)**	**pH**	**log S (M)**
pH 2	2.12	-4.69±0.003	2.08	-5.40±0.015	2.11	-4.34±0.027
Captisol	2.16	-4.46±0.021	2.17	-5.32±0.009	2.17	-3.89±0.036
Cavasol	2.16	-4.75±0.029	2.14	-4.82±0.132	2.13	-4.25±0.032
Klucel	2.11	-4.71±0.004	2.13	-5.29±0.111	2.12	-3.86±0.011
Kolidon	2.11	-4.67±0.010	2.09	-4.92±0.181	2.09	-3.99±0.017
PS630	2.01	-4.64±0.015	2.03	-4.80±0.087	2.06	-3.88±0.028
pH 5.8	5.83	-4.68±0.017	5.82	-4.68±0.044	5.82	-3.82±0.039
Captisol	5.92	-4.49±0.022	5.97	-4.52±0.065	5.95	-3.92±0.028
Cavasol	5.94	-4.74±0.072	5.93	-4.45±0.134	5.91	-3.80±0.061
Klucel	5.94	-4.67±0.029	5.91	-4.66±0.114	5.87	-3.59±0.050
Kolidon	5.84	-4.63±0.019	5.84	-4.29±0.058	5.86	-3.55±0.060
PS630	5.85	-4.67±0.025	5.94	-4.10±0.109	5.90	-3.49±0.082
pH 6.5	6.54	-4.61±0.012	6.55	-4.07±0.041	6.50	-3.56±0.060
Captisol	6.67	-4.43±0.071	6.68	-3.92±0.152	6.67	-3.47±0.087
Cavasol	6.61	-4.56±0.102	6.60	-3.91±0.109	6.53	-3.31±0.105
Klucel	6.60	-4.54±0.040	6.58	-3.90±0.104	6.62	-3.04±0.083
Kolidon	6.54	-4.54±0.011	6.52	-3.85±0.020	6.43	-3.06±0.013
PS630	6.57	-4.57±0.045	6.57	-3.66±0.073	6.58	-2.97±0.100
pH 3.5	--	--	--	--	3.58	-4.65±0.026
Captisol	--	--	--	--	3.47	-4.29±0.056
Cavasol	--	--	--	--	3.42	-4.44±0.059
Klucel	--	--	--	--	3.65	-4.11±0.009
Kolidon	--	--	--	--	3.36	-4.20±0.051
PS630	--	--	--	--	3.39	-4.06±0.012

A5: *average experimental logS for benzthiazide, isoxicam and piroxicam in BDM, with and without excipients*

BDM/ Excipient	***Bzt***	
	pH	***log S (M)***
	Bzt	
FeSSIF	5.89±0.00	-4.49±0.03
Captisol	5.91±0.00	-4.60±0.09
Cavasol	5.82±0.00	-4.62±0.01
Klucel	5.77±0.01	-4.52±0.01
Kolidon	--	--
PS630	5.83±0.01	-4.31±0.01
FaSSIF	6.53±0.10	-4.62±0.03
Captisol	6.63±0.06	-4.59±0.06
Cavasol	6.47±0.03	-4.73±0.08
Klucel	6.54±0.03	-4.60±0.03
Kolidon	6.49±0.00	-4.38±0.01
PS630	6.49±0.00	-4.28±0.03
	Iso	
FeSSIF	5.90±0.01	-4.50±0.01
Captisol	5.92±0.01	-4.39±0.09
Cavasol	5.82±0.00	-4.34±0.06
Klucel	5.78±0.08	-4.36±0.07
Kolidon	--	--
PS630	5.83±0.00	-4.15±0.04
FaSSIF	6.58±0.01	-4.02±0.01
Captisol	6.60±0.01	-3.98±0.15
Cavasol	6.49±0.00	-3.93±0.02
Klucel	6.53±0.00	-3.81±0.07
Kolidon	6.50±0.00	-3.85±0.03
PS630	6.53±0.00	-3.66±0.00
	Pir	
FeSSIF	5.87±0.00	-3.48±0.01
Captisol	5.91±0.02	-3.44±0.02
Cavasol	5.81±0.00	-3.50±0.01
Klucel	5.82±0.06	-3.43±0.05
Kolidon	--	--
PS630	5.82±0.01	-3.38±0.03
FaSSIF	6.48±0.01	-3.21±0.05
Captisol	6.56±0.00	-3.45±0.03
Cavasol	6.41±0.00	-3.13±0.04
Klucel	6.46±0.02	-2.99±0.03
Kolidon	6.38±0.02	-3.00±0.02
PS630	6.40±0.00	-2.98±0.00

Figure S1: DSC of sodium-glimepiride salt

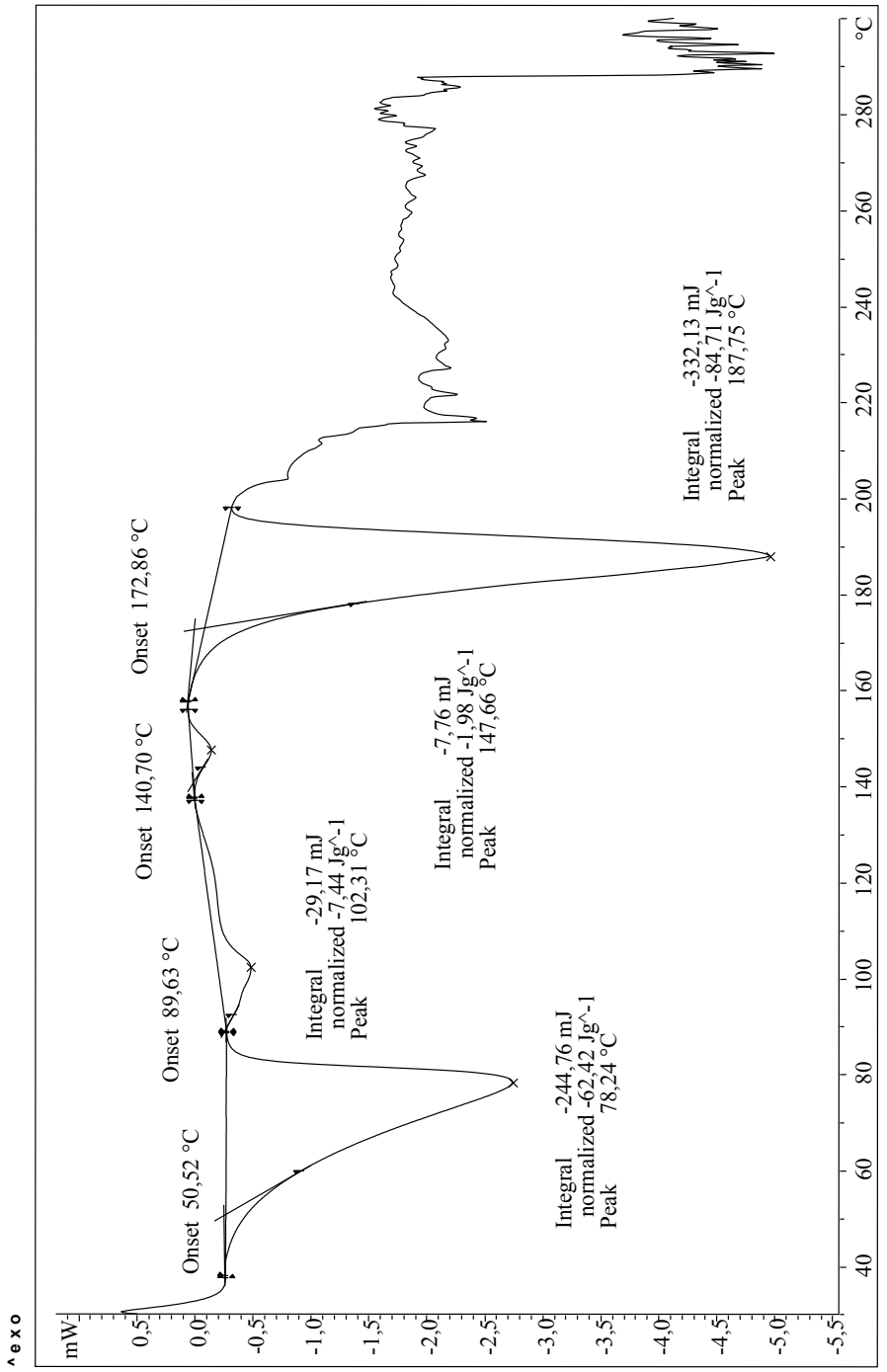

Figure S2: TGA of sodium-glimepiride salt

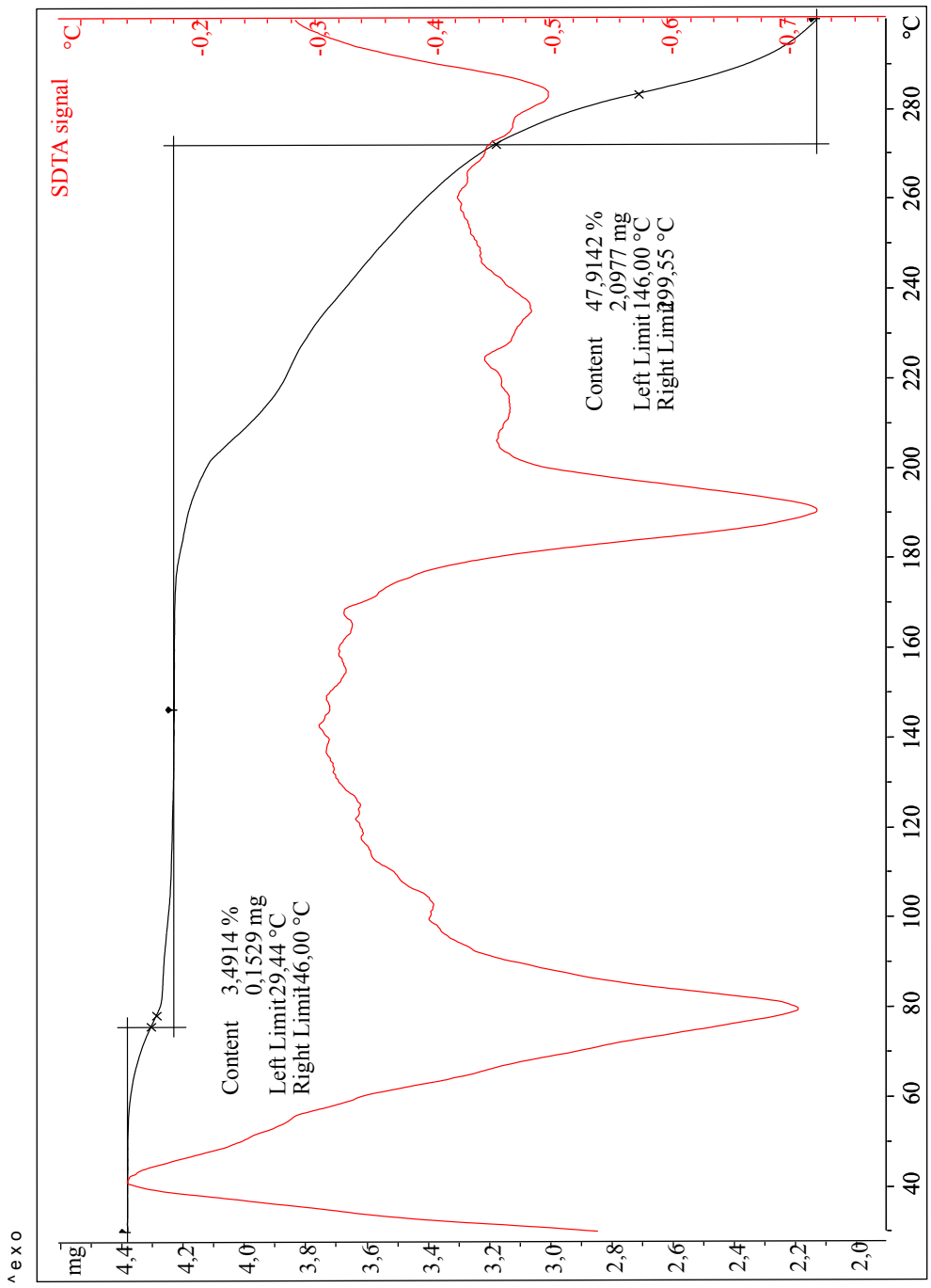

Figure S3: PXRD of sodium-glimepiride salt

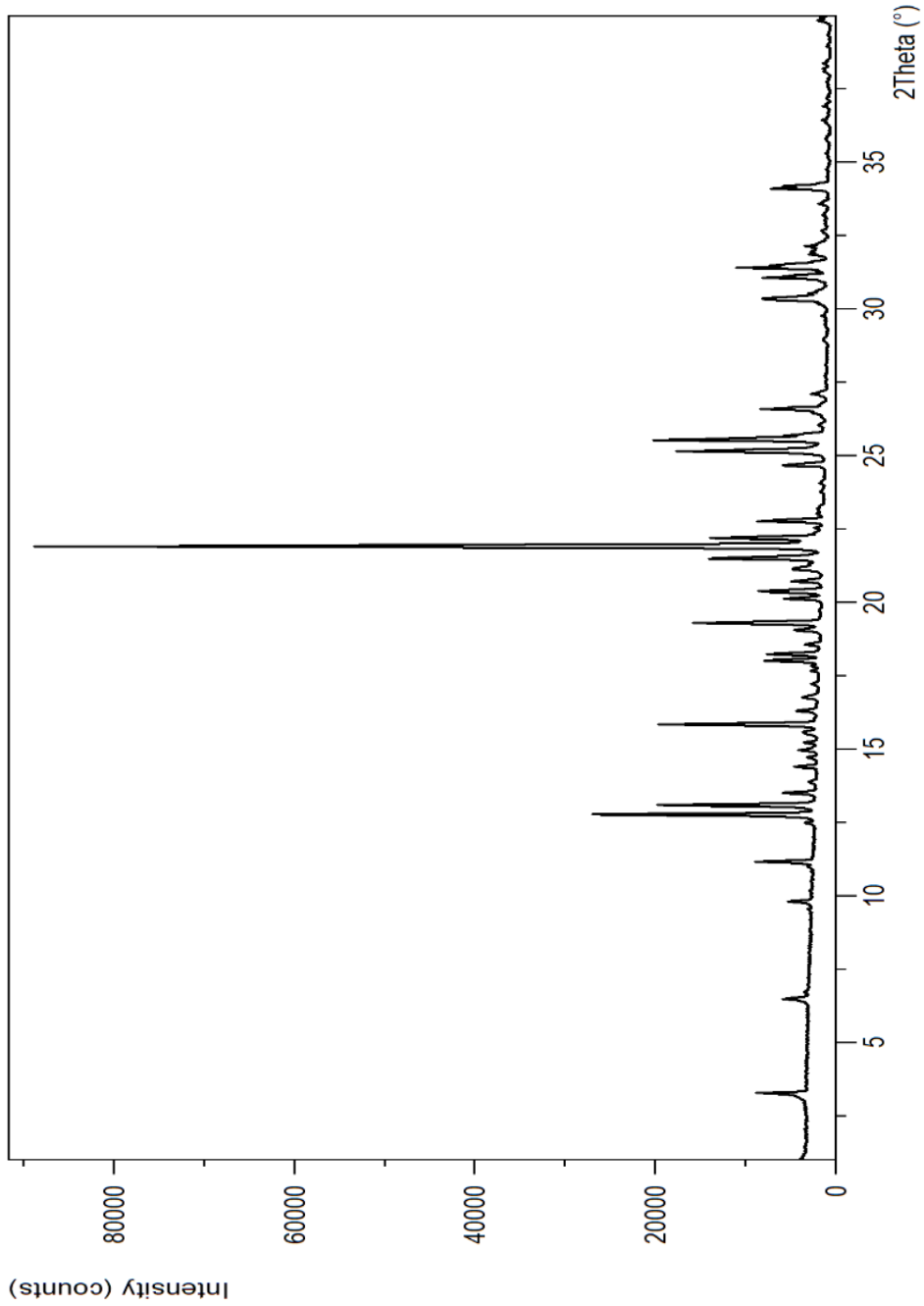

Figure S4: The XRPD diagram of Form SIBU-TFA has been indexed with the following monoclinic cell: a=17.439(2) Å, b=10.434(1) Å, c=11.422(1) Å, β= 102.230(5)º, V=2031.1(4) Å^3 (Figures of Merit: M= 27, F= 70), according to systematic absences $P2_1/n$ or $P2_1/c$ space groups are compatible with the cell.
The powder diffractogram was indexed and the lattice parameters were refined by means of the LeBail method, program Dicvol04[8], and the space group was determined from the systematic absences. The cell volume is compatible with 1 molecule of sibutramine and 1 molecule of phosphoric acid in the asymmetric unit, Z=4, (assuming a density value of 1.2).

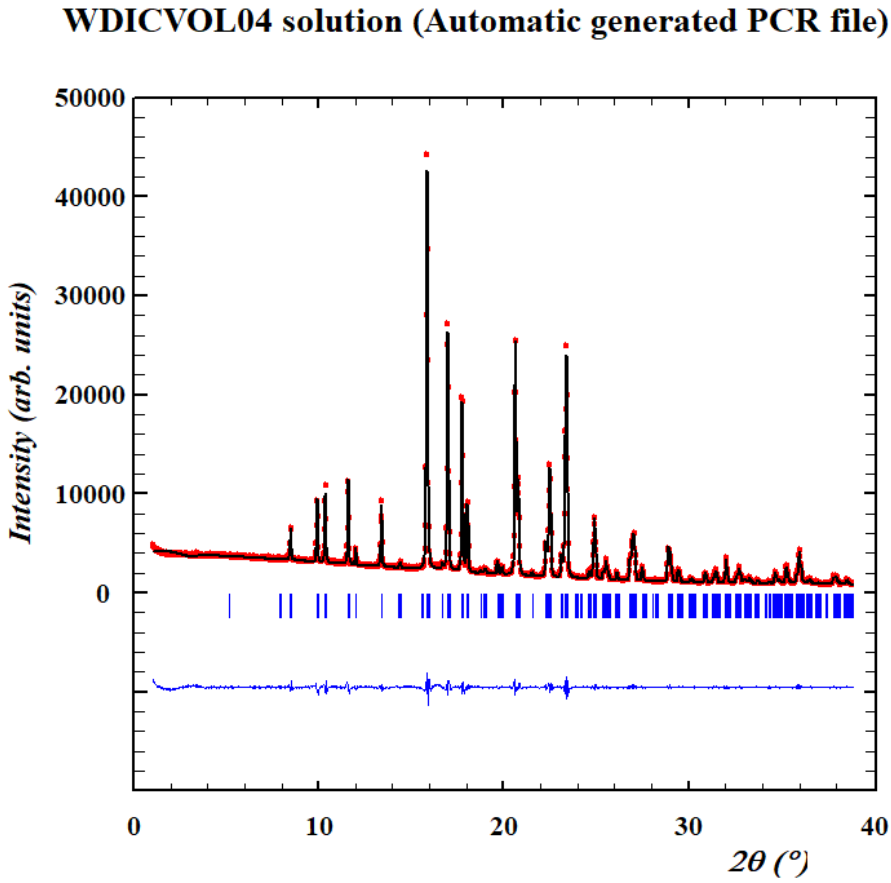

Figure S5: The XRPD diagram of Form SIBU-phosphate has been indexed with the following triclinic cell: a=30.920(6) Å, b=19.905(3) Å, c=9.342(1) Å, α= 49.193(9)º, β= 134.517(8)º, γ= 146.692(6)º, V=2217.9(6) Å^3 (Figures of Merit: M= 45, F= 152).

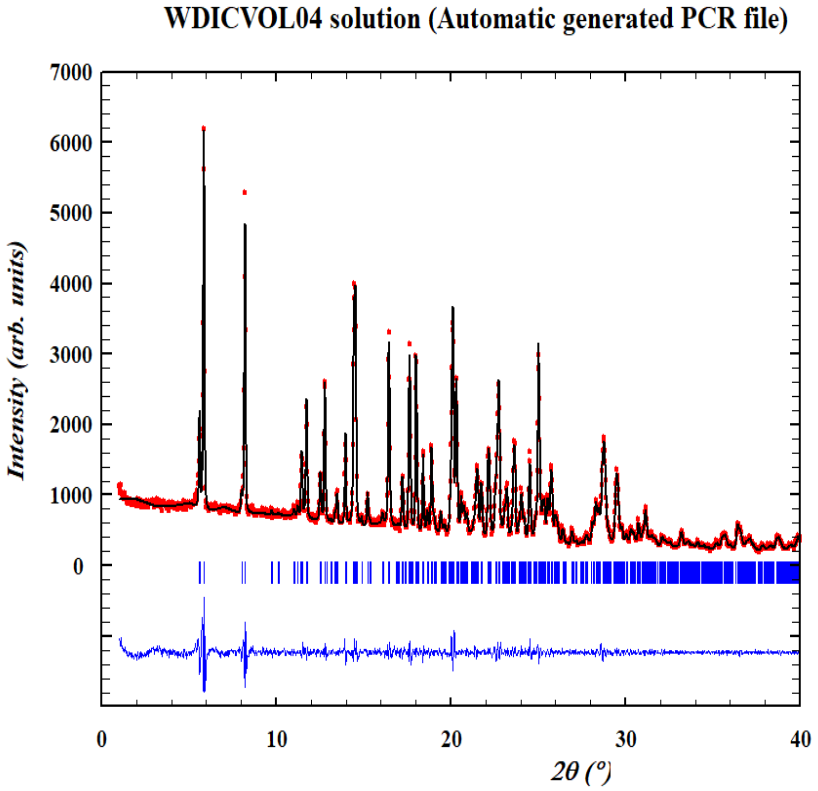

Figure S6: *DSC of sibutramine-TFA salt*

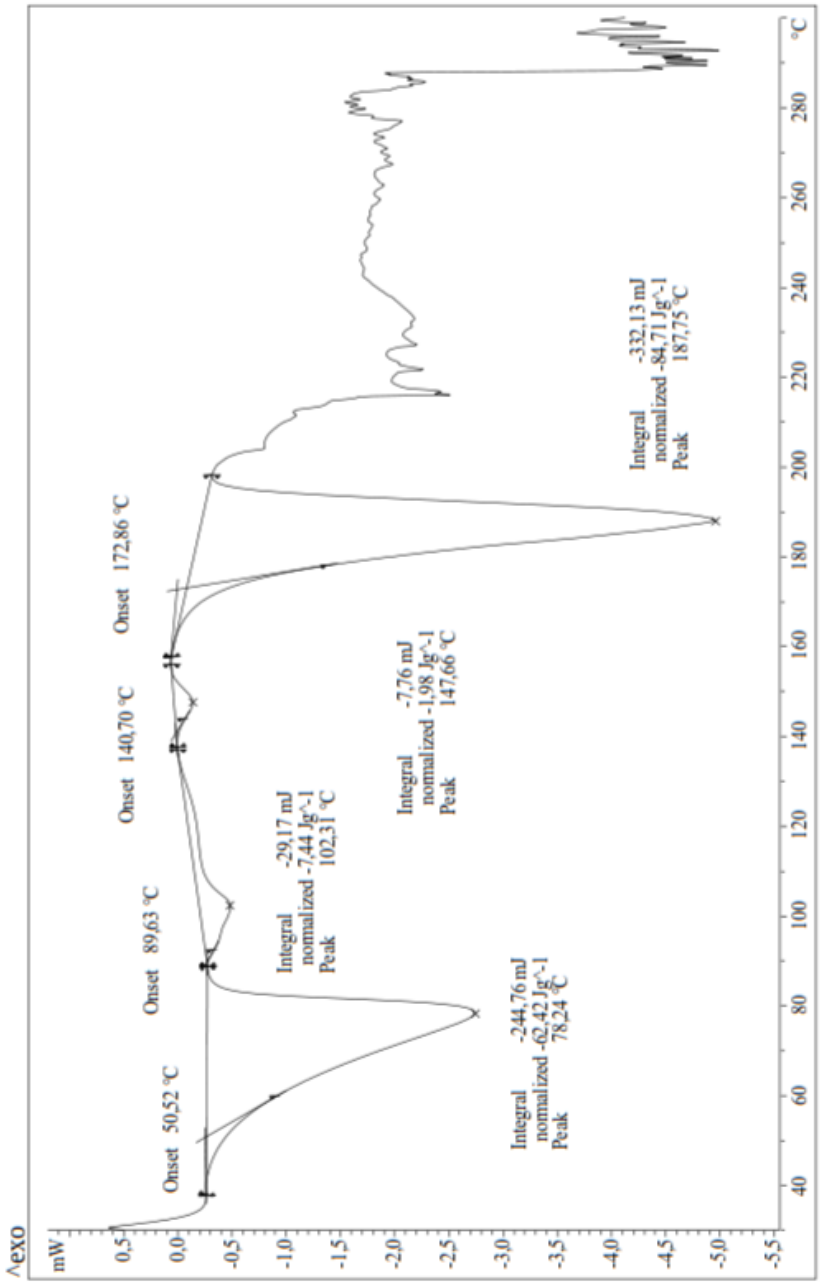

Figure S7: TGA of sibutramine-TFA salt The powder

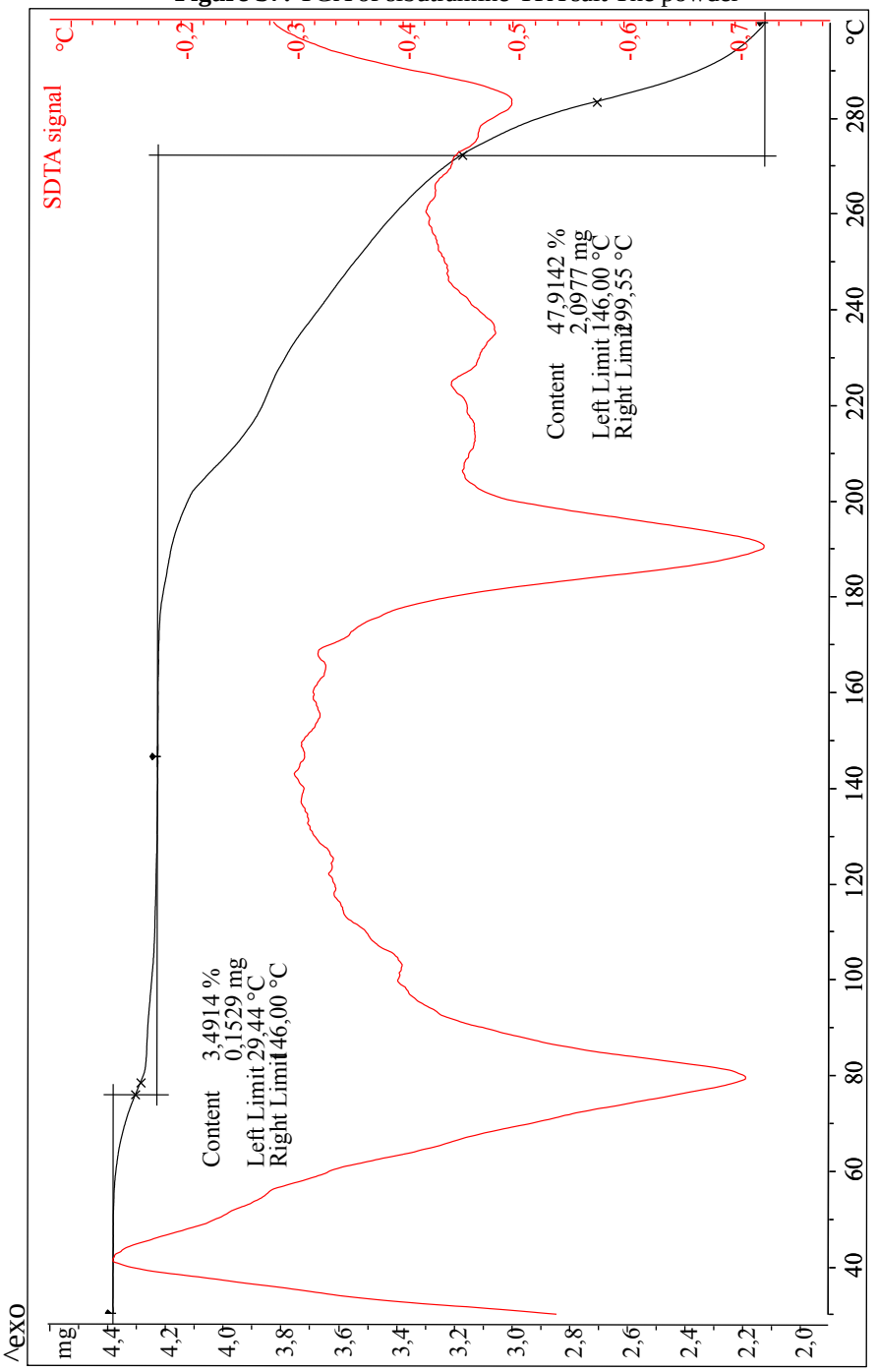

Figure S8: *Diffractograms for Bzt, Iso and Pir collected after the assays, where they are as the raw material*

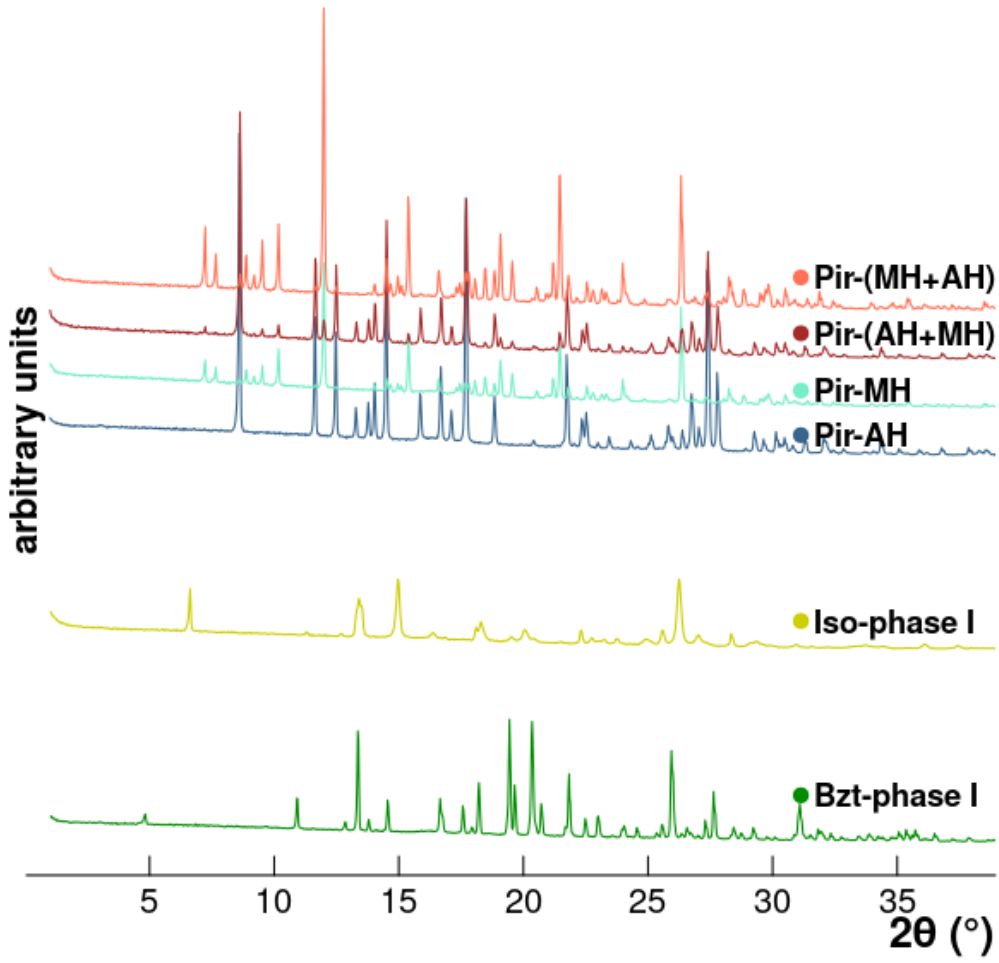

Bzt-phase I: crystalline phase I for benzthiazide, which is matching with diffractogram in Cambridge database
Iso: crystalline form found for Iso, no available diffractogram to compare.
Pir-AH: phase of piroxicam anhydrate crystallographic form
Pir-MH: the monohydrate crystal form of piroxicam, both found in[125].
Pir-(AH+MH): sample mixed with both Pir phases but no more than 10% of the second form is present.
Pi-(MH+AH): exactly as the previous but with inverted order of the components.

References needed for the Appendix section:

[1] F. Tian, A. Zimmerman, Method for preparing glimepiride α crystal form, CN106866486A, 2017.
[2] F. Tian, A. Zimmerman, β Crystal form of glimepiride and preparation method thereof, CN106883161A, 2017.
[3] F. Tian, A. Zimmerman, Glimepiride γ crystal form and preparation method thereof, CN106699631A, 2017.
[4] F. Tian, A. Zimmerman, Method for preparing glimepiride δ crystal form, CN106866485A, 2017.
[5] F. Tian, A. Zimmerman, Preparation of glimepiride crystal form ε, CN106866487A, 2017.
[6] W. Grell, R. Hurnaus, G. Griss, R. Sauter, E. Rupprecht, M. Mark, P. Luger, H. Nar, H. Wittneben, P. Mueller, Repaglinide and Related Hypoglycemic Benzoic Acid Derivatives., J. Med. Chem. 41 (1998) 5219–5246. doi:10.1021/jm9810349. (CCDC code: TOHBUN01)
[7] M. Iwata, H. Nagase, T. Endo, H. Ueda, Glimepiride, Acta Crystallogr. Sect. C Cryst. Struct. Commun. 53 (1997) 329–331. doi:10.1107/S0108270196002363. (CCDC code: TOHBUN02)
[8] A. Boultif, D. Louër, Indexing of powder diffraction patterns for low-symmetry lattices by the successive dichotomy method, J. Appl. Crystallogr. 24 (1991) 987–993. doi:10.1107/S0021889891006441.